

Republic of Iraq
Ministry of Higher Education
and Scientific Research
University of Babylon
College of Engineering
Mechanical Engineering Department



Investigation of the Characteristics of a Two-phase Flow Inside Straight and Tapered Two-pass Channels with Rib Turbulators

A Thesis Submitted to the
College of Engineering / University of Babylon in
Partial Fulfillment of the Requirements a ward of Degree
of Master in Engineering / Mechanical Engineering /
Power

By

Barakat Hassan Abd Alameer

Supervised By

Prof. Dr. Riyadh S. Saleh Al-Turaihi

2022

1444

بِسْمِ اللَّهِ الرَّحْمَنِ الرَّحِيمِ

وَتَرَى الشَّمْسَ إِذَا طَلَعَتْ تَزَاوَرُ عَنْ
كَهْفِهِمْ ذَاتَ الْيَمِينِ وَإِذَا غَرَبَتْ
تَقَرَّبُ إِلَيْهِمْ ذَاتَ الشِّمَالِ وَهُمْ فِي فَجْوَةٍ
مِنْهُ

صدق الله العظيم

Dedication

To the one soul that taught me the real meaning of lost That the sorrow and the grieve surrounds you at your happiest comforting moments, when you realise that the one you used to share it with had gone for good

My precious beloved father this is for you

To my dearest mother

Every and all treasures are non comparing to you , it's you that I felt well trusted and hope .. You are my greatest achievement.

To My lovely family .

Barakat 2022

Certification

I certify that this thesis entitled “**Investigation of the Characteristics of a Two-phase Flow Inside Straight and Tapered Two-pass Channels with Rib Turbulators**” was prepared by Barakat Hassan Abd Alameer Under our supervision at the University of Babylon in a partial fulfillment of the requirements for the degree of Master of Science in Mechanical Engineering (Power).

I recommend that this thesis be forwarded for examination in accordance with the regulation of the University of Babylon.

Signature

Prof. Dr. Riyadh S. Saleh Al-Turaihi

(Supervisor)

Acknowledgment

First, I would like to express my gratitude and thanks to Almighty God for all the blessings I have had. I would like to express my deepest thanks and sincere gratitude to my supervisor Prof. Dr. Riyadh Saleh Al-Tarihi for his guiding comments, invaluable instructions, help and constant encouragement during the preparation of my study..

Special thanks to the staff of the University of Babylon, Department of Mechanical Engineering, for their support and teaching. Last but not least, a special thanks and gratitude to my supportive mom, my lovely sisters, my siblings, as well as all my friends for their help during this work

Barakat 2022

Abstract

Gas turbine blades are typically tapered from hub to tip to reduce thermal loading. These channels exist inside high-performance turbine blades for providing effective cooling to the blade external surface, which is exposed to high-temperature gas flow. Heat transfer measurements are presented for both the straight and tapered square channels including the turn region with and without rib turbulators

In this work, a two-phase flow (water - air) was studied in the presence of heat transfer in straight and tapered horizontal ribbed rectangular channels. The study was conducted theoretically to test the effect of the shape of the channels, the effect of entry velocity and the geometrical shape of ribs at a constant heat flow on the temperature distribution inside the test channel, as well as the heat transfer coefficient. The velocity of water and air used is between (1.154 - 0.3845 m/s) and (13.89 - 4.624 m/s) in sequence. The heat flow is constant ($10000\text{W}/\text{cm}^2$).

Solid work 2018 program was used to design the three-dimensional geometric shape. The simulation was carried out using Ansys fluent 20.R1 program. The dimensions of the straight channel are 60 cm and the cross section is $5 \times 2.2 \text{ cm}^2$, they are equal at the entry and the bending area. As for the tapered channel, the dimensions of the bend area are half of the entry area, to be at the entry $5 \times 2.2 \text{ cm}^2$, and at the bend $2.5 \times 2.2 \text{ cm}^2$, so that it is in the form of a tapered channel. Three geometric shapes of square, house and trapezoid ribs were tested, and they were placed at the top of the channel and at the base to be opposite each other. Three geometric shapes of holes were made inside trapezoid ribs and their effect on the heat transfer coefficient was tested.

Numerical results showed that the local heat transfer coefficient improved by (12%,6%) (21%) inside the test channel equipped with an rib when compared with the smooth channel, it improved by (12%, 6%) inside the test channel equipped with a trapezoid -shaped rib when compared with the other ribs. The other, and it improved by (20%) inside the test channel equipped with a slit rib when compared with the solid rib, when the water velocity increased from (1.154 -0.3845 m/s), and when the air velocity increased from (13.89 - 4.624 (m/s), sequentially, at a constant heat flux (10000 W)

Contents

Chapter One: Introduction	1
1.1. General	1
1.2. Two phase flow	2
1.3. Two pass channel	5
1.4. Rib.....	6
1.5. Object of this work.....	8
Chapter Two: Literature Review	11
2.1. Previous Studies about straight and tapered two pass channels and ribbed channel	11
2.1.1 Effect of solid and slit rib shape on heat transfer and pressure drop.....	11
2.1.2 Effect of rib spacing ,orientation and angle on heat transfer and pressure drop.....	18
2.1.3 Channel geometry , aspect ratio and turn configuration.....	21
2.2.4 Two-phase flow phenomena.....	24
2.3. Scope of this work.....	27
2.4. Summary.....	29
Chapter Three: Mathematical Model and Numerical Simulation	47
3.1 Introduction.....	47
3.2 Design Consideration	47
3.3. Geometry of Ribs.....	51
3.4. Mesh Generation.....	53
3.1 Grid Independence Test.....	47

3.6.	Problem Assumptions	56
3.7 .	Governing Equations.....	57
3.8.	Turbulence Model.....	59
3.9.	Boundary Condition.....	60
3.10.	Convergent Criteria.....	61
3.11.	Fluids and Material Properties.....	62
Chapter Foure: Results and Discussion		65
4.1.	Introduction.....	65
4.2.	Program Validation	65
4.3	The result of work.....	67
4.3.1	Effect of channel shape.....	68
4.3.2	Effect of Rib Shape on two pass tapered 2channel.....	69
4.3.2.1	Temperature distribution.....	69
4.3.2.2	Pressure distribution.....	70
4.3.2.3	Heat transfer coefficient.....	71
4.3.3.	Slit rib.....	73
4.3.3.1	Compare between the solid and slit rib.....	73
A.	Velocity vector	73
B.	Temperature distribution....	74
C.	Heat transfer coefficient.....	76
4.3.3.2	shape of slit.....	77
A.	The effect of shape of slit on the rib in Temperature Distribution...	77
B.	The effect of shap of slit on the rib in H T C.....	79

4.3.3.3. Effect of increasing air superficial velocity on circle slit trapezoidal rib.....	80
A. Temperature distribution.....	80
B Velocity vector.....	81
C. pressure distribution.....	86
D. Heat transfer coefficient.....	87
4.3.3.4 Effect of increasing water superficial velocity on circle slit trapezoidal rib.....	89
A. Temperature distribution.....	89
B. Velocity vector.....	92
C. pressure distribution.....	92
D. Heat transfer coefficient.....	96
Chapter five: conclusion and suggestions for future works.....	98
5.1. Conclusions.....	98
5.2. Suggestions for future work	99
Reference.....	100
الخلاصة.....	107

Nomenclature

Latin Symbols		
Symbol	Description	Units
b	Rib width	m
D_h	Channel hydraulic diameter	m
E	Energy	J
h_x	Local heat transfer coefficient	$W/m^2.K$
I	Turbulent intensity	-
k	Thermal conductivity	$W/m.K$
P	Pressure	N/m^2
q	Wall heat flux	W/m^2
Q	Volume flow rate	m^3/s
Re	Reynolds number	-
t	Time	sec
T	Temperature	K
U	Superficial velocity	m/s
v	Mass averaged velocity	m/s
e	Rib height	m

Greek Symbols		
Symbol	Description	Units
ΔP	Pressure drop	Pa
ΔT	Temperature difference	K
μ	Dynamic viscosity	kg/m. s
ε	Turbulent dissipation rate	m^2/s^3
α	Volume fraction	-
ρ_m	Mass density of mixture	kg/m^3
K	Turbulent kinetic energy	m^2/s^2

Subscripts	
Symbol	Description
k	Phase
a	Air
dr	Drift velocity
in	Inlet
m	Mixture
r	Rib
t	Turbulent

w	Water
x, y,z	Variables Coordinate

Abbreviations	
Abbreviation	Description
Ansys	Analysis of System
CFD	Computational Fluid Dynamics
CFX	Computational Fluid Xerography
CNC	Computer Numerical Control
HTC	Heat Transfer Coefficient
TKE	Turbulent Kinetic Energy
TPF	Thermal Performance Factor

CHAPTER ONE

INTRODUCTION

Introduction

1.1 General

Gas turbines are extremely important in today's society, and as power demand rises, the thermal efficiency and power output of the engine should be maximized. Enhancing the input temperature of the hot gases through the internal channels is one approach of increasing both power output and thermal efficiency. The turbine input temperature of the gases in sophisticated gas turbines can reach 1700° C - 2000° C. These temperatures are higher than the melting points of the turbine components. As a result, cooling the turbine components is critical in order for them to tolerate these severe temperatures. Current cooling techniques reduce the temperature to over 1000° C, allowing them to tolerate this severe environment.

To cool a current gas turbine blade, several approaches such as jet impingement, film cooling, rib turbulators, curved internal cooling passageways, and dimple cooling are used, as illustrated in Figure (1.1). Jet impingement is employed to cool the leading edge, pin fin cooling at the trailing edge, and rib turbulators to cool the interior channels. The current research focuses on the interior cooling of turbine blades employing rib turbulators.

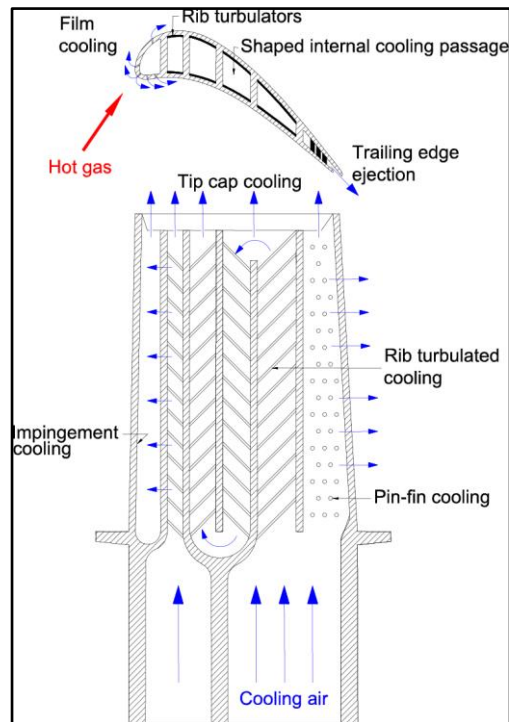


Fig (1.1) : Different cooling techniques employed in turbine blades.

1.2 Two phase flow

The intake temperature of a gas turbine is gradually increasing as gas turbine technology advance. The widely used ways of cooling the blades with air or steam today have certain drawbacks, such as limited cooling efficiency and high working fluid consumption. Because water mists have a larger heat transfer coefficient than air or steam, when the working fluid is a mist/steam two-phase flow, the cooling efficiency of the blades is greatly enhanced, the working fluid consumption is reduced, and the thermal efficiency of the gas turbine rises [1].

Dispersed bubbly two-phase flow is a flow in which the gas phase exists as bubbles in the liquid phase. Channels and pipes with ribs or grooves are frequently utilized in a variety of applications such as ventilation, turbine blades, heat exchangers, and refrigeration. This is due to its favorable properties such as high heat and mass transfer rates between phases, temperature uniformity, and excellent phase mixing[2].

The properties of two-phase flow via these applications should be stated so that they may be employed in the design of their systems. The existence of an interface between the phases complicates the description of two-phase flow, which is dependent on a vast number of variables such as channel design, flow orientation, flow rate, and physical characteristics of the liquids. Recognizing a flow pattern is required for the study of two phase flow with heat transfer systems. Because thermal and hydrodynamic conditions, such as temperature and pressure gradients, fluctuate with flow patterns[3].

Most common class for multiphase flows are two-phase flows and these include the following

1- Gas-liquid flows, which are probably the most important form of multiphase flow and is found widely in industrial applications. Such flow exists in a range of industrial plant which includes evaporators, condensers, boilers, distillation towers, chemical reactors, air ejectors, pipelines for oil and natural gas, turbines, etc.

2- Gas-solid flows, where solid particles are suspended in gases, which are of industrial importance in pneumatic conveying, in the combustion of pulverized fuel and in fluidized beds.

3- Liquid-solid flows, which are widely encountered in hydraulic conveying of solid material. Suspensions of solids in liquids also occur in crystallization systems.

4- Liquid-liquid flows, which include emulsion flows of oil and water in pipelines (of interest in the present context) and flows through packed columns, pulsed columns, nuclear reactors, distillation columns, stirred reactors and pipeline reactors in liquid-liquid solvent extraction. Two-phase flow is classified into many major types based on their

interfacial structure. Separated flows, transitional or mixed flows, and scattered flows are the categories that can also be referred to as flow regimes or flow patterns, as seen in figures (1.2) and (1.3). Two-phase flow may be labeled as one component two-phase flow, such as a condition of steam water glide flow, but air water flow may be labeled as two components two-phase flow. [4]

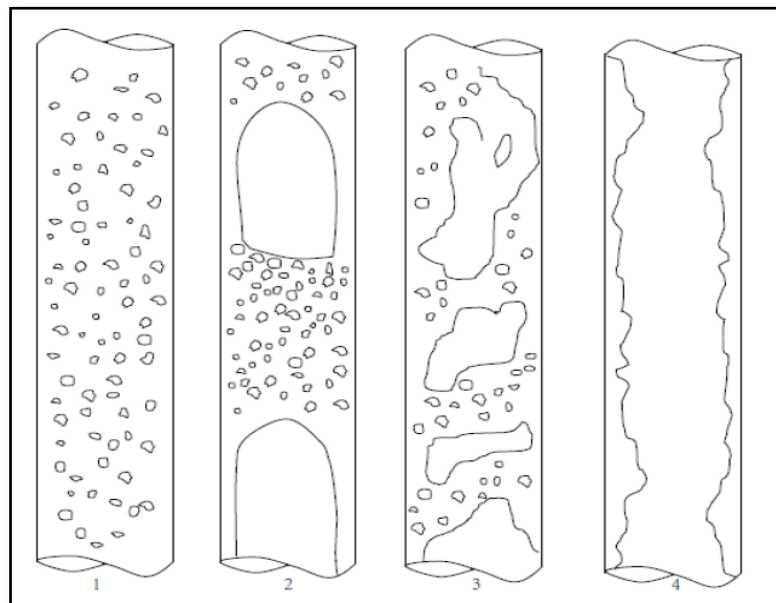


Fig (1.2) Vertical flow patterns: (1) bubble; (2) slug; (3) churn; (4) annular[4]

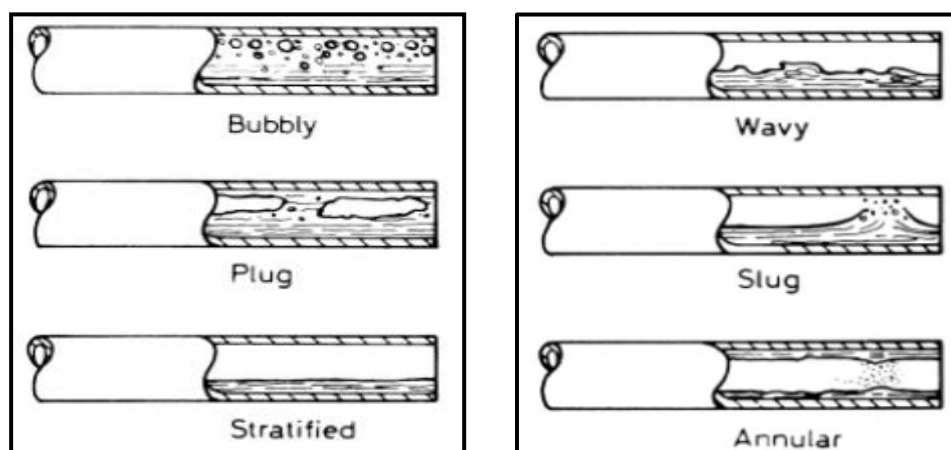


Fig (1.3) horizontal flow patterns[4]

1.3 Two pass channel

Internal turbine blade cooling is affected by the U-shaped bend produced secondary flow. Varied turn design provide different flow fields in the multi-pass channel's turn zone. Secondary flow, flow separation, flow impingement, and flow reattachment all affect the flow characteristics around the curve. Thus, in internal turbine blade cooling, the turn zones play an essential role in heat transfer increase and a pressure drop penalty. The improved gas turbine design need both smaller pressure drops and increasing heat transfer improvement over its stream wise length. As a result, it is critical to pick a turn arrangement that meets the aforementioned design requirement [5].

Gas turbine blades often feature a tapering from hub to tip to decrease thermal stress concentration caused by rotating. The interior channels that provide cooling to the inside of the blade likewise vary in cross-sectional area from hub to tip. The local heat transfer coefficient of these channels is estimated using the local Reynolds number and a database of straight channel correlations for turbulated channels as shown in figure (1.4)[6].

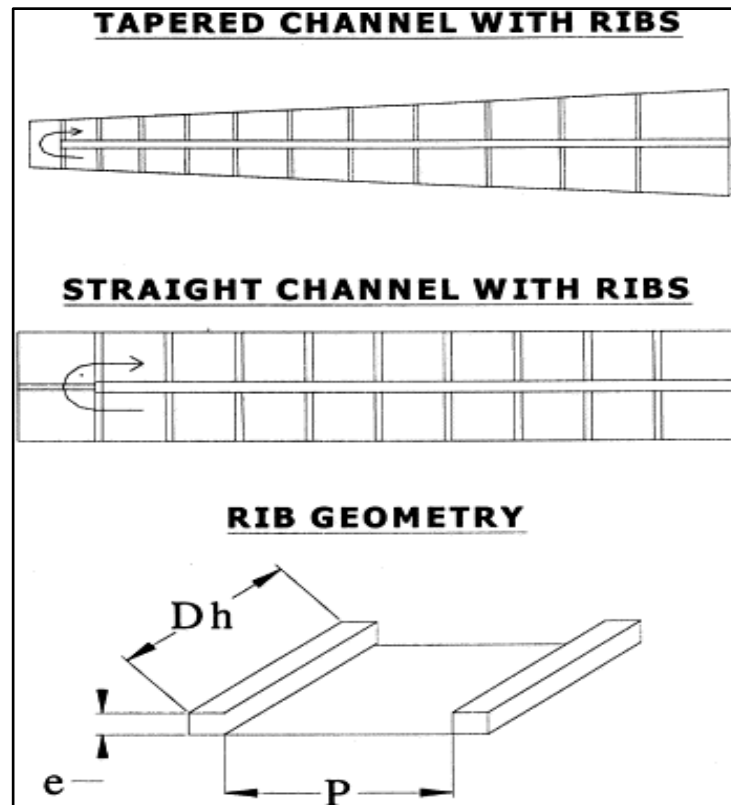


Fig (1.4)Straight and tapered channels [6].

1.4 Ribs

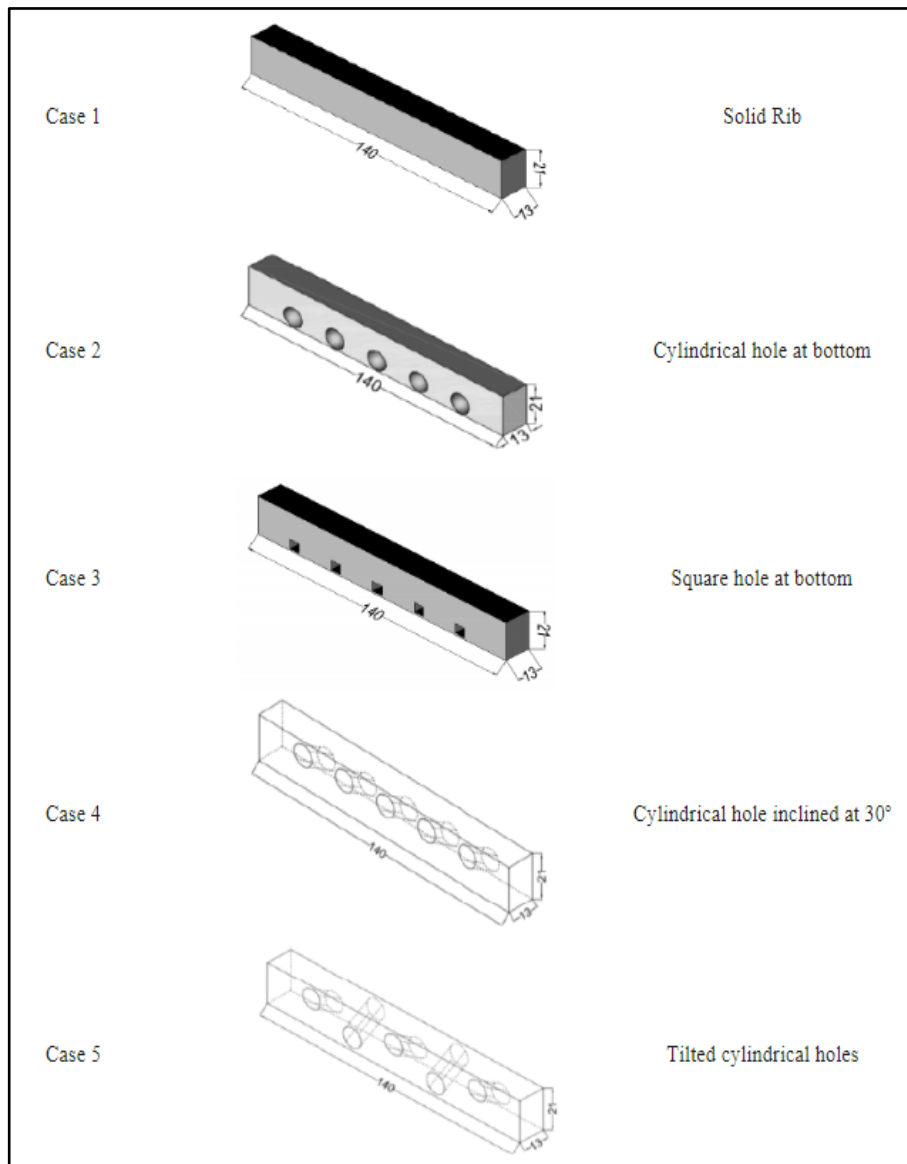
The introduction of the ribs at regular intervals is intended to improve heat transmission rates. Man-made protrusions that are carefully positioned along the walls. The rib produces flow separation, which increases frictional loss. The improved heat transmission has a downside in the form of higher pressure drop, which can be several times more than in a smooth channel. The height of the rib has considerable influence on pressure drop and heat transmission. Although the ribs can be oriented in many way, the pitch is determined by the size of the rib and the distance between two subsequent ribs. The heat transfer performance of the ribbed channel is determined by the channel aspect ratio, rib arrangement. [7].

The ribbed channel's heat transfer coefficient increases as a result of the detached and the reattached barrier layer. The rib creates secondary

flow, which improves heat transmission from the wall to the coolant layer. The rib also causes turbulent mixing in the channels, which enhances flow velocity[8].

The mainstream flows in the smooth and ribbed channels are entirely different. In a smooth channel, the mainstream flow develops easily along the stream, and the thickness of the boundary layer progressively grows until it stable, resulting in a poor heat transmission on the end wall surface .In ribbed channels, the mainstream flows near the end wall immediately impinges on the ribs, causing a recirculation before the ribs .Then it passes over the rib, causing separation; another recirculation is formed after the rib, and secondary flow being generated by the rib develops on the end wall, promoting mass and heat exchange in the mainstream flow along the end wall surface. Finally, the major flow strikes the end wall between the ribs and reconnects with it. [9].

Permeable ribs have the advantage of not developing hot patches while having higher local heat transfer coefficient (HTC) and a lower pressure drop than solid ribs. As the open area ratio grows, the critical (Re) for the initiation of flow permeability decreases. When the perforation inclination angle, open area ratio, rib pitch to hydraulic diameter ratio, and Reynolds number decrease, heat transfer augmentation increases as shown in figure(1.5). [10].



Fig(1.5) slitted ribs [11]

1.5 Objectives of the work

The objective of this work is to investigate numerically the impact of water and air superficial velocities, as well as the three shapes of ribs and three shapes of rib slits, on heat transfer coefficient and temperature distribution in a rectangular two pass straight and tapered channel with

compound turbulators (ribs), and compare the results to a smooth channel. The operating fluids are water and air, with varying discharge rates.

The numerical analysis in this work was accomplished, by utilizing [ANSYS FLUENT (20.R1)] commercial computational fluid dynamics software to study the effect of superficial velocity of water and air, and the three shape of ribs(square ,trapezoid ,house rib) and three shape of slit of ribs(circle , square and ellipse) on heat transfer coefficient and temperature distribution in a rectangular two pass straight and tapered channel tubulated and smooth channel. The Solid Works 2018 software was used to numerically model the geometry of the duct using three-dimensional models combined with Ansys Workbench 20.0 R1. For the straight channel, the inlet and exit cross-section areas are $5 \times 2.2 \text{ cm}^2$, the cross section area at the turn is the same as that at inlet and outlet .For the tapered channels, the cross-section area at the turn are $3.75 \times 2.2 \text{ cm}^2$ and $2.5 \times 2.2 \text{ cm}^2$.

CHAPTER TWO
LITERATURE REVIEWS

Literature Review

Several researchers have explored the behavior of this approach theoretically and experimentally, with varying improvements.

2.1 Straight and Tapered Two-pass Channels and Ribbed Channels

2.1.1 Effect of Solid and Slit rib Shape on Heat Transfer and Pressure Drop

Sharma et. al [12] ,conducted an experimental analysis of the detailed heat transfer and flow field characteristics in a rectangular duct with different types of prismatic ribs on the bottom surface. The truncated prismatic ribs are formed by tapering the square rib from both sides to the middle to provide a rib height at the ends of 0, 2, 4, 6 and 8 mm. A broad range of Reynolds numbers (9400-58,850) of air are used to analyze the effect of rib configurations on the flow parameters as well as on the increase in heat transfer. Many of the truncated prismatic ribs had a higher Nusselt number rise (approximately 25.15 percent) and lower penalty pressure (approximately 54.65 percent) than those with square ribs.

Abraham and Vedula. [13] , investigation experimentally of the local heat transfer coefficients of the converging channel with the cross-section being maintained square from inlet to exit with rib roughening elements. In order to quantify thermal efficiency based on constant pumping power and constant heat transfer area parameters, the total average heat transfer coefficient was used along with the estimated pressure decrease through the test channel. They used Reynolds number between 5000 to 35000 of air. The proportion of rib height to mean hydraulic duct diameter (e/D_h , m) is maintained constant at 0.08. Data for

three pitch-to-height ratios (P/e) equal to 6, 10 and 17.5 are recorded for straight and V ribs. The ratio P/e based on constant pumping power thermal performance criterion was observed to be equal to 10 and this is the only configuration studied for W ribs. The findings indicated that the difference in thermal efficiency between the V and W ribs is within the limits of uncertainty.

Elwekeel et.al [14] , carried out an a numerical analysis of turbulent forced convection in a three-dimensional channel with periodic ribs on the bottom channel wall. The bottom wall is exposed to a constant heat flow, while the top wall is insulated .The purpose of their research was to look at forced convection, flow friction, and performance factors in a horizontal air and air/mist cooled rectangular duct with varied shaped ribs. Over a range of Reynolds numbers (8000–20,000), calculations are performed for square, triangular, and trapezoidal rib cross sections .Computations using the finite volume approach are used to study the impacts of three turbulence models: the conventional k- Ω , and shear stress transport turbulence models. The average mist cooling improvement is determined to be around 1.8 times. With trapezoidal-shaped ribs, air/mist gave better heat transfer increase than air (38°) .

Rasool and Qayoum [15], examined the heat transfer and friction factor for turbulent air flow through a two-pass square channel with ribs of varying cross sections. For a comparative roughness pitch (p/e) of 10, the focus was on exploring the possible influence of different rib shapes. For the Reynold's number range of 5000-52000 of air, four distinct test cases are examined: square, boot, trapezoidal, and house rib shapes.The Nusselt number results are confirmed by comparing them to experimental and computational data from previous research conducted under comparable conditions. The effect of the Reynold's number on the overall performance

of different rib forms has also been studied. In comparison to square ribs, the average Nusselt number increases by 1.19. The investigation reveals that rib design has a major impact on heat transfer distribution and fluid flow in between the ribs, with the boot-shaped rib design showing superior heat transfer performance than standard square ribs, ensuring improved thermo-hydraulic performance.

Singh and Ekkad [16], investigated the heat transmission and pressure drop characteristics of a two-pass channel ($AR= 1$) with ribs alone, dimples alone, and a combination of ribs and dimples. The ribs are V-shaped, with a 0.125 rib height to hydraulic diameter ratio and a 16 rib pitch to rib height ratio. Dimples have a depth-to-print diameter ratio of 0.3 and are cylindrical in form. Transient Liquid Crystal Thermography was used to determine the heat transfer coefficient, and comprehensive Nusselt values were recorded and examined. Additionally, static pressure measurements were taken at various points to quantify the overall pressure drop throughout the two pass channels as well as the local variation of the pressure coefficient. The tests were conducted for a wide range of Reynolds numbers (19,500–69,000) to cover the whole range of Reynolds numbers often seen in both land-based and air-breathing engines. When compared to ribs alone and dimples alone designs for the Reynolds number range investigated, the combination of ribs and dimples resulted in better heat transfer augmentation.

Kumar and Amano[17], compared ribs of various height to 90 degree ribbed channels and smooth channels in terms of computational analysis. ANSYS Fluent, a flow modeling simulation program, was used for the numerical analysis. The flow is considered to be steady state, and the $k-\epsilon$ with Standard Wall Functions is used to describe flow turbulence. For varied Reynolds numbers, local heat transmission in a square duct

roughened with 90 degree ribs of variable height are explored .The pitch of a rib was 10 times the height of the rib, which is 0.0635 m. The channel's square cross section is.0508x.0508 m². At the channel's middle, the rib to rib height ratio ranges from 10 to 20. A rib was also taken into account in the turn section. In comparison to the 90 degree ribbed channel and smooth channel, the numerical simulation demonstrated greater heat transmission for the changing height ribs.

Moon et.al [18],used three-dimensional Reynolds-averaged Navier–Stokes equations, the heat transfer and friction loss performances of rib-roughened rectangular cooling channels with a range of cross-sectional rib forms. Square, isosceles triangular, fan-shaped, house-shaped, reverse cut-trapezoidal, cut-trapezoidal, reverse boot-shaped, boot-shaped, reverse right-angle triangular, right-angle triangular, reverse pentagonal, pentagonal, reverse right-angle trapezoidal, right-angle trapezoidal, isosceles trapezoidal, reverse right-angle trapezoidal, isosceles trapezoidal, reverse right-angle trapezoidal .The pitch, height, and breadth of the rib in relation to the channel's hydraulic diameter were set at 10, 0.047, and 0.047, respectively. To study turbulence, the Reynolds stress model was combined with the Speziale–Sarkar–Gatski pressure–strain model. The area-averaged Nusselt number computations were confirmed by comparing them to experimental data collected under the identical conditions. For Reynolds numbers of 5000–50,000 and rib pitch-to-width ratios of 5.0–10.0, the impacts of the Reynolds number and rib pitch-to-width ratio on the performances of various ribs were also explored. With a pressure drop equivalent to that of the square rib, the new boot-shaped rib design demonstrated the optimum heat transfer performance.

Chang et.al.[19], in this experimental was Detached S-ribs are proposed to be arranged in a staggered fashion around two parallelogram

straight channels intertwined with a 180-degree smooth-walled sharp bend for heat transfer enhancements. Using the steady-state infrared thermography process, the precise Nusselt number distributions over the two opposite channel end walls are determined at the Reynolds numbers of 5000, 7500, 10,000, 12,500, 15,000 and 20,000 of air. Having acquired the average heat transfer properties, the thermal efficiency factors are determined according to the constant consumption of pumping power criterion. The comparative thermal efficiency between the two identical twin-pass parallelogram channels with detached 90 and S-ribs shows higher regional heat transfer rates over the turning area, contributing to lower thermal output factors for the S-rib test channel

Singh et.al. [20], studied the flow and heat transfer numerically and experimentally in a two-pass channel with a square cross-section, a 1:1 aspect ratio, and four ribs of geometric shapes V, M and N with an angle of 45, and the rib pitch to rib height ratio (p/e) is 16 and the rib height to channel hydraulic diameter (e/D_h) is 0.125. The study is carried out using the range Reynolds number of 19500 to 69,000 of air. The experimental study was carried out using transient liquid crystallography to calculate the heat transfer coefficients. The numerical study was carried out using (ANSYS FLUENT) to solve the complex flow field to explain and understand the heat transfer processes numerically. The results showed that the ribs with V shape and at an angle of 45 have the best improvement in slightly higher heat transfer and hydraulic performance compared with other ribs that have M, N shapes as well.

Abed et.al.[21], investigated the forced convective two-phase convective flow (i.e. air and water) through a rectangular ribbed channel with a vertical orientation, numerically and experimentally. Three different rib-groove shapes have been studied (Ribs – groove shapes; Triangular,

Trapezoid, and Semi-Trapezoid ribs – groove) .The study testing was performed with continuous heat flux across the set of surface water and air inlet velocity values between 0.105 – 0.316 m/s and 0.263 – 1.320 m/s, respectively .The findings demonstrate that the triangle rib-groove has a high coefficient of heat transfer and a smaller temperature difference than in other cases against a different number of Reynolds. The experimental evidence was compared to the numerical findings for ribs – grooved channel with a variance of around 1.0 %– 7 %.. Finally, the triangle rib-groove increases the heat transfer value relative to the trapezoidal and semi trapezoidal rib-groove channel at constant pumping power.

Sharma et.al. [22], investigated the local heat transmission of pentagonal ribs placed on the bottom heated wall of a rectangular channel. The emphasis was on evaluating and analyzing the possible influence of changing chamfering angle (0 to 20)deg and rib pitch to height ratio (6 to 12) on overall heat transfer augmentation and distribution on the surface. Experiments are carried out at a variety of Reynolds numbers ranging from 9400 to 58850.Liquid crystal thermography was used to assess the temperature distribution on the ribbed surface and then to illustrate the local heat transfer coefficient. The results indicated that the local augmentation Nusselt number distribution was axisymmetric and has two dimensions in the heat transfer distribution. Pentagonal ribs demonstrate a substantial improvement for the low heat transfer zones in the leeward area of the square rib, especially at higher Reynolds numbers, and are thus viewed as a possible advantage in terms of avoiding hotspots.

Tariq et.al. [23], investigation experimentally of detailed aerothermal properties within a duct with an array of solid and permeable pentagonal ribs installed on the bottom wall and a parallel and inclined slit. The fixed rib height-to-hydraulic diameter ratio, rib pitch-to-height ratio, and open

area ratio during trials are 0.125 percent, 12%, and 25%, respectively. The primary aim of the research is to determine the impact of inter-rib area flow features on local heat transfer fields. Performance indices demonstrate that pentagonal ribs with slanted slits outperform alternative designs in both directions. Aerothermal characteristics in the inter-rib area were investigated using time-averaged streamlines, mean velocities, fluctuation statistics, vorticity, turbulent kinetic energy (TKE) budget terms, and local and spanwise-averaged Nusselt numbers, as well as augmentation Nusselt numbers. The magnitude of stream wise velocity, fluctuation statistics, vorticity, and TKE budget terms at the downstream corner are significantly affected by the flow emanating from the inclined-slit pentagonal rib, whereas the dissipation term of TKE budget correlates well with the surface heat transfer distribution.

Ali et.al.[24], studied the heat transmission and fluid flow (air) properties of various rib turbulator shapes. Particle image velocimetry and liquid crystal thermography were utilized to investigate the flow field and heat transfer using a trapezoidal rib with variable downstream chamfering and a centrally positioned longitudinal slit. Experiments were conducted in a rectangular duct for flow over rib with a 12.5 percent blockage ratio and a 25% open area ratio for hydraulic diameter based Reynolds numbers of 61480. Angles of chamfering ranged from 0 to 20 degrees. When compared to its solid counterpart, the slitted rib causes a shorter reattachment length and a lower pressure penalty.

Zhenga et .al. [25], conducted a study to verify the improvement of the thermal performance of cooling ducts by placing slit ribs, which are of different shapes ribs with rectangular slits, V-shaped slits, anti-V-shaped slits, broken V-shaped slits and broken anti-V-shaped slits. The effect of slit shapes on the thermal performance of cooling channels was studied. Air

was used as the coolant with Reynolds numbers ranging from 1000 to 2500. The results showed that the channels in which with broken slits have a higher thermal performance in heat transfer due to the intensity of the turbulence, in contrast high pressure losses that have an effect on the thermal performance.

2.1.2 Effect of Rib Spacing ,Orientation and Angle on Heat Transfer and Pressure Drop

Xu et.al.[26],the effect of rib spacing on heat transmission in a rotating two-pass square channel was examined experimentally. Reynolds and rotation numbers range from 20000 to 50000 and 0 to 0.8, respectively. The 90-degree ribs are placed asymmetrically on the leading and trailing surfaces, with a height-to-hydraulic diameter (e/D_h) ratio of 0.1. On the pressure side, the rib pitch-to-height (p/e) ratio changed from 3.8 to 14.4 in the positive rotating direction, while it remained constant at 10 on the suction side .The results showed that the rib spacing impact is stronger in the first radially outward flow passage than in the second. Except for the trailing wall of the first passage, rotation minimized the impact of rib spacing, and $p/e=10$ has the optimum surface average heat transfer improvement. In most situations, however, rotation causes a lesser pressure decrease at a low rotation number. For positive rotating direction, the very tight rib spacing of $p/e=3.8$ provides the optimum thermal performance. The optimum rib spacing ratio for negative direction was $p/e=10$.

Olewi and Al-Turaihi [27], investigated experimentally and numerically the two phase flow(air-water) in vertical duct ribbed for both sides with rectangular ribs .The experimental rig dimensions ($4 \times 6 \times 70$ cm) , the duct was made from Pyrex material . The duct had internal ribs with ($4 \times 1 \times 1$ cm) dimensions and the distance of (3 cm) separate each rib

from the other .The flow behavior of the duct was photographed and the results compared to the volume fraction images obtained by ANSYS fluent 15.0. The same CFD model compared to the experimental results was used with other ribs in height to show the difference between the height of the ribs. Three ratios of Rib height to duct width were studied (0.083, 0.167, and 0.25).

Gao et al. [28], investigated the correlation nine various rib orientations and the 180-degree bend forced convection in the U-shaped tunnel was using the ANSYS CFX commercial CFD program when $Re = 30000$. The vortex core approach was used to display the whole history of secondary flow, which was colored by turbulence kinetic energy. The qualitative results demonstrate that the upstream shape had a significant impact on the Nu ratio in the downstream passage (Passage 2).The qualitative results demonstrated that the upstream shape had a significant impact on the Nu ratio and total pressure loss in the downstream passage (Passage 2). The N-type rib orientation in Passage 1 provided more disturbance energy into Passage 2, where the P-type rib orientation can lower the momentum loss and pressure loss of the upstream secondary flows. Based on the study of secondary flow interaction around the bend, a new bend shape with a 9 percent thermal performance improvement over the existing optimal rib orientation was presented. This research reveals that the vortex core approach was a potential visualization tool for flow management and optimization in U-shaped channels.

Gao et al.[29], numerically investigated the combined effects of rib orientations (N-type and P-type) and four rib angle (30° , 45° , 60° , 75°) on flow and heat transfer in two-pass ribbed channels. By using commercial software ANSYS CFX 14.0, the 3D steady Reynolds-averaged Navier-Stokes equations coupled with SST $k-\omega$ model are solved by commercial

software ANSYS CFX. The findings demonstrated that transporting more secondary flows into the downstream passage without weakening the local secondary flow and energy dissipation of the upstream secondary flow was the key factor for local heat transfer enhancement. In addition, the rib orientation in passage two should take into account the effect of the rib angle so that the secondary flow of the local main flow had the same rotational direction with the most strong upstream secondary flow to decrease the energy loss and speed up the development of the secondary flow of the local main flow as much as possible channel with angled ribs.

Lei et.al. [30], investigated the influence of rib spacing on heat transmission in a revolving two-passage channel (aspect ratio, AR 14 2:1) at a 135 deg orientation angle. At a flow angle of 45 degrees, parallel ribs were attached to the leading and trailing walls of the spinning channel. The rib-height-to-hydraulic-diameter (e/D_h) ratio was 0.098. The investigated rib-pitch-to-rib-height (P/e) ratios were 5, 7.5, and 10. Tests were performed at five Reynolds numbers ranging from 10,000 to 40,000 for each rib spacing, and experiments are carried out at four rotational speeds ranging from 400 rpm to 400 rpm for each Reynolds number. The results demonstrated that the heat transfer enhancement rised when P/e decreases from 10 to 5 under non rotation circumstances. However, the effect of rotation on heat transfer enhancement stays almost constant as P/e varies from 10 to 5.

Kaewchoothong et.al.[31], studied the effect of the arrangement of the ribs on the distribution of the local heat transfer coefficient in a square-section channel. The ribs that were used in this study have a square cross-section placed on both sides of the channel, as well as the ratio of rib height to hydraulic diameter ratio (e/D_h) and rib-to-height ratio (e/D_h) at 0.133 and 10, respectively. Three types of ribs arrangement are used, inclined ribs

,V-shaped ribs , and inverted V-shaped ribs .The rib angle used varied between 30 to 90 degrees for the inclined sides and 45 to 90 for both V-shaped and inverted V-shaped ribs, and the Reynolds number used in this study was fixed ($Re=30000$) . The results showed that the average Nusselt number on the surface with an angle of inclination of the side at 60 , 45 degrees V - shape ribs is improved about 20%, 25% and 30% higher than the case of the angle 90 and the ribs inclined at an angle of 60 V- shape ribs . The ribs in the form of V-shape ribs have a higher Nu compared to the other cases.

Al-Turaihi and Oleiwi [32], (CFD) model was used to study the flow of water and air in a ribbed and smooth duct. The temperature was applied at the top and bottom of the channel where the ribs are located . Three types of ribs was studied rectangular, trapezoidal, and triangle . Three air velocities and three water velocities are used (0.12, 0.15, and 0.18 m/s),and (0.4, 0.6, and 0.8 m/s) ,respectively. It was show that, the heat transfer coefficient of the ribbed channels was compared with the smooth channel to be increased by 73.97 % for rectangular ribbed channel, and 135.65 % for triangle ribbed channel . It was found that increased as the velocity of air / water increased and also found the heat transfer coefficient increased by adding ribs .

2.1.3 Channel geometry ,Aspect ratio and Turn Configuration

Liu et. al [33], heat transfer properties in a two-pass channel with integrated film cooling holes and ribs with a variable cross-section were investigated experimentally. Two opposing walls were roughened by rectangular ribs angled at 60 degrees to the main flow. Along the second pass, the film cooling holes were spread on the rib-roughened surfaces .The studies were conducted at between 10000 and 60000 Reynolds numbers.The main conclusions may be drawn from the experimental

results: increasing the hole opening ratio increased heat transfer. The heat transmission impact was variable depending on the position of the cooling holes.

Gaoa et.al. [34], the combined influence of rib orientation and bend form on heat transmission in U-shaped channels at Reynolds number of 30,000 with 60° and 45° ribs is numerically studied and evaluated using vortex core technology. The results demonstrate that the rotation direction and transverse location of secondary flow in straight passageways are determined by the rib orientation, but the bend shape influences the delivery of upstream secondary flow and the production of local secondary flow. The optimal bend form was based on an intuitive representation of secondary flow development, which gave insight into geometry optimization for heat transfer applications.

Erelli et.al.[35], the experimentally and numerically work was studied of the turbulent flow and heat transfer in a two-pass smooth square duct. In this study was used four different turn configurations (cases-1, 2, 3, and 4) having various divider and outer turn geometries. Infra-red thermography (IR) technique has been employed to obtain the local temperature distribution on the heated surface for three different Reynolds numbers namely, 25,000, 35,000, and 45,000. Measurement of the average Nusselt number of different turn configurations shows that the computational simulations adopt the same behavior as experimentally found, but the heat transfer increase in the bend area is not expected by the chosen turbulence model. Case-3 (sharp 180 bend with circular divider average) thermal efficiency is higher than that of the other three instances.

Saha and Acharya [36] A numerical comparison of turbulent flow inside a two-pass internal cooling channel with varied bend geometry is presented in this work. The objective is to create a shape that minimizes

bend-related pressure loss while also improving the total heat transfer coefficient. The heat transfer and pressure loss for nine various bend geometries are compared to the baseline example, which is a square channel with a round U-bend. Changes to the bend geometry are made along the channel divider wall and at the 180-degree bend's end wall. (1) a turning vane geometry, (2) an asymmetrical bulb, (3) three distinct symmetrical bulbs, (4) two different bow shaped geometries at the end wall, (5) a bend with an array of dimples in the bend zone, and (6) a combination of bow geometry and dimples were all investigated. The bend shape of a two-pass channel was discovered to have a substantial impact on its overall performance. Nusselt number ratios and thermal performance factors (TPF) are used to compare the adjusted bend geometries to the baseline. The TPF increases in all adjusted bend geometries, with the symmetrical bulb shape exhibiting a roughly 30% gain in thermal performance. The symmetrical bulb with a bow along the outer walls and surface dimples has the highest TPF (41 percent increase above baseline).

Liue et.al.[37], the characteristics of the flow field in a U-shaped channel of square cross-section and different curvature shapes (square - square, circle - square and circle - circle) were studied by using the velocity measurement of particle images. The Reynolds number that was used in this study depends on the hydraulic diameter being 8888, 13 333, or 17 777. A number of conclusions were drawn based on the results, where the size and number of vortices were reduced in the bending region due to the increase in Reynolds, which makes the flow stronger, as well as there is a high percentage of turbulent kinetic energy in the bending region, which is shaped like a circular inside and outside (circle - circle)

Wang et.al.[38], the influence of ribs on heat transfer performance and cooling air flow characteristics in different aspect ratios (AR) U-shaped

channels under varied operating circumstances are quantitatively studied .The ribs angle and channel orientation are 45° and 90° , respectively, while the aspect ratios are 1:2, 1:1, and 2:1. The inlet Reynolds number varies from 10000 to 40000, and rotational speeds include 0 rpm, 550 rpm, and 1,100 rpm. The three major criteria for measuring channel heat transfer are the local heat transfer coefficient, the end wall surface heat transfer coefficient ratio, and the augmentation factor .Ribs considerably enhance the heat transfer area and improve the heat transfer coefficient of ribbed surfaces, particularly in the first pass, but the end wall surface contributes more to channel heat transmission due to its greater area and lower heat transfer coefficient. The broad channel (AR = 2:1) has a higher augmentation factor than the small channel (AR = 1:2), and the weight of the ribs heat transfer rises as the inlet Reynolds number increases. The trailing surface in the first pass is the major influence object of rotating, since it decreases the ribs heat transfer weight in the channel.

2.1.4 Two-phase Flow Phenomena

Hayashi et.al.[39], studied the pressure drops in horizontally oriented U-bends was measured for air-water bubbly, plug, slug and annular flows to test the applicability of the available relations to the data .They used the inner diameters of the U-bends, D , were 8 and 16 mm, and the bend ratios were 3 and 6, $D * B = 2RB/D$, where RB is the curvature bend radius . The findings show that the bend disturbed the flow and caused significant drops of pressure not only in the bend but also in the downstream-side straight pipe. As a result, the bend pressure drop was measured as the amount of the pressure drop induced in the bend and the additional pressure drop caused in the re-developing area in the downstream-side straight pipe .

Dhanasekaran and Wang [40], the current research employs numerical modeling to apply mist cooling to the revolving mist/air internal cooling

tube with rib turbulators. The first section validates the computational fluid dynamics (CFD) models of smooth and ribbed channels without mist and rotation using experimental data from the literature. The predicted and experimental values match within 3% variance in the lower Reynolds number (Re) range, and within 10% deviation in the higher Reynolds number range. The smooth channel has high agreement with the experimental result throughout the whole range of Re values. The rotating impact on smooth and ribbed channels is anticipated and examined in the second section. The mist cooling enhancement on the ribbed channel with rotation is simulated in the last section. The secondary flows generated by channel bend and rotation are studied in detail. The findings reveal that with 2% mist injection, the mist cooling enhancement is about 30% at the trailing surface and about 20% at the leading surface of the first passage. Both surfaces are expected to get 20% augmentation in the second transit.

Al-Turaihi and kareem [41], experimentally and numerically studied in order to analyze characteristics of the mixture (water, air) in a rectangular Placed vertically by using internal rib with different volume flow rates of water and air ,and constant heat power. A test section with a rectangular cross section (8 cm×3cm) and a length (70 cm) was used. Using computational fluid dynamics CFD software to analyze the unstable two-phase flow turbulence for several water and air velocities with smooth expansion, a numerical investigation was carried out. Three different water flow rate values (2.5,5.8 l/min), five different air flow rate values (8.33, 10.83,12.5,14.167,16.67 l/m) and three different heat power values (120,140, 160 watt) are included. The findings showed that as the discharge of air and water increases.

Al-Turaihi [42], experimental was test to study the effects of air and water discharge for straight hydrofoil attacks at various angles and

designed an experimental rig to study the two-phase flow. in this work The rectangular cross section (10 cm×3cm) and length (70 cm) test section shows the behavior of the two-phase flow (gas and liquid) around the straight hydrofoil and tests the difference in pressure and documents this behavior. Three different angles of attack (almost = 0 °, 15 ° and 30 °) are considered in this work. Water discharge (Q_w) was taken at different amounts ($Q_w=12, 17, 27$ and 37 L/min) and different air discharge ($Q_a=5, 15, 25$ and 35 L/min). In the test section, the maximum inlet velocity for air is (4,758 m/s) and for water is (1,217 m/s). The results show that the pressure differential increased at the inlet and outlet of the rectangular channels as the angle of attack increased at constant air and water discharge amounts. The findings demonstrate that the pressure differential increased at the inlet and outlet of the rectangular channels when both water and air discharge were at a constant angle of attack.

Habeeb and Al-Turaihi [43], investigated experimental and numerical was study the two-phase flow phenomena around straight hydrofoil at different angles of attack in a rectangular enlarging channel with dimensions (10 x 3 x 70 cm) extended from a two-phase circular assembly tube. Experiments are carried out in the air-water flow channel with varying air and water flow rates. The purpose of these experiments is to visualize the two phase flow phenomena as well as to research the effect of the difference in pressure through the channel with the presence of the hydrofoil. In this experiment, all sets of experimental data were collected by means of a pressure transducer and visualized by a video camera for different discharges of water and air (20, 25, 35 and 45 l/min), (10, 20, 30 and 40 l/min) respectively and different attack angles (0, 15 and 30 degrees). The numerical simulation carried out by using commercial Fluent CFD software. The findings demonstrate that the pressure difference

increases at the inlet and outlet of the rectangular channel when the angle of attack increases with constant air and water discharge, or when air discharge increases with constant water discharge and angle of attack, or when water discharge increases with constant water discharge and angle of attack

2.2 Scope of This Work

Experimental and Numerical (CFD) studies were carried out in smooth and ribbed two-pass channels. The researchers studied the characteristics of heat transfer and flow behavior experimentally and studied the effect of the turn geometry ,aspect ratio of the two-pass channel on heat transfer, pressure drop ,temperature distribution and flow behavior. The fluids used in most of the previous research were air, water, air/mist ,water/mist ,mist/steam and nanofluid.

In this work, the characteristics of heat transfer, flow, pressure drop, as well as temperature distribution of two-phase flow in straight and tapered horizontal two-pass channels and having a rectangular cross-section .

- 1) The three two-pass channels (straight and two tapered) are tested and the optimum channel are choosed at constant air-water discharge and constant heat flux.
- 2) The optimum channel with and without ribs are tested at constant air-water discharge and constant heat flux.
- 3) The three shape of ribs (square ,house and trapeziodal) inside the tapered channel are tested, and choose the optimum shape of rib at constant air-water discharge and constant heat flux .

- 4) The optimum rib with three shape of slit (square, ellipse and circle) are tested and choose the optimum shape of slit at constant air-water discharge and constant heat flux.
- 5) Finally, the optimum slit rib inside the two-pass channel were tested with three air-water discharge at constant heat flux.

The ribs are located at the top and the bottom of the heated section of the channel. The liquid used in this work is water and air. The study were carried out numerically (CFD simulation) by using AnsysFluent20.0R1.

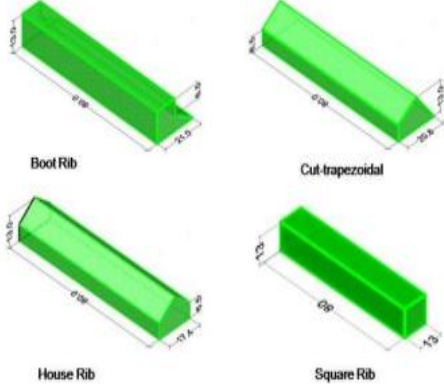
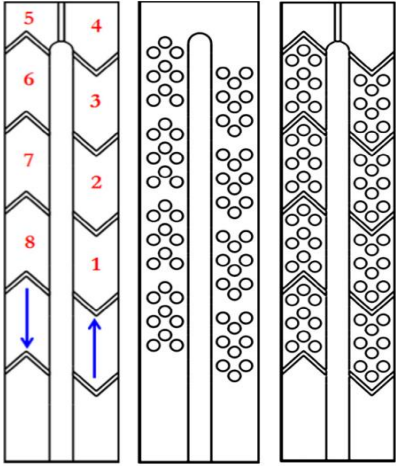
2.3.Summary

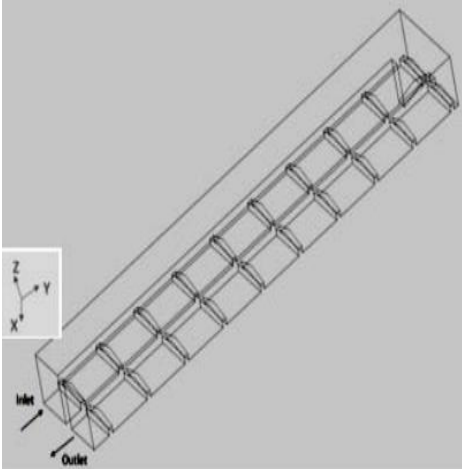
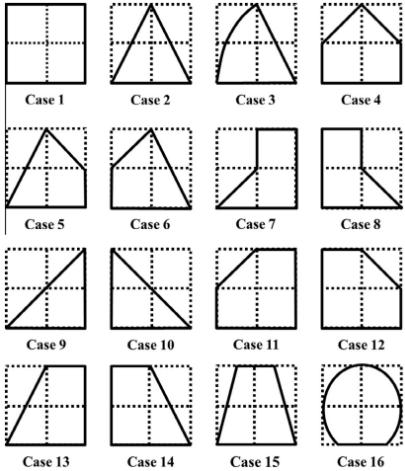
The literature presented in this chapter are summarized in Table (2.1)

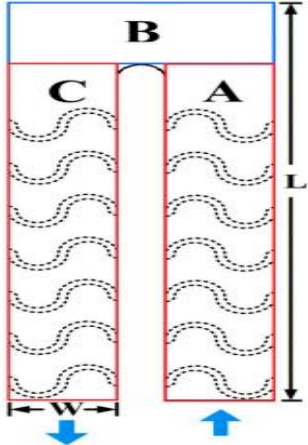
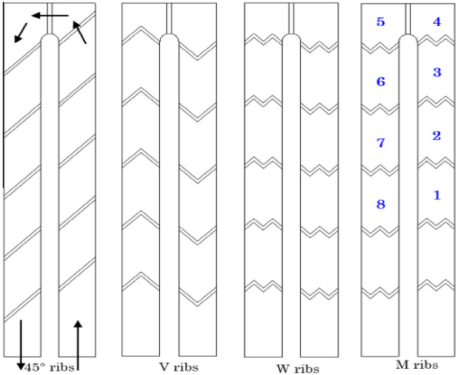
Table (2.1): Summary for the Previous Literatures

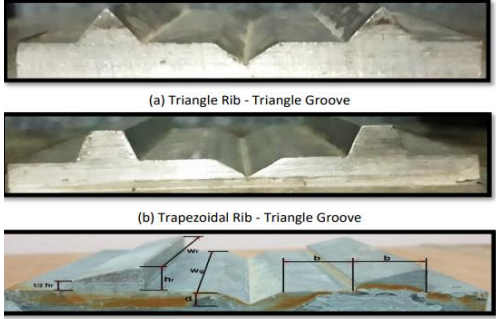
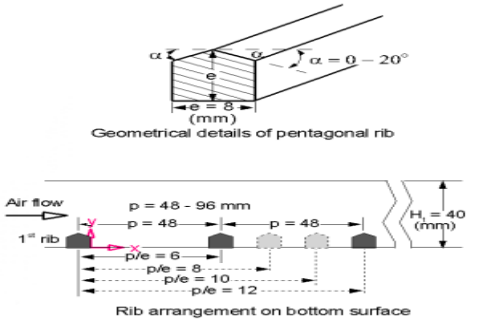
Authors	Type of investigation	Type of flow and flow parameter	The research aim	Conclusion	Teast section
Sharma et. Al [12] 2018	Exp.	Air, Reynolds numbers (9400-58,850)	Detailed heat transfer and flow field characteristics in a rectangular duct with different types of prismatic was conducted.	Truncated prismatic ribs provide higher augmentation Nusselt number , lower, pressure penalty and provide better thermohydraulic performance than the square rib,	<p>Fig. 2. Different rib configurations with arrangement on the bottom wall.</p>

<p>Abraham and Vedula [13] 2015</p>	<p>Exp.</p>	<p>Air, Reynolds number between 5000 to 35000</p>	<p>Explanations of the local heat transfer coefficients of the converging channel with the cross-section being maintained square from inlet to exit with rib roughening elements.</p>	<p>The W ribs a better choice as an enhancement unit.</p>	
<p>Elwekeel et.al [14]2014</p>	<p>Num.</p>	<p>Air and Air/mist Reynolds numbers (8000–20,000)</p>	<p>Analysis of forced convection, flow friction, and performance factors in a horizontal air and air/mist cooled rectangular duct with varied shaped ribs</p>	<p>With trapezoidal-shaped ribs, air/mist gives a better heat transfer increase than air .</p>	

<p>Rasool and Qayoum [15]2018</p>	<p>Num.</p>	<p>Air Reynolds numbers 5000-52000</p>	<p>Examines the heat transfer and friction factor for turbulent air flow through a two-pass square channel with ribs of varying cross sections</p>	<p>With the boot-shaped rib design showing superior heat transfer and friction factor performance than standard square ribs</p>	
<p>Singh and Ekkad [16] 2017</p>	<p>Exp.</p>	<p>Air Reynolds numbers 19,500 to 69,000</p>	<p>The heat transmission and pressure drop characteristics of a two-pass channel with ribs alone, dimples alone, and a combination of ribs and dimples are investigated.</p>	<p>The combination of ribs and dimples resulted in better heat transfer augmentation as well as higher thermal hydraulic performance.</p>	

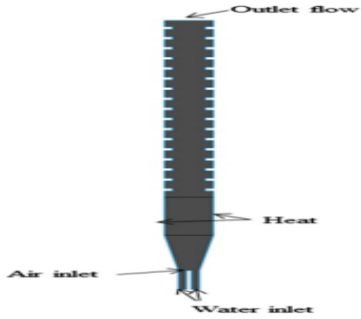
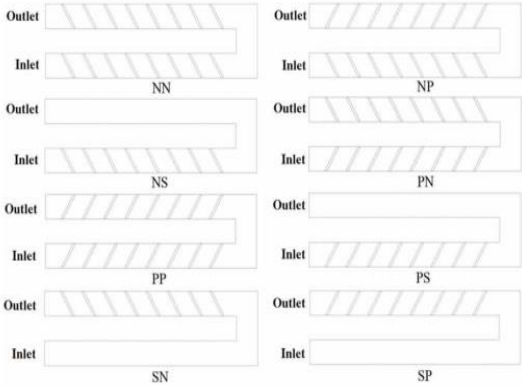
<p>Kumar and Amano [17]2012</p>	<p>Num.</p>	<p>Air Reynolds numbers 70000 to 17500</p>	<p>Compare ribs of various height to 90 degree ribbed channels and smooth channels in terms of computational analysis</p>	<p>In comparison to the 90 degree ribbed channel and smooth channel, the numerical simulation demonstrated greater heat transmission for the changing height ribs.</p>	
<p>Moon et.al [18]2014</p>	<p>Num.</p>	<p>Air Reynolds numbers 5000-50,000</p>	<p>The heat transfer and friction loss performances of rib-roughened rectangular cooling channels with a range of cross-sectional rib forms were investigated</p>	<p>The new boot-shaped rib(case-8) design demonstrated the optimum heat transfer performance and lower friction losses than the other cases.</p>	

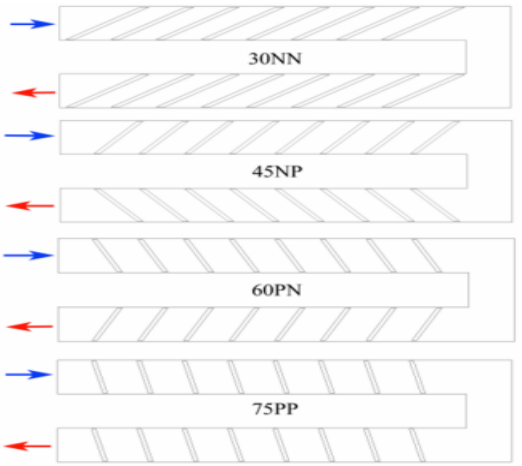
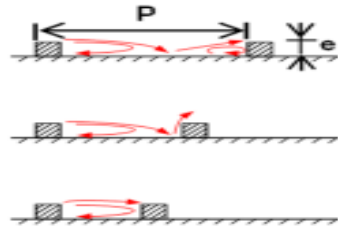
<p>Chang et.al.[19]2018</p>	<p>Exp.</p>	<p>Air, Reynolds numbers are used 5000-20,000.</p>	<p>Detached S-ribs installed near the opposite endwalls of the twin-pass parallelogram channels</p>	<p>shows higher regional heat transfer rates over the turning area and higher fanning friction factors, contributing to lower thermal output factors for the S-rib test channel</p>	
<p>Singh et.al [20] 2016</p>	<p>Exp. and Num.</p>	<p>Air, Reynolds number range from 19,500 to 69,000</p>	<p>The flow and heat transfer were studied in a two-pass channel with a square cross-section and four ribs of geometric shapes V , M and N.</p>	<p>The ribs with V shape and at an angle of 45 have the best improvement in slightly higher heat transfer and hydraulic performance compared with other ribs .</p>	

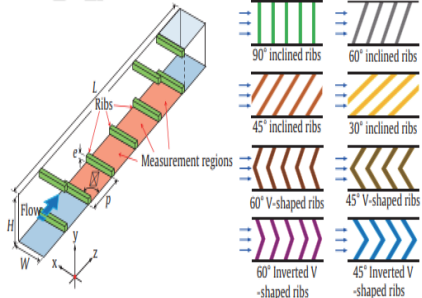
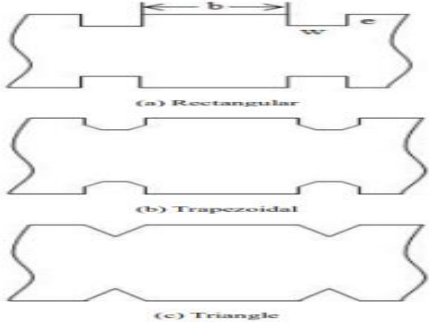
<p>Abed et.al. [21] 2020</p>	<p>Exp. And Num.</p>	<p>Air and water.</p>	<p>Investigated the forced convective two-phase flow through a rectangular ribbed channel. Three different rib-groove shapes have been studied</p>	<p>The triangle rib-groove increases the heat transfer value relative to the trapezoidal and semi trapezoidal rib-groove channel .</p>	 <p>(a) Triangle Rib - Triangle Groove (b) Trapezoidal Rib - Triangle Groove (c) Triangle Groove-Semi-Trapezoidal Rib</p>
<p>Sharma et.al. [22]2018</p>	<p>Exp.</p>	<p>Air, Reynolds numbers ranging from 9400 to 58850</p>	<p>Investigated the local heat transmission and friction factor of pentagonal ribs placed on the bottom heated wall of a rectangular channel.</p>	<p>Pentagonal ribs demonstrate a substantial improvement for the low heat transfer zones in the leeward area of the square rib.</p>	 <p>Geometrical details of pentagonal rib Rib arrangement on bottom surface</p>

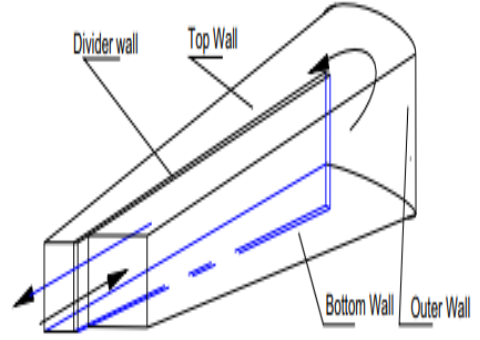
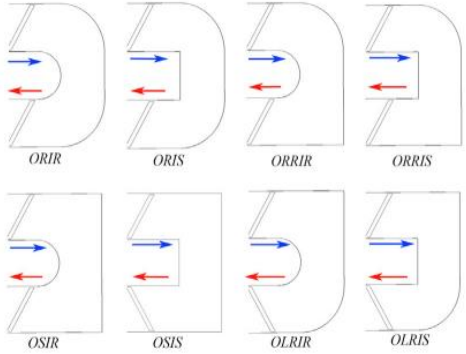
<p>Tariq et.al. [23]2018</p>	<p>Exp.</p>	<p>Air, Reynolds numbers: 26,160, 42,500, and 58,850</p>	<p>Investigated detailed aerothermal properties with in a duct with an array of solid and permeable pentagonal ribs installed on the bottom wall and a parallel and inclined slit</p>	<p>Performance indices demonstrate that pentagonal ribs with slanted slits outperform alternative designs in both directions.</p>	
<p>Ali et.al [24]2012</p>	<p>Exp.</p>	<p>Air, Reynolds numbers of 61480</p>	<p>The heat transmission and fluid flow properties of various rib turbulator shapes have been investigated</p>	<p>When compared to its solid counterpart, the slitted rib causes a shorter reattachment length and a lower pressure penalty</p>	

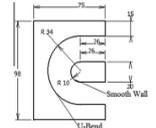
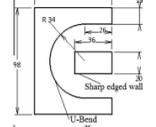
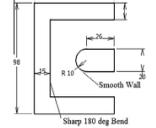
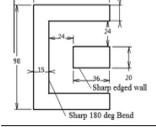
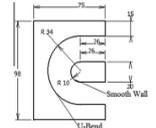
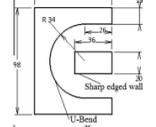
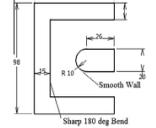
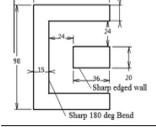
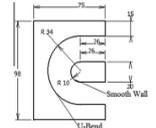
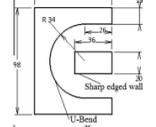
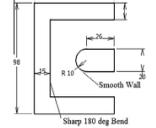
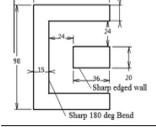
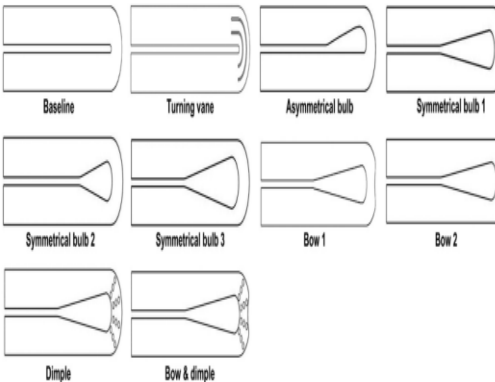
<p>Zhenga et.al. [25] 2019</p>	<p>Num.</p>	<p>Air Reynolds numbers ranging from 1000 to 2500.</p>	<p>This study was conducted to verify the improvement of the thermal performance of cooling ducts by placing slit ribs</p>	<p>The results showed that the channels in which with broken slits have a higher thermal performance in heat transfer</p>	
<p>Xu et.al. [26] 2015</p>	<p>Exp.</p>	<p>Air. Reynolds numbers ranging from 20000 to 50000</p>	<p>The effect of rib spacing on heat transmission and friction in a rotating two-pass square channel is examined experimentally</p>	<p>$p/e=10$ has the optimum surface average heat transfer improvement</p>	

<p>Oleiwi and Al-Turaihi [27] 2019</p>	<p>Exp. And Num.</p>	<p>Air and water</p>	<p>Investigated experimentally and numerically the two phase flow(air-water) in vertical duct ribbed for both sides with rectangular ribs</p>	<p>The same CFD model compared to the experimental results was used with other ribs in height to show the difference between the height of the ribs</p>	
<p>Gaoaet et.al. [28] 2018</p>	<p>Num.</p>	<p>Air. Re=30000</p>	<p>Studies the coupling of nine different rib orientation and the 180-degree bend on overall friction loss and forced convection .</p>	<p>The heat transfer coefficient is increased as the e/w ratio increased and the velocity increase of air and water.</p>	

<p>Gao et.al. [29] 2018</p>	<p>Num.</p>	<p>Air. Re=30000</p>	<p>Studied the combined effects of rib orientations (N-type and P-type) and four rib angle (30°, 45°, 60°, 75°) on flow and heat transfer in two-pass ribbed channels.</p>	<p>Compared with smooth channel, the highest heat transfer enhancement of 85.86 % is observed in 60NP case.</p>	
<p>Lei et.al. [30] 2011</p>	<p>Exp.</p>	<p>Air. Reynolds numbers ranging from 10,000 to 40,000</p>	<p>The influence of rib spacing on heat transmission in a revolving two-passage channel was investigated</p>	<p>Heat transfer enhancement rises when P/e decreases from 10 to 5 under non rotation circumstances.</p>	

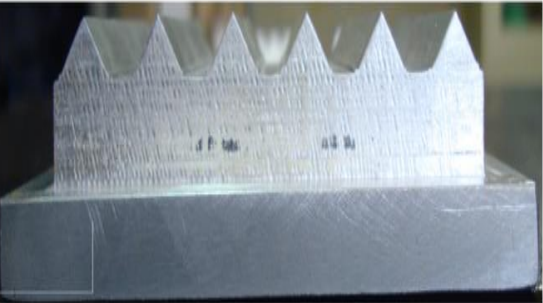
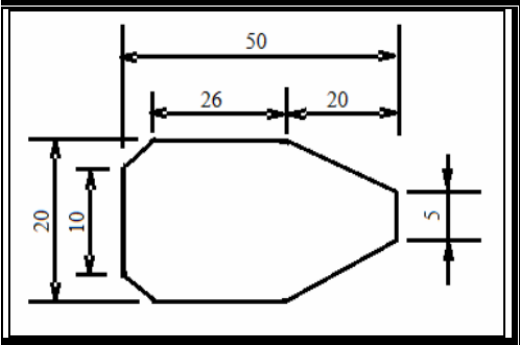
<p>Kaewchoothong et.al. [31] 2017</p>	<p>Exp.</p>	<p>Air Re=30000</p>	<p>The effect of the arrangement of the ribs on the distribution of the local heat transfer coefficient in a square-section channel was Studied</p>	<p>The ribs in the form of V-shape ribs have a higher Nu compared to the other cases.</p>	
<p>Al-Turaihi and Oleiwi. [32] 2016</p>	<p>Num.</p>	<p>Air and water Re from 16000 to 40000</p>	<p>(CFD) model was used to study the flow of water and air in a ribbed and smooth duct</p>	<p>It was found that increased as the velocity of air water increased and also found the heat transfer coefficient increased by adding ribs .</p>	

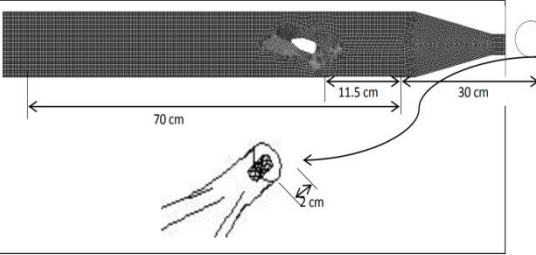
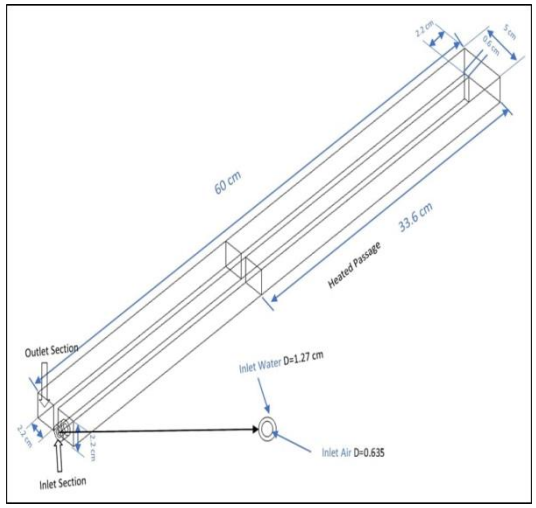
<p>Liu et. al [33]</p>	<p>Exp.</p>	<p>Air Reynolds numbers =10000 to 60000</p>	<p>Heat transfer properties in a two-pass channel with integrated film cooling holes and ribs with a variable cross-section</p>	<p>The higher the hole-opening ratio and the different hole locations produce different heat transfer effect.</p>	
<p>Gaoa et.al. [34] 2019</p>	<p>Num.</p>	<p>Reynolds number of 30,000</p>	<p>The combined influence of rib orientation and bend form on heat transmission and friction loss in U-shaped channels</p>	<p>The rotation direction and transverse location of secondary flow in straight passageways are determined by the rib orientation</p>	

<p>Erelli et.al [35] 2015</p>	<p>Exp. and Num.</p>	<p>Air. Reynolds numbers 25,000, 35,000, and 45,000.</p>	<p>In this study was used four different turn configurations (cases-1, 2, 3, and 4) having various divider and outer turn geometries</p>	<p>Case-3 (sharp 180bend with circular divider average)has thermal efficiency is higher than that of the other three instances.</p>	<table border="1"> <thead> <tr> <th>Turn configuration</th> <th>Experimental/numerical study</th> <th>Surface condition</th> </tr> </thead> <tbody> <tr> <td></td> <td>Re = 25,000, 35,000, 45,000</td> <td>Smooth walls with one wall heated</td> </tr> <tr> <td></td> <td>Re = 25,000, 35,000, 45,000</td> <td>Smooth walls with one wall heated</td> </tr> <tr> <td></td> <td>Re = 25,000, 35,000, 45,000</td> <td>Smooth walls with one wall heated</td> </tr> <tr> <td></td> <td>Re = 25,000, 35,000, 45,000</td> <td>Smooth walls with one wall heated</td> </tr> </tbody> </table>	Turn configuration	Experimental/numerical study	Surface condition		Re = 25,000, 35,000, 45,000	Smooth walls with one wall heated		Re = 25,000, 35,000, 45,000	Smooth walls with one wall heated		Re = 25,000, 35,000, 45,000	Smooth walls with one wall heated		Re = 25,000, 35,000, 45,000	Smooth walls with one wall heated
Turn configuration	Experimental/numerical study	Surface condition																		
	Re = 25,000, 35,000, 45,000	Smooth walls with one wall heated																		
	Re = 25,000, 35,000, 45,000	Smooth walls with one wall heated																		
	Re = 25,000, 35,000, 45,000	Smooth walls with one wall heated																		
	Re = 25,000, 35,000, 45,000	Smooth walls with one wall heated																		
<p>Saha and Acharya [36]</p>	<p>Num.</p>	<p>Air. Reynolds numbers</p>	<p>Comparison of turbulent flow inside a two-pass internal cooling channel with varied bend geometry</p>	<p>The symmetrical bulb with a bow along the outer walls and surface dimples has the highest thermal performance factor.</p>																

<p>Liue et.al. [37] 2020</p>	<p>Exp.</p>	<p>Air Reynolds numbers 8888, 13 333, or 17 777.</p>	<p>The characteristics of the flow field in a U- shaped channel of square cross-section and different curvature shapes were studied</p>	<p>High percentage of turbulent kinetic energy in the bending region, which is shaped like a circular inside and outside (circle - circle)</p>	
<p>Wang et.al [38] 2017</p>	<p>Num.</p>	<p>Air Reynolds number varies from 10000 to 40000</p>	<p>The influence of ribs on heat transfer performance and cooling air flow characteristics in different aspect ratios (AR) U-shaped channels .</p>	<p>The channel (AR = 2:1) has a higher augmentation factor than the small channel (AR = 1:2), and the weight of the ribs heat transfer rises as the inlet Reynolds number increases.</p>	

<p>Hayashi et.al. [39] 2020</p>	<p>Exp.</p>	<p>Air and water</p>	<p>Studied the pressure drops in horizontally oriented U-bends was measured for air-water bubbly, plug, slug and annular flows to test the applicability of the available relations to the</p>	<p>The bend pressure drop was measured as the amount of the pressure drop induced in the bend and the additional pressure drop caused in the re-developing area in the downstream-side straight pipe</p>	
<p>Dhanasekaran and Wang [40]2013</p>	<p>Num.</p>	<p>Mist/air Reynolds number varies from 5,000 to 40,000</p>	<p>A CFD model was developed to predict mist/air cooling enhancement in a rotating ribbed rectangular channel.</p>	<p>with 2% mist injection, the mist cooling enhancement is about 30% at the trailing surface and about 20% at the leading surface of the first passage</p>	

<p>Al-Turaihi and kareem [41] 2016</p>	<p>Exp. and Num.</p>	<p>Air and water</p>	<p>Analyze characteristics of the mixture (water, air) in a rectangular Placed vertically by using internal rib with different volume flow rates of water and air ,and constant heat power</p>	<p>The discharge of air and water increases, the exit temperature decreases and the coefficient of local heat transfer increases due to the existence of a rib that raises the area of heat transfer</p>	
<p>Al-Turaihi [42] 2013</p>	<p>Exp.</p>	<p>water and air</p>	<p>Effects of air and water discharge for straight hydrofoil attacks at various angles and designed an experimental rig to study the two-phase flow</p>	<p>The pressure differential increased at the inlet and outlet of the rectangular channels as the angle of attack increased at constant air and water discharge amounts</p>	

<p>Habeeb and Al-Turaihi [43] 2013</p>	<p>Exp. and Num.</p>	<p>Water and air</p>	<p>Study the two-phase flow phenomena around straight hydrofoil at different angles of attack in a rectangular enlarging channel extended from a two-phase circular assembly tube</p>	<p>pressure difference increases at the inlet and outlet of the rectangular channel when the angle of attack increases with constant air and water discharge.</p>	
<p>The present work</p>	<p>Num.</p>	<p>Air and Water</p>	<p>The study was conducted theoretically to test the effect of the shape of the channels, the effect of entry velocity and the geometrical shape of ribs at a constant heat flow on the temperature distribution inside the test channel, as well as the heat transfer coefficient.</p>	<p>The results showed that the local heat transfer coefficient improved inside the test channel equipped with an rib when compared with the smooth channel, it improved by (12%, 6%) with a trapezoid -shaped rib when compared with the other ribs, and it improved by (20%) with a slit rib when compared with the solid rib</p>	

Chapter Three

Mathematical Model and Numerical Simulation

Mathematical Model and Numerical Simulation

3.1 Introduction

The numerical component of this study, which comprises of the simulation program's mathematical governing equations, is described in this chapter (CFD FLUENT software). The distinct water-air flow (two-phase flow) regulating parameters will next be addressed. In two circumstances, these parameters travel through a straight and tapered rectangular two pass channel: when it is smooth and when it is turbulated .Computational fluid dynamics (CFD) is a branch of fluid dynamics that explores a problem by numerically solving the governing equations and providing practical methods for replicating real flow. ANSYS- Fluent 20.0R1 is used to analyze the three-dimensional turbulent two-phase of flow(Water-Air) and heat transfer characteristics through smooth and turbulated channel . Heat transfer coefficient and the temperature distribution were investigated in both cases of the channel (smooth, turbulated) with changing the three shape of ribs and three shape of slit and with the changing the superficial velocities of water and air .

3.2 Design Consideration

The Solid Works 2018 software is used to numerically model the geometry of the duct using three-dimensional models combined with Ansys Workbench 20.0 R1. The geometrical model is contracted from Ekkad [6] experiment model in 2000 to make it more equivalent to the size of real turbine blades. As indicated in Fig (3.1), the width of the divider wall is shortened to reduce the high temperature area that could not be cooled by working fluid due to a lack of a cooling path.

The cross section of the channel are 60 cm long from entrance to turn .For the straight channel, the inlet and exit cross-section areas are $5 \times 2.2 \text{ cm}^2$, the cross section area at the turn is the same as that at inlet and outlet .For the tapered channels, the cross-section area at the turn are $3.75 \times 2.2 \text{ cm}^2$ and $2.5 \times 2.2 \text{ cm}^2$ as shown in figure (3.2).This produces a decrease of four times in the cross-section area from inlet to turn in the first pass and an increase of four times in cross section area from turn to exit in the second pass. Both channels have the same entrance .The divider wall thickness is 0.6 cm thick , the inlet of water and air from the bottom edge of the channel In turbulent flow at the range of Reynolds range 7000 to 12000. as shown in fig(3.2), the entrance length is substantially shorter, as predicted, and its dependency on the Reynolds number is smaller. Many practical tube flows have entrance effects that become minor beyond a tube length of 10 diameters, and the hydrodynamic and thermal entry lengths are approximated to be $L_{h \text{ turbulent}} \approx L_{t \text{ turbulent}} \approx 10Dh$, and the flow may be considered to be completely developed for $X > 10Dh$ [50] ,in this work will take the entrance region as $X=12Dh$, $X=26.4 \text{ cm}$ is entrance region (unheated passage) and the heated passage is 33.6 cm as shown in figures (3.1) .

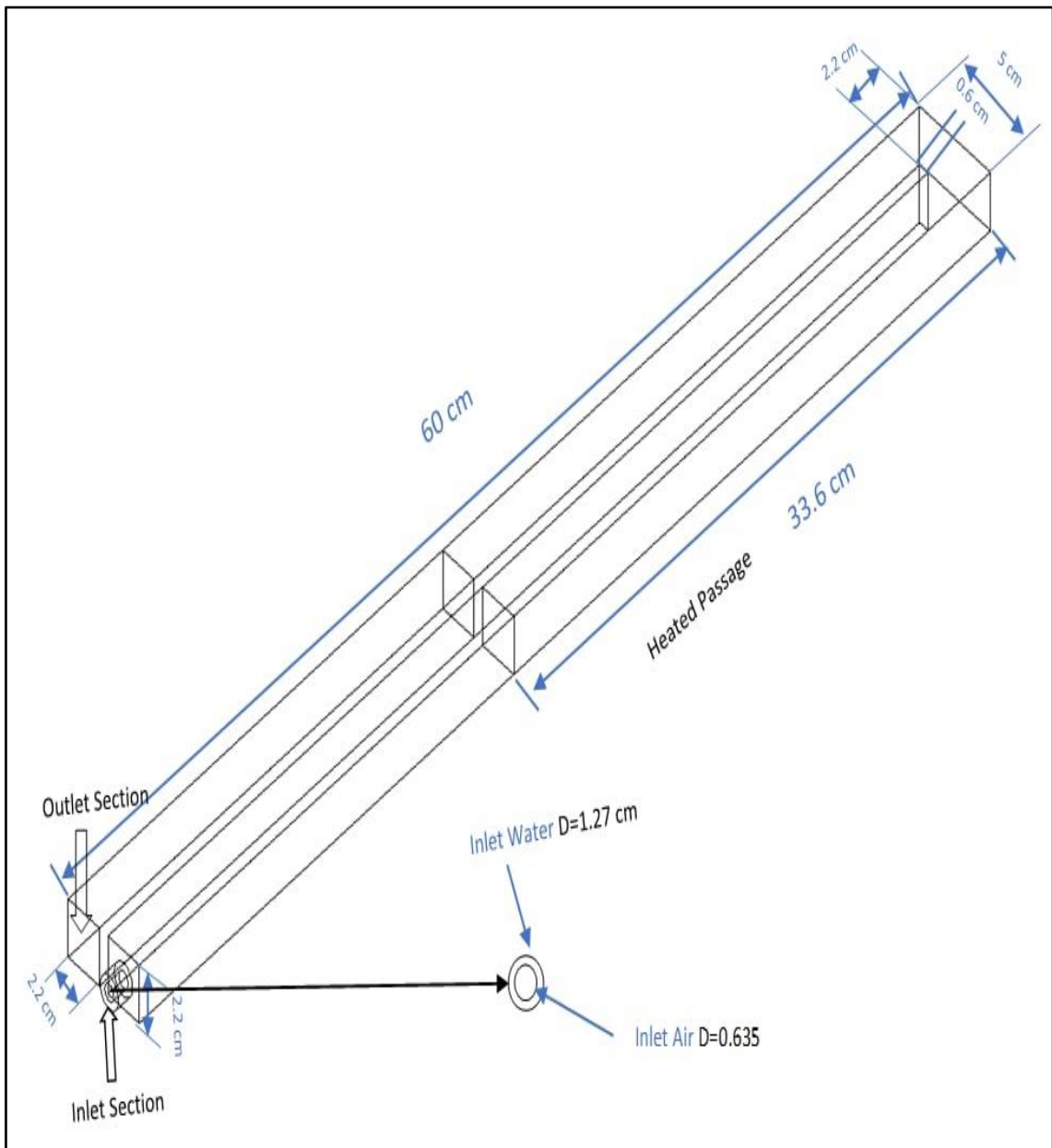
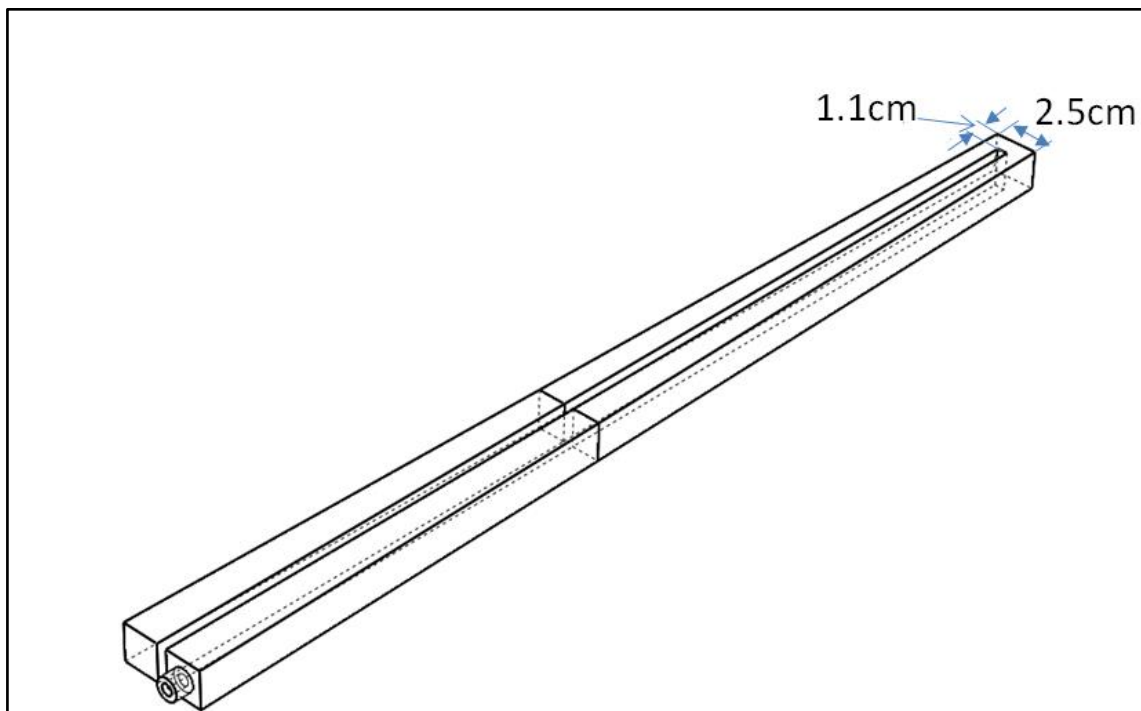
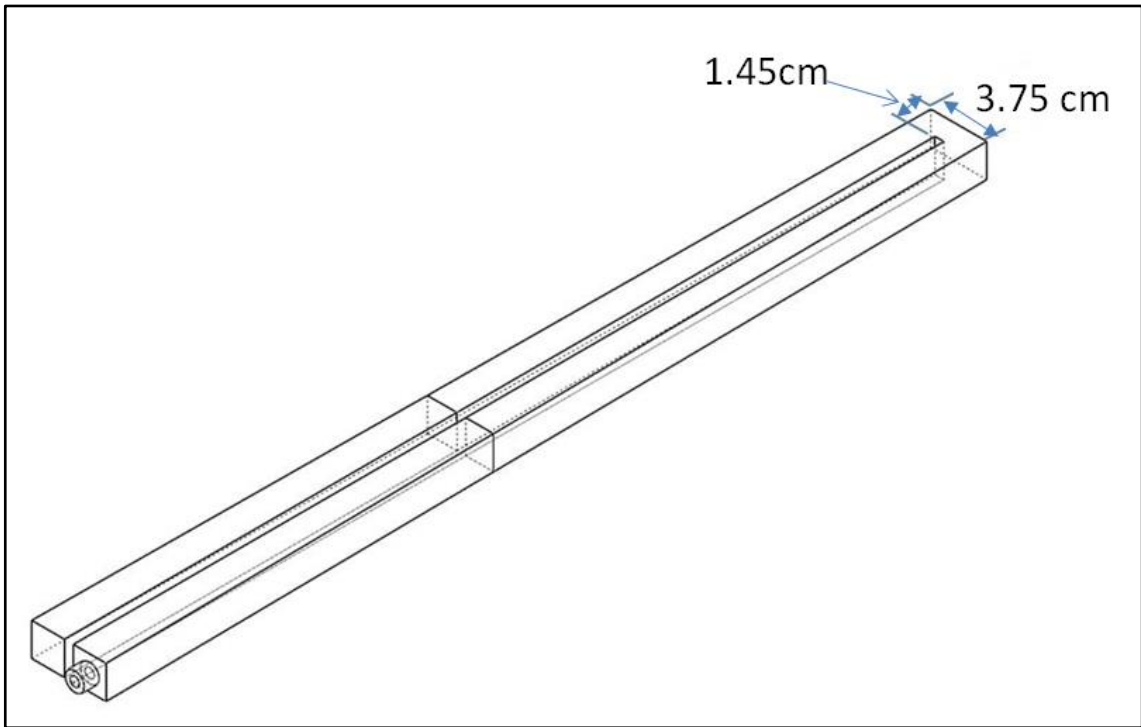


Fig (3.1) A-Smooth Straight channel



Fig(3.2) A.Tapered channel 1 , B. Tapered channel 2

3.3 Geometry of Ribs

The rib pitch is 10 rib heights ($p/e = 10$), Surface average heat transfer improvement is optimal when $p/e = 10$ [26]. The actual physical pitch distance between ribs decreases as the hydraulic diameter decreases. This causes the local rib height (e) and rib pitch (p) to decrease along the tapered channel, $b = e$ and $e = 0.1D_h$ as shown in figure (3.3), tapered channel 2 with ribs as shown in figure (3.4).

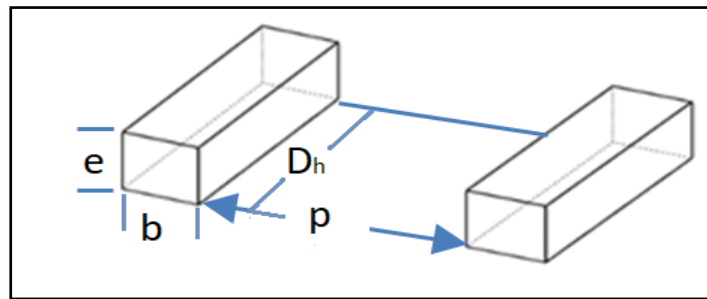
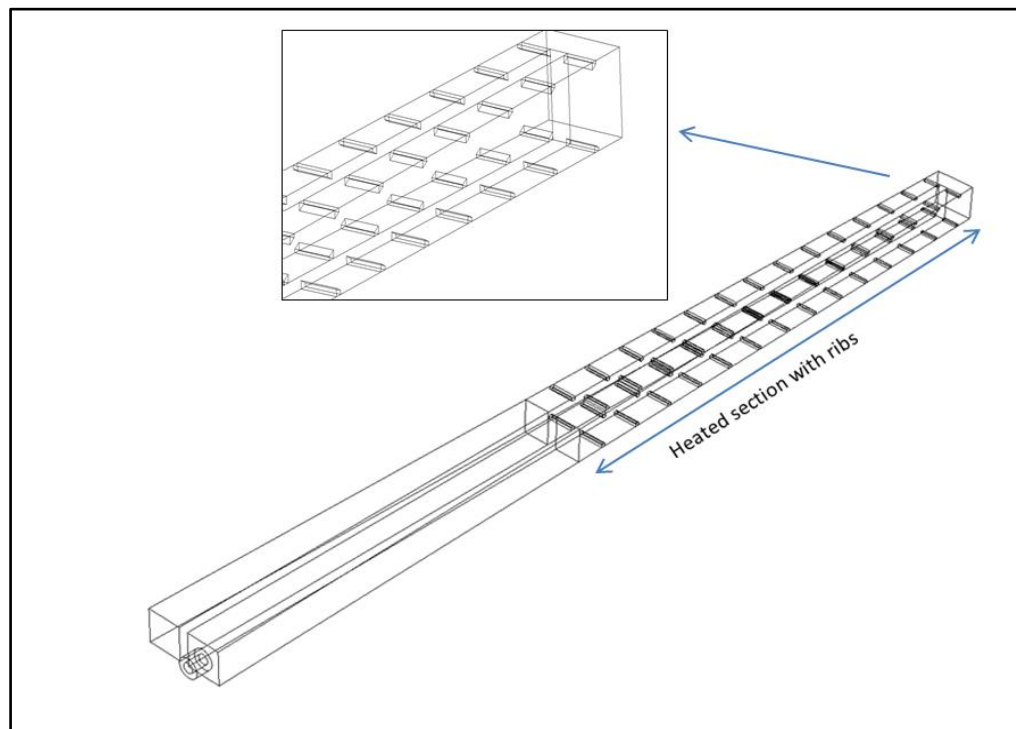


Fig (3.3) Pitch of rib

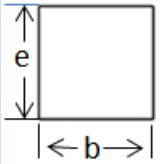
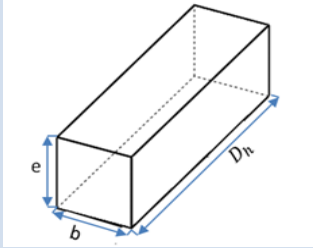
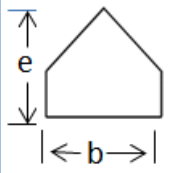
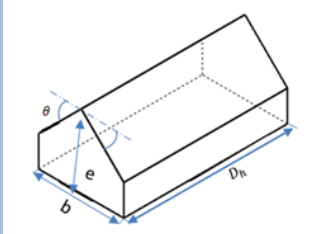
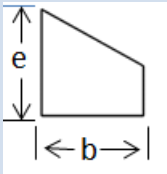
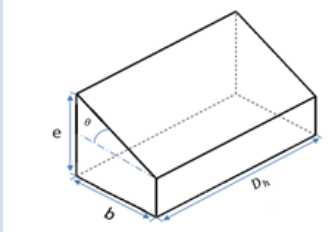


Fig(3.4) Ribbed channel

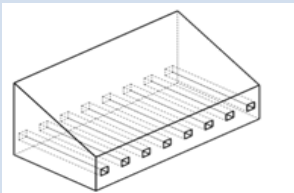
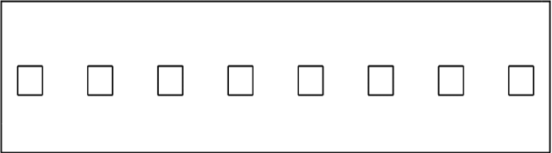
3.3.1 Types of ribs

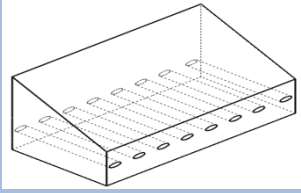
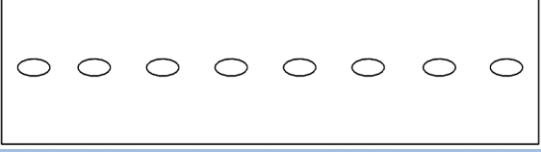
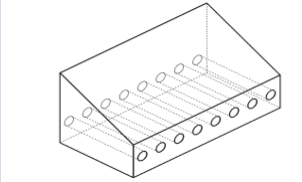
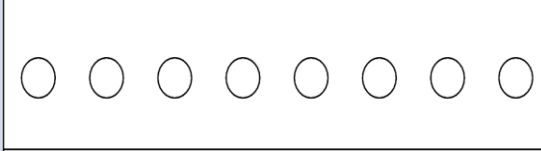
In this section the shape of the solid and slit rib that used in this study

1- Solid ribs

<p>Square rib</p>		
<p>House rib</p>		
<p>Trapezoidal rib</p>		

2- Slit ribs

<p>Square slit rib</p>		
-------------------------------	---	--

<p>Ellipse slit rib</p>		
<p>Circle slit rib</p>		

3. 4 Mesh Generation

There are many types of mesh, such as coarse , medium , and fine mesh. Choosing the type of mesh depended on several factors, such as, the system geometry, the type of flow, and complexity .

In this work, the geometry of the rectangular channel was divided into small square element (Quadrilateral structured grid) using the Meshing combined with Ansys Workbench 20.R1 with maximum and minimum size equal to (0.002 m) through fine relevance center and medium smoothing mesh near the wall of channel and straight to give Y^+ less than 5 to solve the laminar sub layers. The model governing equations would be solved at each element of the model geometry. [46].

As shown in figure (3.5). Also, table (3.1) displays the number of elements and nodes for each case in this study.

Table 3.1: The number of elements and nodes used in this study

Case	Nodes No	Elements No
Smooth straight Channel	708694	1773564
Smooth tapered Channel 1	665044	1649703
Smooth tapered Channel 2	656234	1607892
Tapered channel with Square ribs	636052	1589183
Tapered channel with house ribs	647241	1616470
Tapered channel with trapezoidal ribs	660487	1658238
Tapered channel with square slit trapezoidal ribs	1898044	5462367
Tapered channel with ellipse slit trapezoidal ribs	1910075	5665233
Tapered channel with circle slit trapezoidal ribs	2014407	5982251

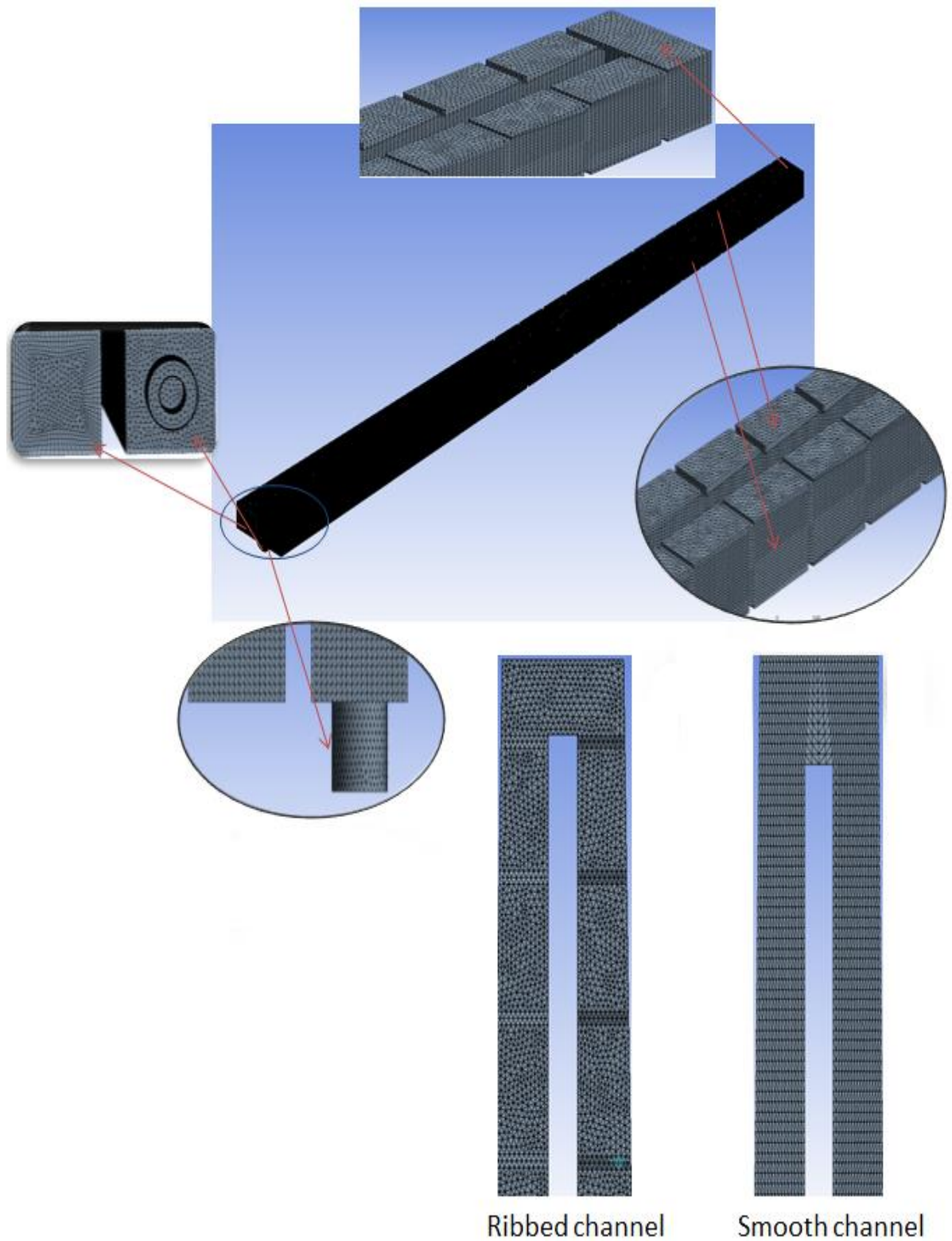


Fig (3.5) Details of the grid.

3.5 Grid independence test

To perform the grid independences by observing the convergent history of the predicted heat transfer coefficient of two-phase flow with a given superficial at a various levels of grid refinement as shown in Fig. (3.6).

It can be shown that the difference in heat transfer coefficient was less than 0.14% as the nodes more than 600000 were employed for smooth and ribbed channel.

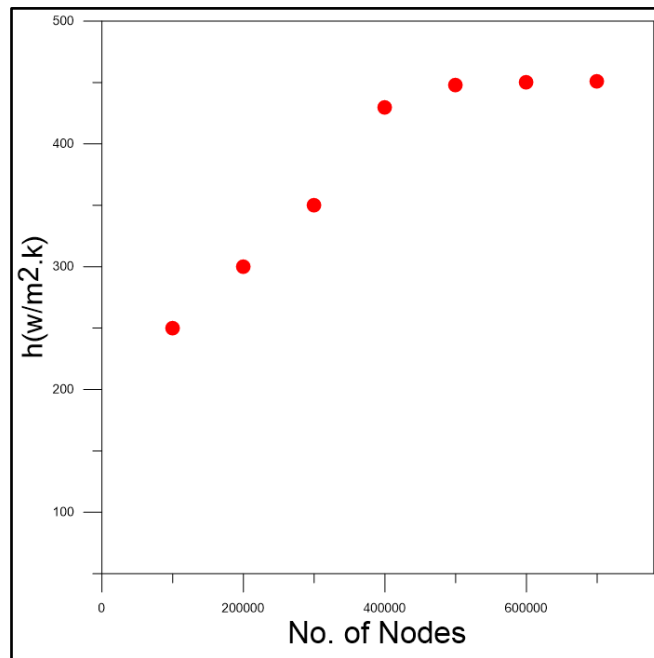


Figure (3.6): Accuracy of Prediction heat transfer coefficient with Number of Nodes for Smooth and Ribbed Channel.

3.6 Problem Assumptions

The following assumptions are used in order to simulate the model:

1. Steady state
2. The flow is assumed to be as a turbulent flow.

3. The pressure is based on the solver
3. The Zone has three dimensions
4. The flow is incompressible
5. Two-phase flow
6. Heat flux is constant

3.7 Governing Equations

The basic control equations for fluid dynamics in theoretical work are the equations of continuity, momentum and energy. A mixture model is used where the phases are stirred at different surface velocities. The governing equations can be written as:[48]:

1. Continuity Equation

The continuity equation was is to calculate the phase volume fraction. The volume fractions of the primary (water) and secondary (air) phase of the control volume can thus be equal to any value between 0 and 1 depending on the area occupied by the primary and secondary phase. [46]

$$\frac{\partial}{\partial t} (\rho_m) + \nabla \cdot (\rho_m \vec{V}_m) = 0 \quad \dots\dots(3.1)$$

The mass-averaged velocity \vec{V}_m is represented as:

$$\vec{V}_m = \frac{\sum_{k=1}^n \alpha_k \rho_k \vec{V}_k}{\rho_m} \quad \dots\dots(3.2)$$

And ρ_m is the density of mixture :

$$\rho_m = \sum_{k=1}^n \alpha_k \rho_k \quad \dots\dots(3.3)$$

α_k is the volume fraction of phase k

2. Momentum Equations

The common form of this equation is given by[46]:

$$\frac{\partial}{\partial t}(\rho_m \vec{v}_m) + \nabla \cdot (\rho_m \vec{v}_m \vec{v}_m) = -\nabla P + \nabla \cdot [\mu_m (\nabla \vec{v}_m + \nabla \vec{v}_m^T)] + \rho_m \vec{g} + \vec{F} + \nabla \cdot \left(\sum_{k=1}^n \alpha_k \rho_k \vec{v}_{dr,k} \vec{v}_{dr,k} \right) \dots\dots\dots (3-4)$$

Where n is the number of phases , \vec{F} is a body force, and μ_m is the viscosity of the mixture, which is given by:

$$\mu_m = \sum_{k=1}^n \alpha_k \mu_k \dots\dots\dots(3.5)$$

Where $\vec{v}_{dr,k}$ is the drift velocity for the secondary phase

$$\vec{v}_{dr,k} = \vec{v}_k - \vec{v}_m \dots\dots(3.6)$$

3. Energy Equations

The general form of this equation is given by[48]:

$$\frac{\partial}{\partial t} \sum_{k=1}^n (\alpha_k \rho_k E_k) + \nabla \cdot \sum_{k=1}^n (\alpha_k \vec{v}_k (\rho_k E_k + P)) = \nabla \cdot (k_{eff} \nabla T) + S_E \dots\dots\dots (3-7)$$

Where k_{eff} is the effective conductivity , $(\sum \alpha_k (k_k + k_t))$ and k_t is the turbulent thermal conductivity. The first term on the right-hand side of eq. (3.7) represents energy transfer due to conduction. The symbol S_E includes any other volumetric heat sources.

3.8 Turbulence Model

The k - ε model is one of the most common turbulence models. Ansys Fluent 20.0R1 displays three methods for k- ε turbulence model in the two-phase flow which are:

1. Turbulence mixture model
2. Turbulence dispersed model
3. Turbulence model for each phase

Relying on the deviation between experimental and numerical results, the selecting of the turbulence k - ε standard mixture model has set for the two phase model which can be realized through these equations[47] .

$$\frac{\partial}{\partial t}(\rho_m k) + \nabla \cdot (\rho_m \vec{v}_m k) = \nabla \cdot \left(\frac{\mu_{t,m}}{\sigma_k} \nabla k \right) + G_{k,m} - \rho_m \varepsilon \quad \dots\dots\dots (3-8)$$

Where ε is the turbulent dissipation rate, G^k is the generation of turbulence kinetic energy, and σ_k is the turbulent Prandtl number for k and ε .

The density and the velocity of the mixture ρ_m and \vec{v}_m , are computed as following:

$$\rho_m = \sum_{i=1}^n \alpha_i \rho_i \quad \dots\dots\dots (3-9)$$

$$\vec{v}_m = \frac{\sum_{i=1}^n \alpha_i \rho_i \vec{v}_i}{\sum_{i=1}^n \alpha_i \rho_i} \quad \dots\dots\dots (3-10)$$

The turbulent viscosity, $\mu_{t,m}$, and the production of turbulence kinetic energy, $G_{\kappa,m}$, are computed as following[47]:

$$\mu_{t,m} = \rho_m C_{\mu} \frac{k^2}{\varepsilon} \quad \dots (3.11)$$

$$G_{\kappa,m} = \mu_{t,m} \left(\nabla \vec{v}_m + (\nabla \vec{v}_m)^T \right) : \nabla \vec{v}_m \quad \dots (3.12)$$

The model constants can be seen in Table (3.2).

Table 3.2: Model Constants of Ansys Simulation

The constant	Value
σ_k	1
σ_{ε}	1.3
$C_{1\varepsilon}$	1.44
$C_{2\varepsilon}$	1.92
C_{μ}	0.09

3.9 Boundary Condition

The fluids used in this study include water, which is intended as the major phase, and air, which is designed as the secondary phase , the values

of the working conditions as shown in (table 3-3) and the model Relaxation factors that used for the numerical simulations in the fluent model as shown in the table (3.4)

Table 3.3 : The values of the working conditions

Wall heat flux (w/m ²)	Water discharge (l/min)	Air discharge (l/min)
10000	3	8
--	6	16.67
--	9	25

Table 3-4 : Model Relaxation factors that used for the numerical simulations in the fluent model

Variable	Relaxation factors
	Two phases (Water-Air)
Pressure	0.1
Momentum	0.1
Volume fraction	0.3
Energy	0.8

3.10. Convergent Criteria

There are errors in every numerical basic solution. The objective is to understand how large the inaccuracies are and whether or not the numerical

findings are acceptable in engineering applications. When the residual curve reached 10^{-4} in the current numerical convergence, it is recognized as complete. Residual error is seen in Table (3.5).

Table (3.5): Residual Error for the Tested Case.

Equations	Continuity	X-Velocity	Y- Velocity	Z- Velocity	Energy	K	E	Volume Fraction
Residual Error	10^{-4}	10^{-4}	10^{-4}	10^{-4}	10^{-6}	10^{-4}	10^{-4}	10^{-4}

3.11 Fluids and Material Properties

The properties of the material that are used in the model at temperature 300 k are shown in Table (3.6).

Table 3.6: Properties of Fluids and Materiel from Ansys Fluent Simulation

Property	Water – Liquid (Ansys Fluent 20.0 R1.Database)	Stainless steel – Solid (Ansys Fluent 20.0 R1.Database)	Air – Gas (Ansys Fluent 20.0R1.Database)

Density (kg/m³)	998.2	2719	1.225
Thermal conductivity (W/m.K)	0.6	202.4	0.0242
Viscosity (kg/m.s)	0.001003	-	1.7894e-05

Chapter four

Results and Discussion

Results and Discussion

4.1. Introduction

This chapter describes the results of the numerical works for the two-phase flow with heat transfer in a straight and tapered two pass channels fitted with several shapes of solid and slit ribs. The numerical data of smooth and ribbed channel are compared in order to show the effect of adding ribs and slit ribs on the rate of heat transfer, temperature distribution, velocity vector and pressure drop.

4.2. Program Validation

In order to demonstrate the validity of the turbulence model and numerical procedure of pervious work for (Hayashi et.al. 2020) [39], an Ansys Fluent software (Version20.) is used to calculate numerically the Pressure distribution along the pipe axis of horizontal U bend pipe, where z is the axial coordinate and $P(0)$ is the pressure at 320 mm upstream from the bend entrance ($D = 8$ mm, $D*B = 6$, as shown in figure (4.1), annular flow at for two phase flow (water-air) $= (10.4$ m/s, 0.13 m/s) respectively. Then, the numerical pressure distribution is compared with the experimental pressure distribution along the pipe axis. The parameters used for the numerical simulations in fluent model are shown in Table (4-1).

The numerical results obtained by using Ansys Workbench 20.R1 are compared with experimental results as shown in Figure (4.2) with maximum deviation of (15 %).

Table (4-1): Relaxation Factor

Variable	Relaxation factors
Pressure	0.1
Momentum	0.1
Turbulent kinetic energy	0.8
Energy	1.0

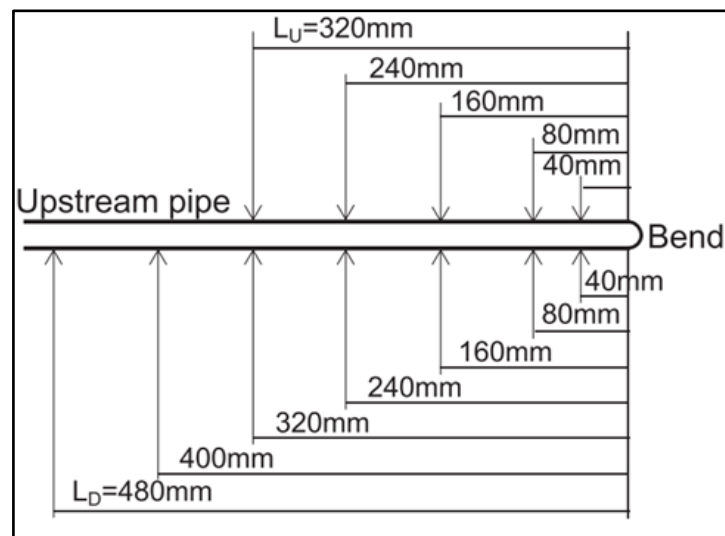
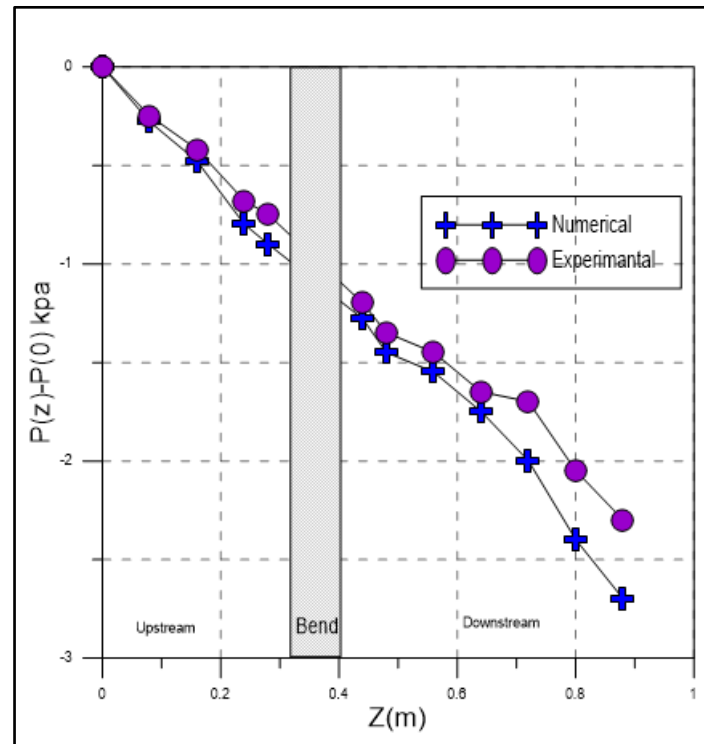


Fig (4.1) :Pressure tap location. The values represent the distance from the bend inlet (or outlet) to a tap location in the upstream pipe (or the downstream pipe).[39]



Fig(4.2) .Pressure distribution along the pipe axis, where z is the axial coordinate and $P(0)$ is the pressure at 320 mm upstream from the bend entrance ($D = 8$ mm, $D*B = 6$, annular flow at (water , air) =(10.4 m/s, 0.13 m/s)).[39].

4.3 The Result of Work

The effect of channels shape (straight and tapered) on pressure drop and the effect of rib shape (solid and slit rib) on temperature distribution , heat transfer coefficient distribution , the velocity vector and pressure distribution in two pass channel are studied ,and the effect of increasing the water superficial velocity from 0.3846 m/s to 1.154 m/s and the air superficial velocity from 4.624 m/s to 13.89 m/s on the temperature distribution , heat transfer coefficient distribution , the velocity vector and pressure distribution in two pass channel numerically are also investigated .

4.3.1 Effect of Channel Shape

Figure (4.3) shows the pressure distributions along the three channels (straight ,tapered 1 and tapered 2). where z is the axial coordinate and $P(0)$ is the pressure at 320 mm upstream from the bend entrance for two phase flow (water-air=(0.3846 m/s, 4.624 m/s)) In the upstream of the bend, the pressure linearly decreases toward the bend as shown in the regression line. The bend effect on the pressure drop in the upstream pipe is therefore small. The pressure gradient after passing through the bend approaches that in the upstream duct (solid line), which means that the flow disturbed in the bend is redeveloped in the downstream channel as shown in the results the pressure drop in the channel that has small area of bend geometry (tapered 2) that has more pressure drop than the straight channel this is result in increase heat transfer coefficient . According to the result the tapered 2 has a high heat transfer coefficient because has more pressure drop compared with the straight and tapered 1 channels as shown in figure (4.3) .

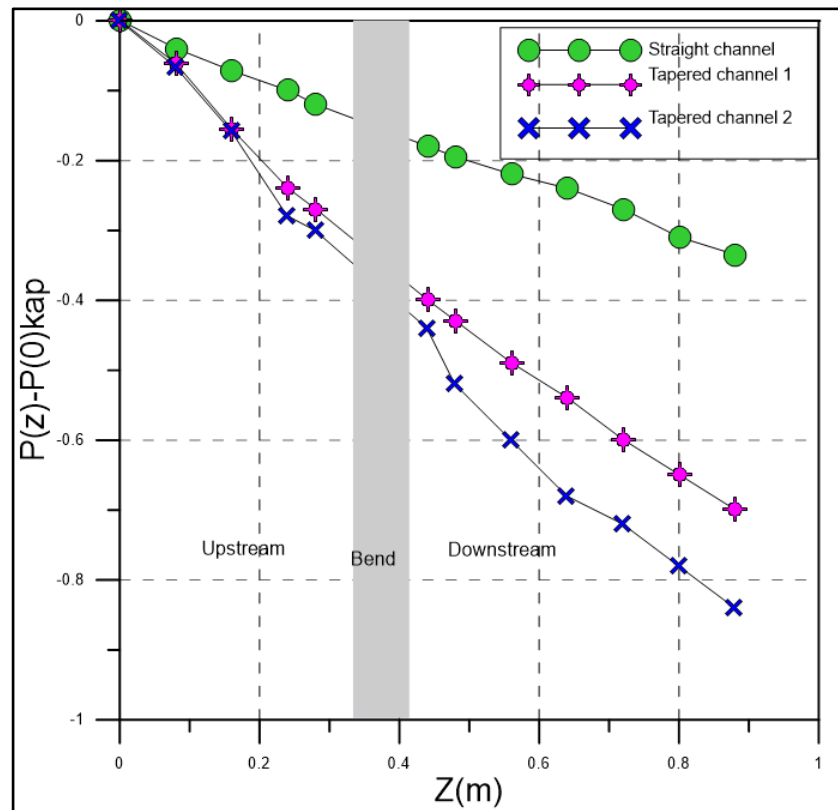


Fig.(4.3) . Pressure distribution along the three channels , where z is the axial coordinate and $P(0)$ is the pressure at 320 mm upstream from the bend entrance

4.3.2 Effect of Rib Shape on Two-Pass Tapered 2 Channel

4.3.2.1 Temperature distribution

Figure (4.4) shows the contour of temperature distribution of three shape of ribs (square , house and trapezoidal rib)

In the first pass, after certain distance the thermal field becomes fully developed. Similarly, the thermal field in the second pass after the bend is found to be developing without showing any symmetry as seen in the first pass. The secondary flow in the turn region is responsible for the asymmetry of then temperature field in the second pass. The temperature field in the turn region shows significant spatial variation in all three cases .It is expected that stronger secondary flow results in the lower wall

temperature because secondary flow becomes effective in cross-transporting the hot fluid away from the wall region causing higher heat transfer. Comparison of the three cases show that all cases has decreased in wall temperature but the case C (trapezoidal rib) has more decreased in wall temperature this is because the structure of trapezoidal rib cause more turbulence and boundary layer separation , the turbulence caused more dissipation in temperature with high heat transfer .

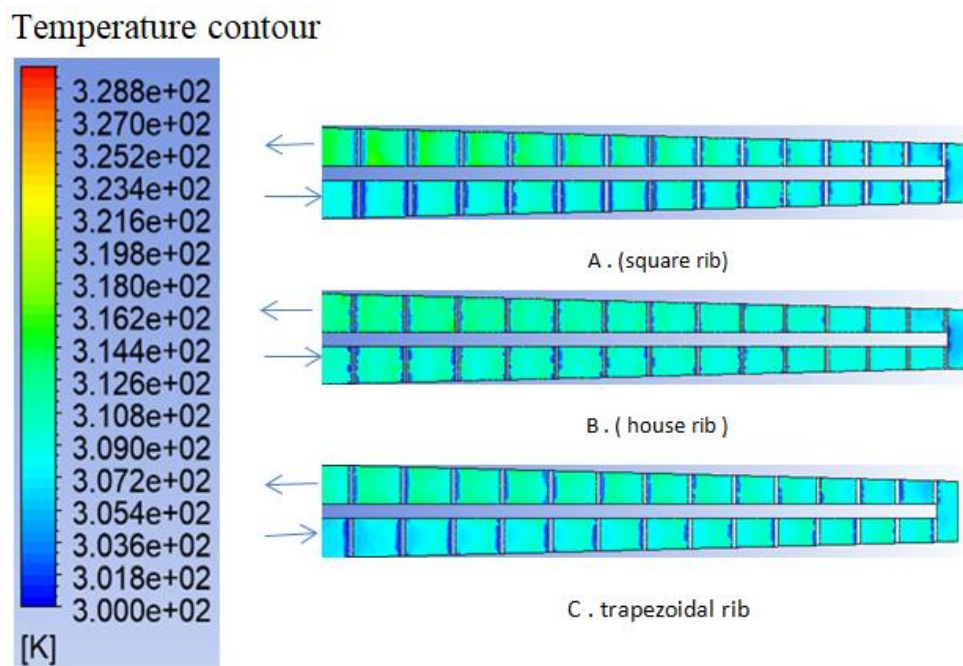


Fig (4.4). contour of temperature distribution of three shape of ribs (square, house rib and trapezoidal)

4.3.2.2 Pressure distribution

Figure (4.5) show the contour of pressure distribution of three shape of ribs (square, trapezoidal and house rib) in tapered two pass channel at two phase flow of water and air superficial velocity (0.3846 ,4.624)m/s respectively. In the first pass of the channel , the pressure linearly decreases toward the bend as shown in the contour . The bend effect on the pressure drop in the upstream duct is therefore small .The presence of the bend

causes a large pressure drop in the bend .The pressure gradient after passing through the bend approaches that in the upstream duct , which means that the flow disturbed in the bend is redeveloping in the downstream. The result clearly showed that because of its larger impinging effect, the trapezoidal-shaped rib (case C) has a higher pressure drop at the following rib. The pressure differential in the inter-rib area changes the position of the detachment.

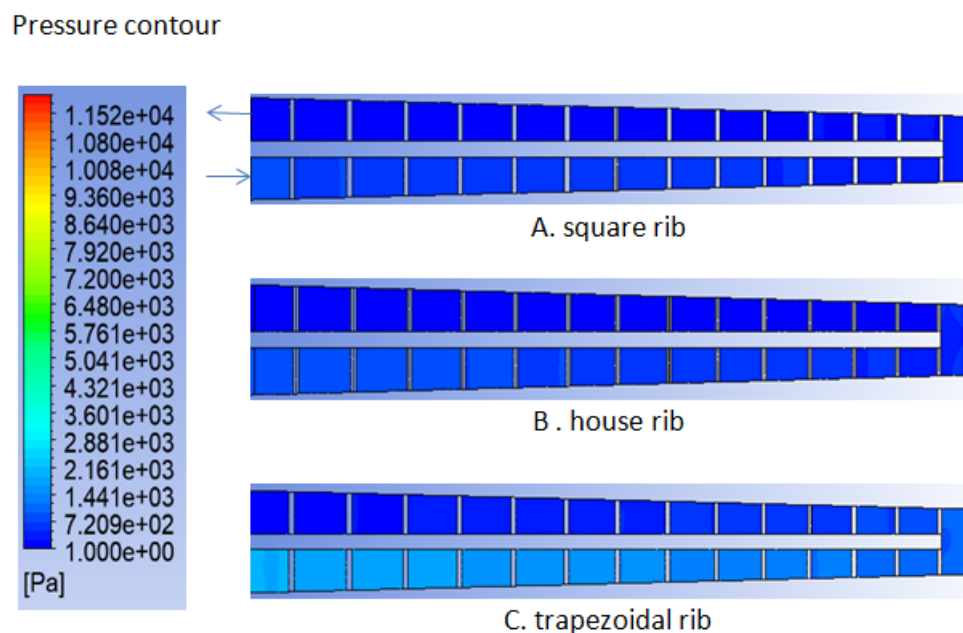


Fig (4.5) pressure distribution with three shapes of ribs

4.3.2.3 Heat Transfer Coefficient

To explore the local heat transfer on the surface of the inner wall and the surface of the ribs The heat transfer coefficient increases with the ribbed channel(square , house and trapezoidal ribs) than the smooth channel about 10 % , 16% , 21 % respectively . When compared the three shapes of ribs, the trapezoidal rib has more heat transfer enhancement than the square and house rib about 12% , 6% respectively ,this is because the structure of trapezoidal ribs cause more turbulence in ribbed ducts, and to explain the difference in heat transfer coefficient between smooth and

ribbed ducts for the value of water and air superficial velocity (0.3846 ,4.624)m/s respectively of smooth channel and channel with three shape of ribs (square, trapezoidal and house rib) at the top and bottom of the channel .The result show that the heat transfer coefficient in the bending region U is the highest, followed by the second pass, and the lowest in the first pass in a smooth channel. This indicates that the secondary flow generated by bending has a strong influence in this channel. and boundary layer separation as shown in figure (4.6) .

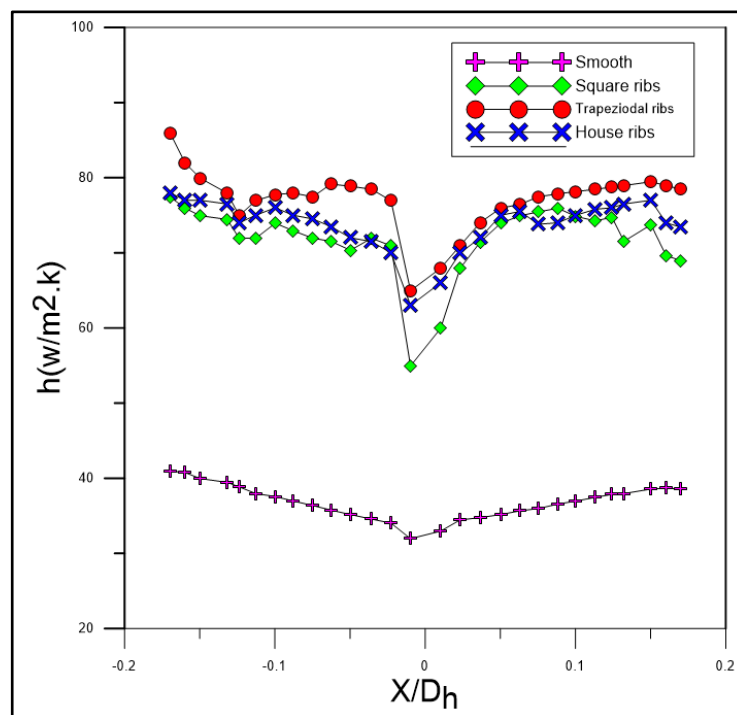
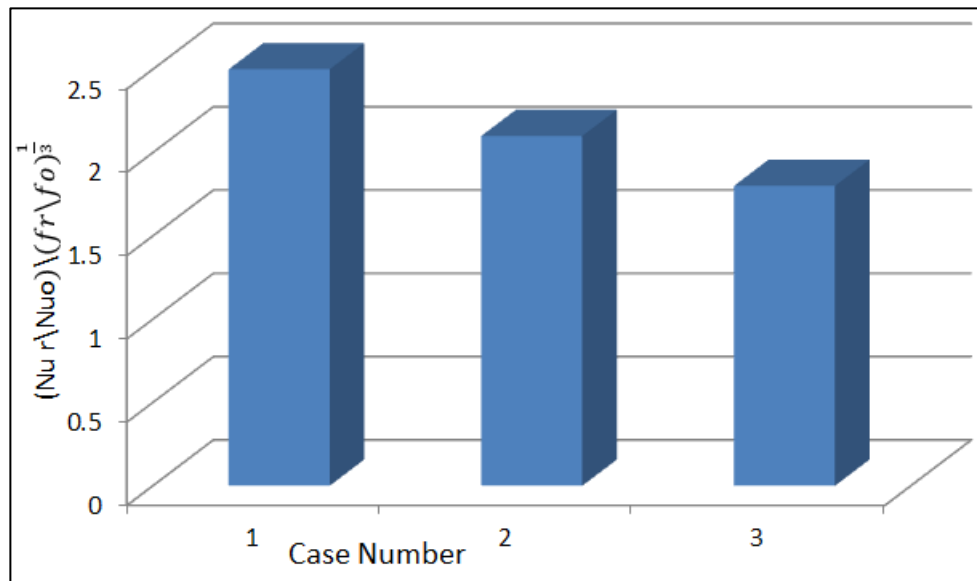


Fig. (4.6). Local heat transfer coefficient of smooth tapered channel and channel with three shape of ribs (square, trapezoidal and house rib)

Figure (4.7) show that the Thermal Performance factor depends upon the Nusselt ratio and friction ratio. It is seen that the Thermo hydraulic Performance factor for case (1)(trapezoidal rib) is highest as compared to the case (2)(house rib) and (3)(square rib)



Fig(4.7). Thermal performance for all cases of ribs (trapezoidal, house and square) respectively ,where Nu_r , Nu_o , f_r , and f_o are the Nusselt Numbers and friction factors for channel with and without ribs respectively.

4.3.3. Slit Rib

4.3.3.1 Compare between the Solid and Slit Rib

A. Velocity Vector

Figure (4.8) shows the instantaneous velocity vector distributions behind solid and a typical slitted rib at superficial velocity of water and air (0.3846,4.624)m/s respectively . The separated shear behind the solid rib is observed to be dominated by large scale unsteady vortical structures. The vortices seem to be originated from the upstream top rib corner and grow in size in later streamwise direction behind the rib, which finally diffuses in the far field. The slitted rib provides perturbation and ventilation of the region just behind the rib, which is otherwise a region of very low velocity with least perturbation in case of solid ribs. The figure clearly shows the high velocity jet like flow through the slit, which is interacting with the separated shear layer resulting decreased reattachment length.

B. Temperature Distribution

Figure (4.9) shows the contour of temperature distribution for the solid and slit trapezoidal ribs in rectangular tapered two-pass channel at superficial velocity of water and air (0.3846,4.624)m/s respectively. The result of the contour it clearly shows the effect of the slit on the temperature distribution that shows a temperature decrease in the channel with the slit rib that is result with the increase of heat transfer coefficient . The decrease in temperature in case of slit ribs because more flow will happen from the slit of the rib and this will prevent the hot spot behind the ribs and more secondary flow will occure that dissipates the temperature and increases the area of heat transfer .

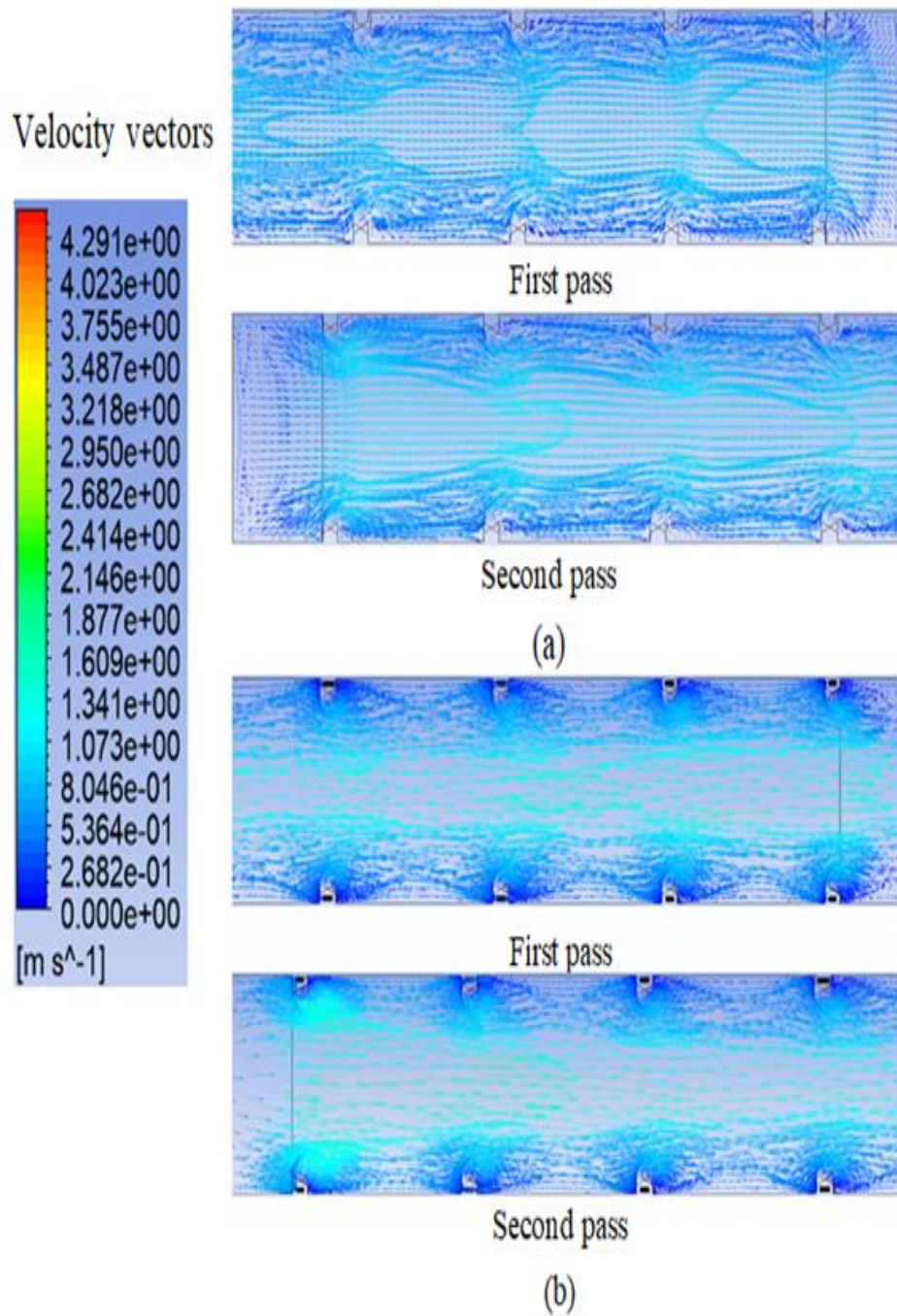


Fig (4-8). Contour of velocity vector of (a) solid rib and (b) slit rib

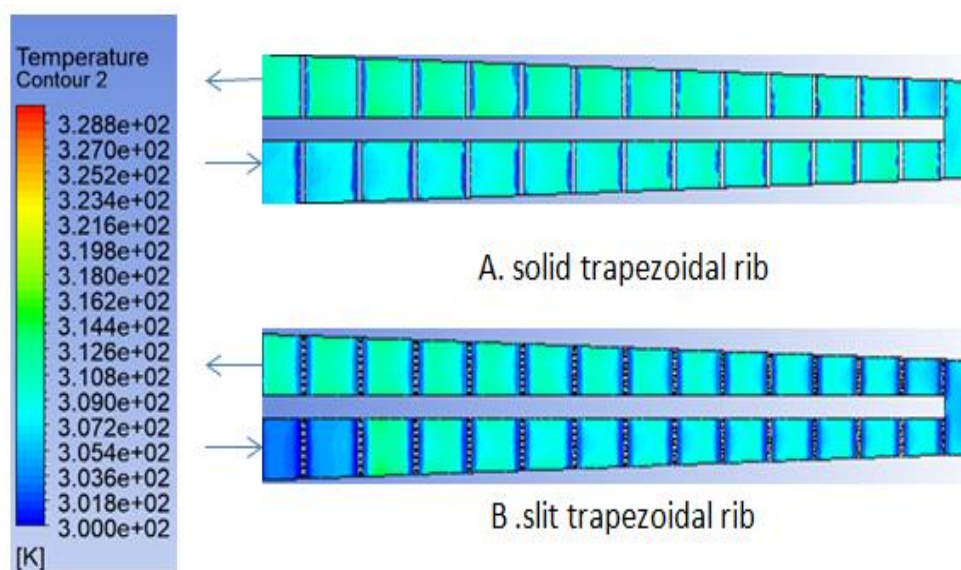


Fig (4.9). contour of temperature distribution for the solid and slit trapezoidal rib

C. Heat Transfer Coefficient

The heat transfer results for solid and slit-ribbed two-pass tapered rectangular channel are presented in this section. Figures(4-10) show the heat transfer coefficient distribution for the solid and slit trapezoidal ribs. Similar to solid ribs the flow past the slit ribs leads to separation due to sudden expansion with subsequent reattachment downstream. In the turn region, heat transfer is enhanced due to the combined effect of the sharp 180° turn and the ribs. At further downstream region, heat transfer coefficient decreases due to the reduction in the turn effect. In the slit rib, the change in heat transfer enhancement can be seen. The flow passing through the slit may induce a change in secondary flow, breaking the vortices between the ribs, resulting in a variance in heat transfer enhancement. The slit rib enhancement heat transfer is compared with the solid rib about 20%.

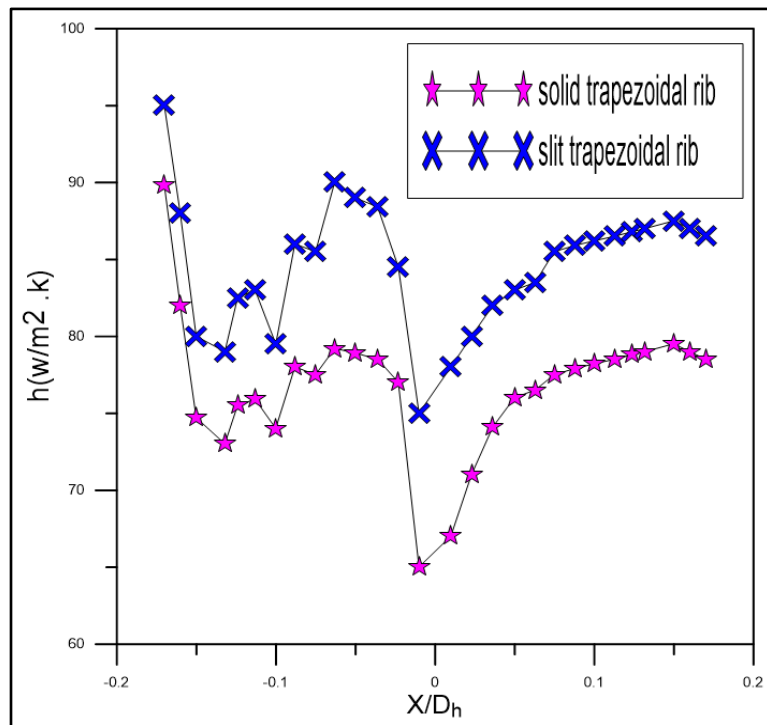


Fig (4-10) . Heat transfer coefficient of the solid and slit ribs

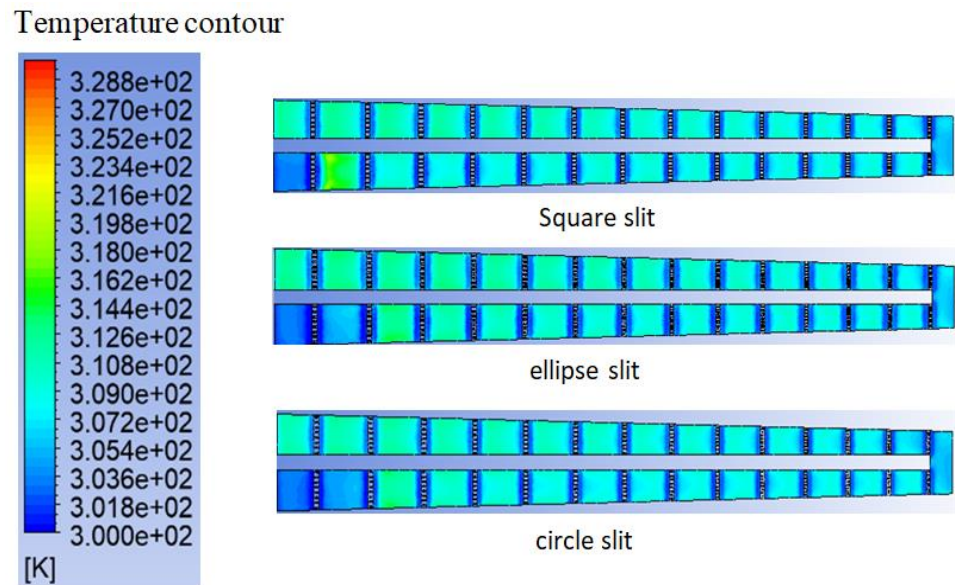
4.3.3.2 Shape of Slit

In this section will be show the effect of the shape of slit ribs on the heat transfer and temperature distribution at superficial velocity of water and air are (0.3846,4.624)m/s respectively in tapered two-pass channel .

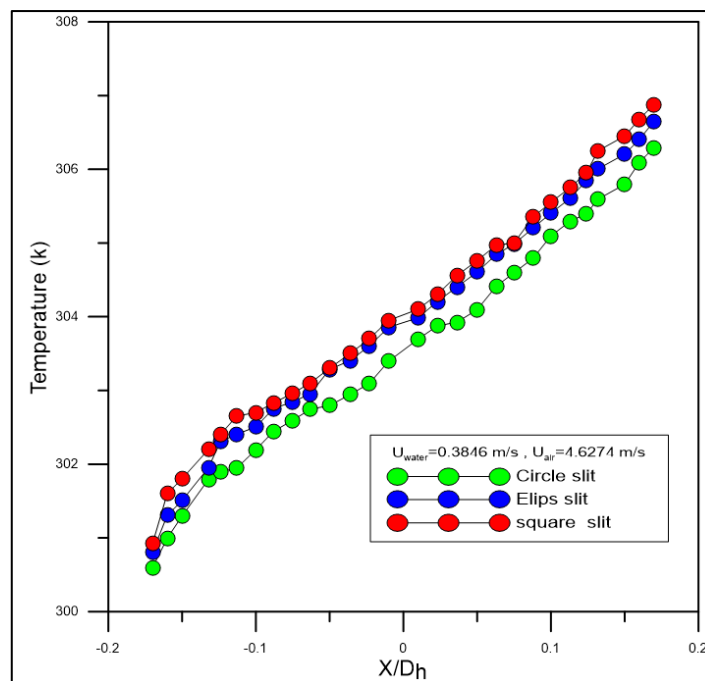
A.The Effect of Shape of Slit on the Rib in Temperature Distribution

Figures (4-11) to (4-12) show the contours of temperature distribution through a tapered channel using several shapes of slit ribs (square ,circle, and ellipse) at the value of water and air superficial velocities and constant heat flux.Through observing these figures, the circle slit rib has the lowest temperature of the other slit ribs because it has a more area for heat transfer and generated a turbulence flow higher than the other slit ribs (square and ellipse).

We can discuss the behavior of the heat transfer improvement as follow, the use of slit ribs inside the channel leads to improve the rate of heat transfer if compared with the solid case, where disturbances is created, surface temperature decrease ,recirculation occurs to improve the rate of heat transfer .



Fig(4-11). contour of temperature distribution for three shape of slit



Fig(4-12) Temperature distribution for three shape of slit

C. The Effect of Shape of Slit on the Rib in H.T.C

It is interesting to note that slitted ribs provide greater heat transfer enhancement than solid ribs in the vicinity of the rib, which may be attributed to the interaction of the jet-like flow emerging from the slit with the separated shear layer, resulting in a reduction in the recirculation bubble size and thus the reattachment length behind any of the slitted rib configurations as compared to solid ribs.

Figure (4-13) shows the heat transfer coefficient distribution for the three shape of slit trapezoidal ribs .The results showed that heat transfer increases with the shape circle slit more than the square and ellipse shape about 11-14% and 6-8 % respectively ,this is because the shape of circle slit has more turbulane flwo behind the ribs and shorter reattachment length which results in shifting of the high heat transfer region towards the rib in case of circle slitted ribs as compared to square and ellipse slit ribs .

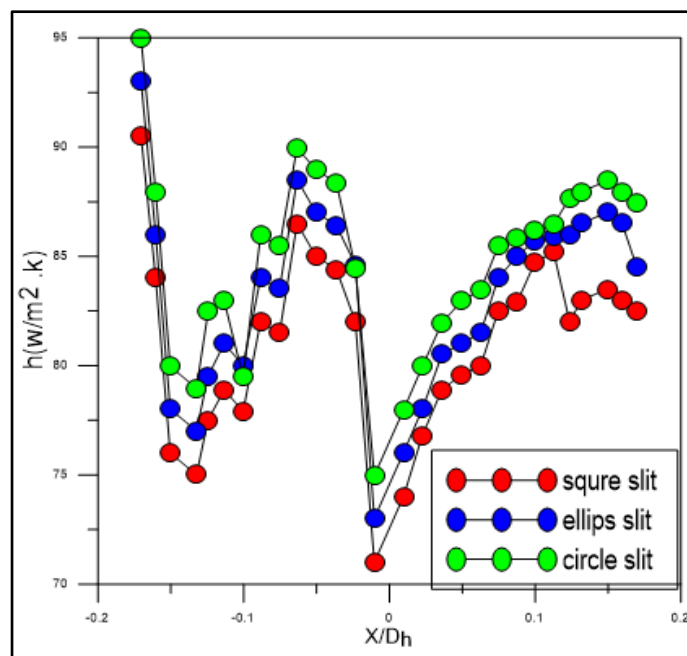
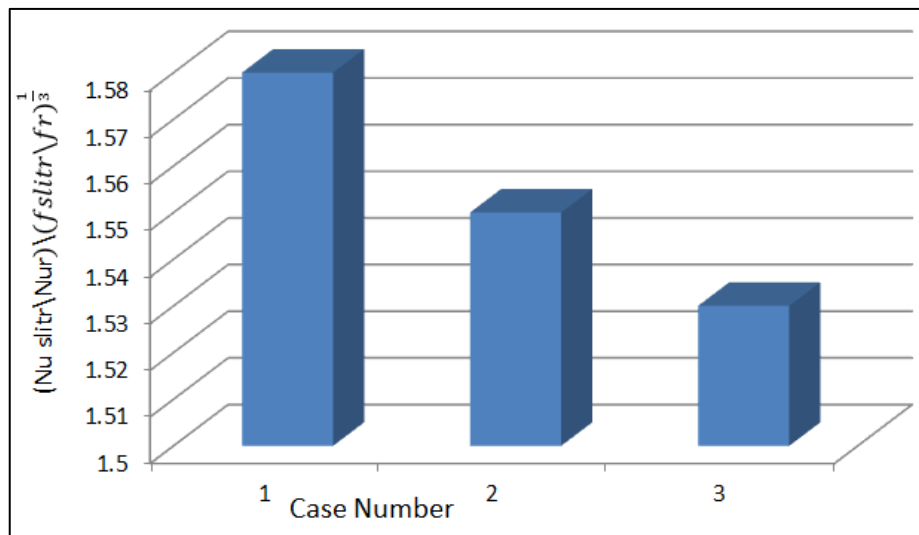


Fig (4-13). Heat transfer coefficient of three shape of slit

Figure (4.14) show that the Thermal Performance factor depends upon the Nusselt ratio and friction ratio. It is seen that the Thermo hydraulic Performance factor for case (1)(circle slit) is highest as compared to the case (2)(ellipse slit) and (3)(square slit).



Fig(4.14) Thermal performance for all cases of three shape slit of trapezoidal rib (circle , ellipse and square) respectively ,where Nu_{slit} , Nu_r , f_{slit} , and f_r are the Nusselt Numbers and friction factors for channel with slit rib and solid ribs respectively.

4.3.3.3. Effect of Increasing Air Superficial Velocity on Circle Slit Trapezoidal Rib

A. Temperature distribution

Figures (4-15) ,(4-16) show the local temperature distribution of circle slit rib in two pass tapered channel with various air superficial velocity respect to water superficial velocity. When air superficial velocity increase, the temperature difference decreases . Heat transfer coefficient increase due to the decrease in the time residence of mixture (water and air) and increase the amount of air increasing inside the channel, where adding of ribs increases surface area of heat transfer and interrupt the development of boundary layer of flow creating turbulence flow inside the channel.

The temperature difference behavior, It can be noted that, the temperature difference decreased as the air superficial velocity increases according to the relation:

$$q = \dot{m} \cdot c_p \Delta T \quad \dots\dots\dots (4-1)$$

Where

$$\dot{m} = \rho v A \quad \dots\dots\dots (4-2)$$

From Eq. (4-1), it can be observed that, the temperature difference inversely proportional with the air superficial velocity

B. Velocity Vector

The figures (4.17) and (4.18) show the contour of velocity vector at different air superficial velocity with respect to water superficial velocity .

The figures show that when increase of air superficial velocity ,It can be seen that the boundary layer separation behind the slit rib. The flow separates after going over the upstream slit rib. There is a primary recirculation bubble, with a small secondary recirculation region directly after the upstream slit rib. Further downstream, the flow reattaches and forms a short recovery region. This flow then impinges on the next slit rib, forming a recirculating region behind it.

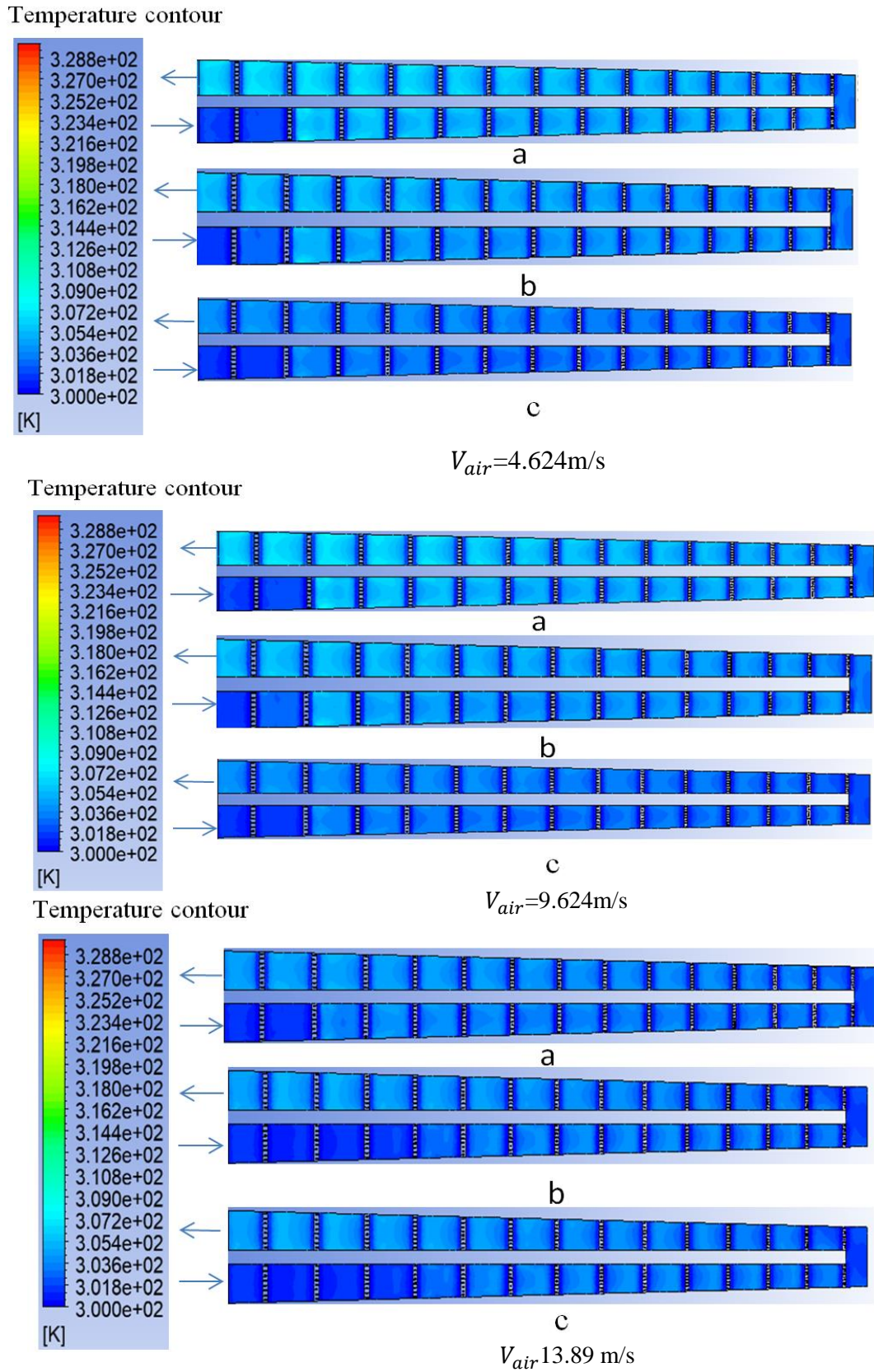


Fig (4-15) . Temperature contour of circle slit ribs of increasing air velocity respect to water velocity V_{water} (a,b ,c)=0.3846,0.769,1.154 m/s respectively

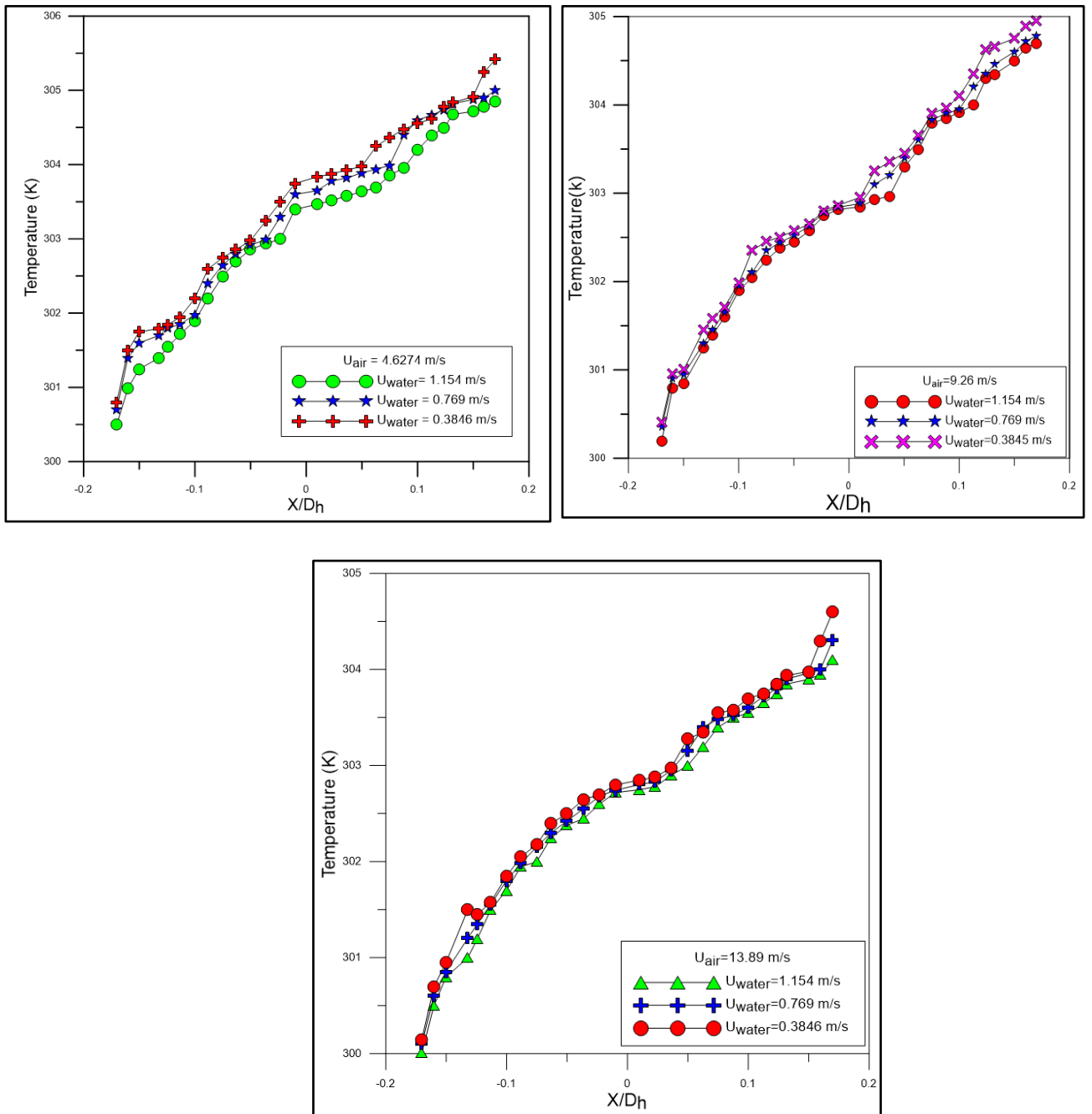


Fig (4-16) . show the local temperature distribution along the tapered two pass channel with trapezoidal rib of circle slit at different air superficial velocity with respect to water superficial velocity .

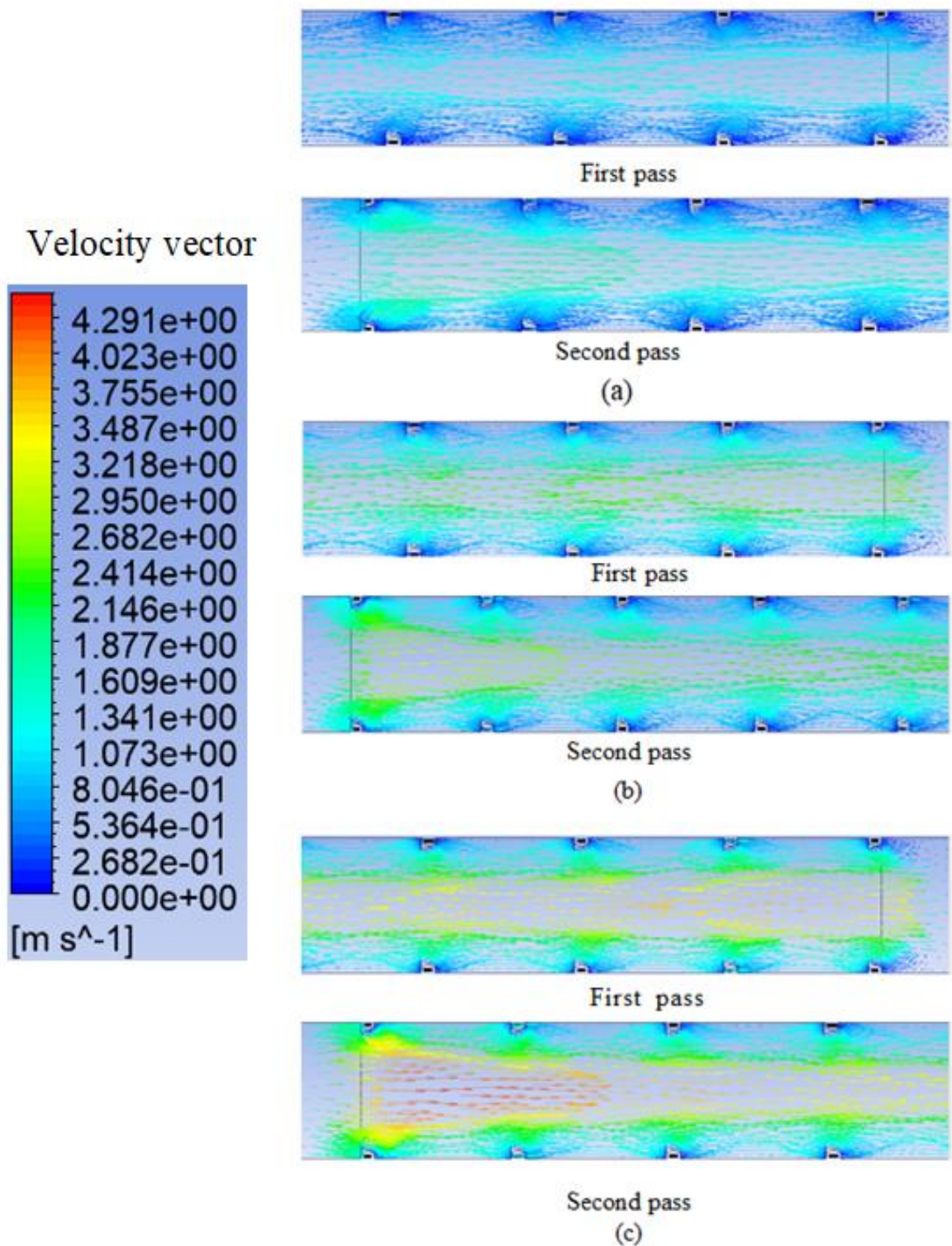


Fig (4-17) . Velocity contour of circle slit ribs of air velocity $V_{air} = 4.624 \text{ m/s}$ respect to water velocity V_{water} (a,b ,c)= $0.3846, 0.769, 1.154 \text{ m/s}$ respectively

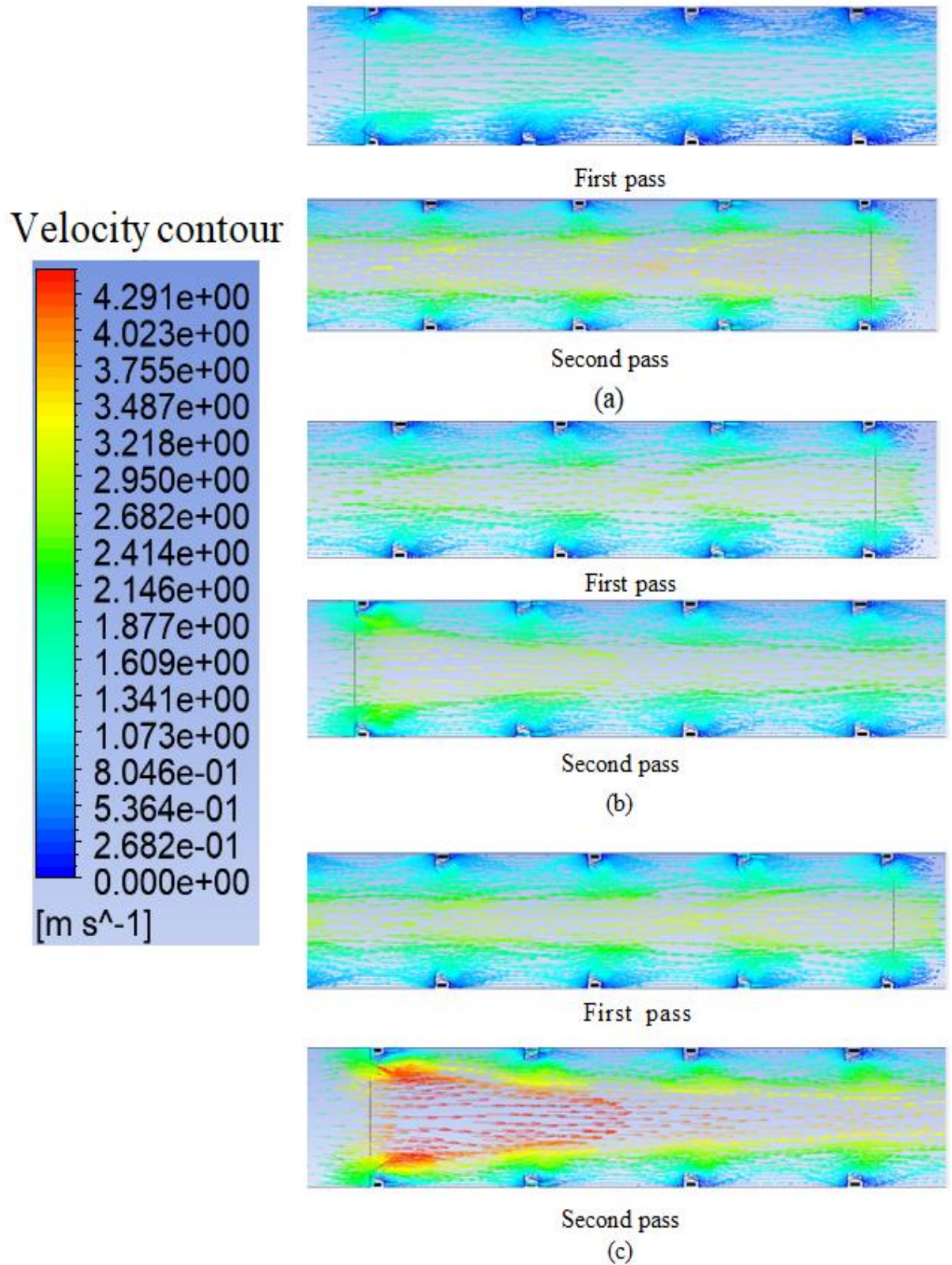
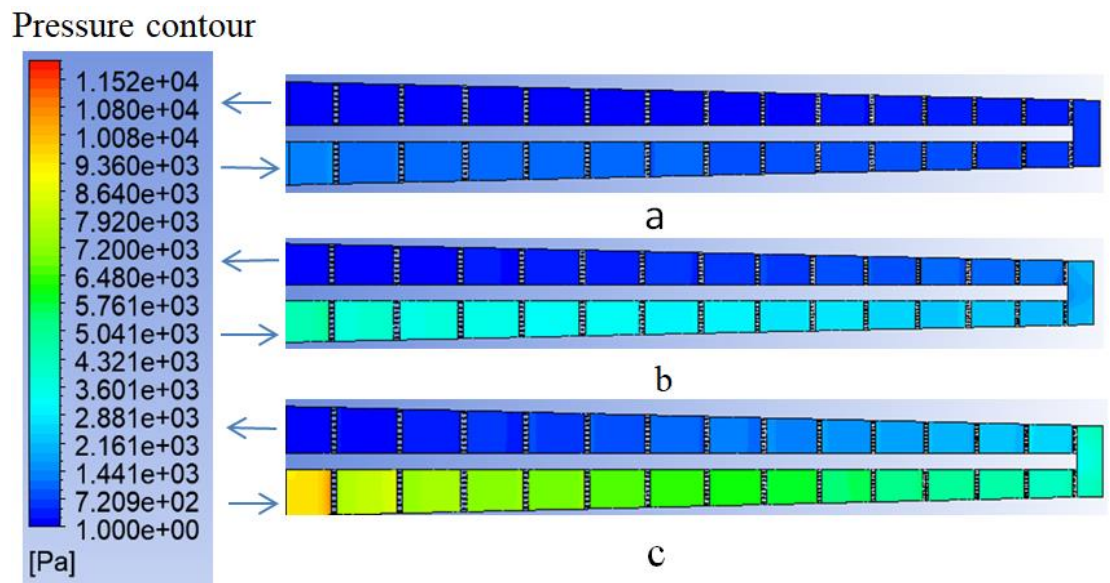


Fig (4-18) . Velocity contour of circle slit ribs of air velocity $V_{air} = 9.624\text{m/s}$ respect to water velocity V_{water} (a,b ,c)= $0.3846,0.769,1.154$ m/s respectively

C. Pressure Distribution

Figure (4.19),(4.120) show the contour of pressure distribution of circle slit trapezoidal ribs in tapered two pass channel at two phase flow of water and air superficial velocity , and the effect of increasing of air velocity with respect to water velocity clearly show in the contour of fig(4-19). In the first pass of the channel , the pressure linearly decreases toward the bend as shown in the contour . The bend effect on the pressure drop in the upstream duct is therefore small .The presence of the bend causes a large pressure drop in the bend .The pressure gradient after passing through the bend approaches that in the upstream duct , which means that the flow disturbed in the bend is redeveloping in the downstream. When the air velocity increases the pressure drop increases. This results in an increase of heat transfer.



$$V_{air}=4.624 \text{ m/s}$$

Fig (4-19) .pressure contour of circle slit ribs of increasing air velocity respect to water velocity V_{water} (a , b, and c)=0.3846 ,0.769 ,1.154 m/s respectively.

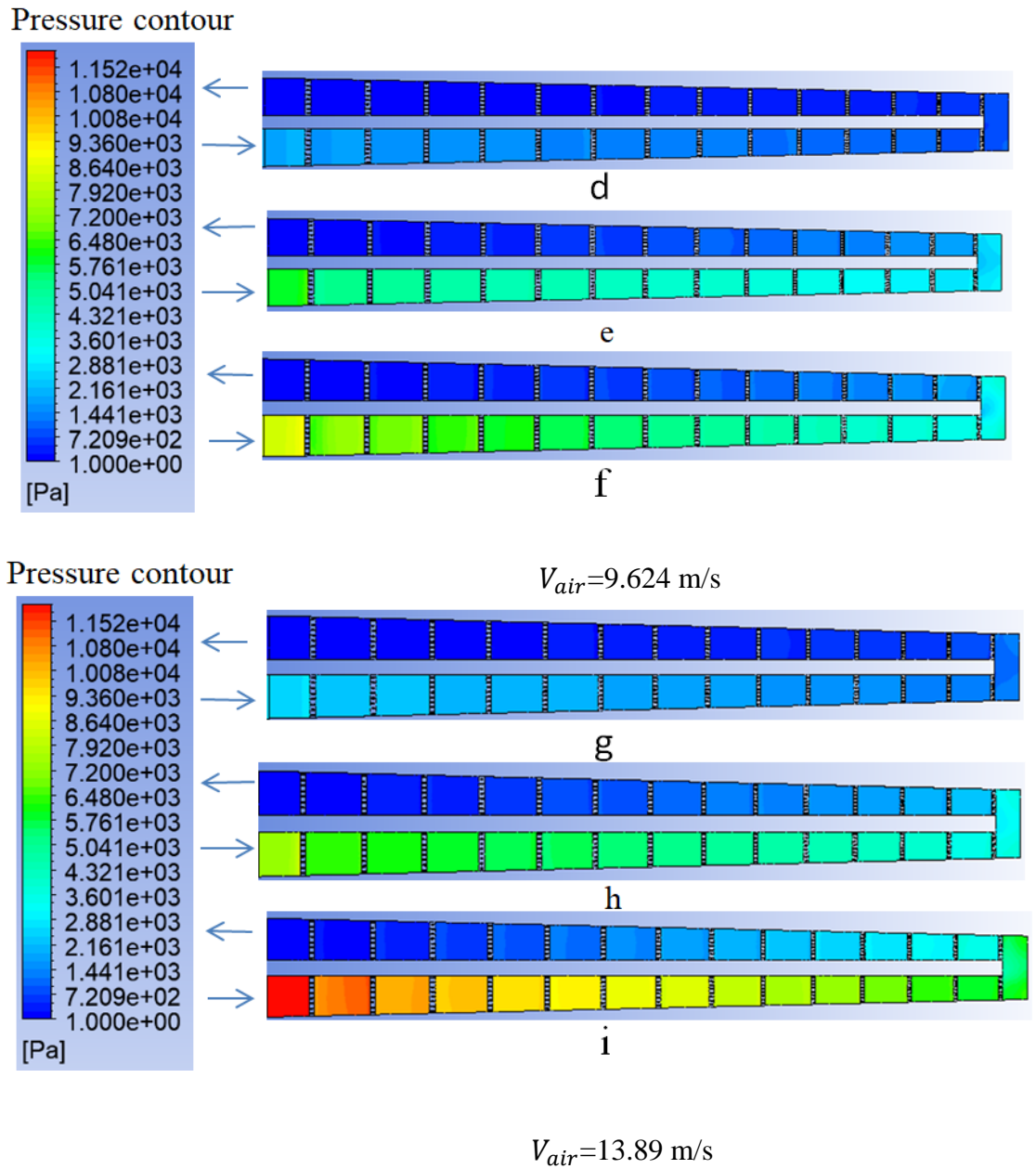


Fig (4.20) .Pressure contour of circle slit ribs of increasing air velocity respect to water velocity V_{water} (d, and g ; e and h ; f and i)=0.3846 ,0.769 ,1.154 m/s respectively

D. Heat transfer coefficient

In this section show the effect of increasing the air superficial velocity on the local heat transfer coefficient with three air superficial

velocity and constant heat flux in the two pass channel with trapezoidal ribs that has circle slit

Figure (4-21) shows the local heat transfer coefficient increased as the air superficial velocity increased, due to a decrease in the time residence of the mixture (water and air) and an increase in the amount of air inside the channel, which has a constant volume that is already filled with water and air. The presence of ribs inside the channel increased the surface area of heat transfer and interrupted the development of the boundary layer of flow, causing turbulence due to the secondary flow generated. The local heat transfer coefficient increased when the air superficial velocity 13.89 m/s as 18% ,10% in comparison with air velocity 4.6247 ,9.26 m/s respectively .

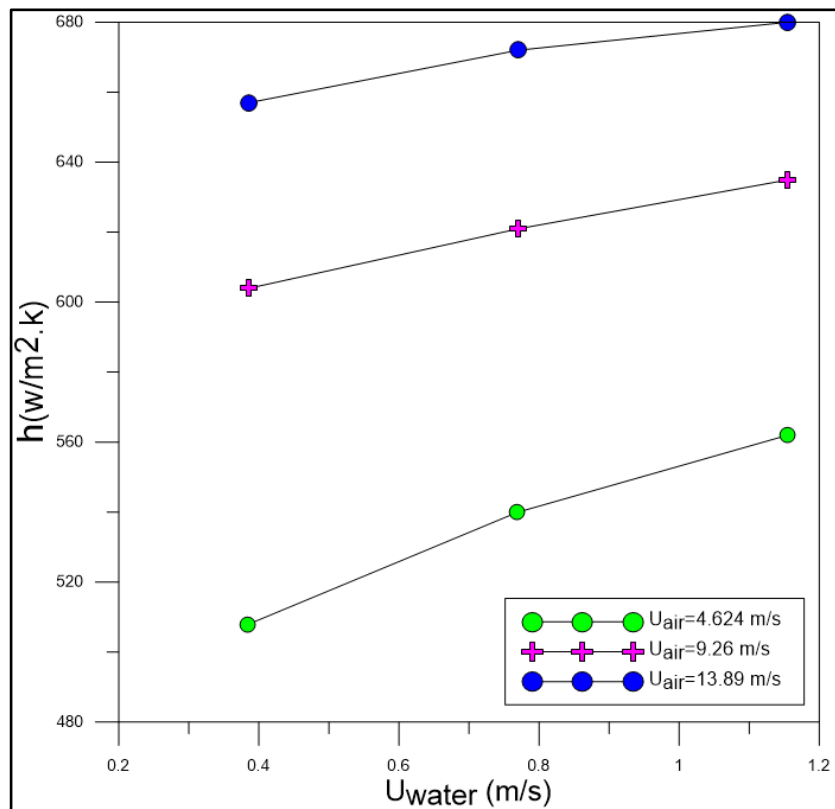


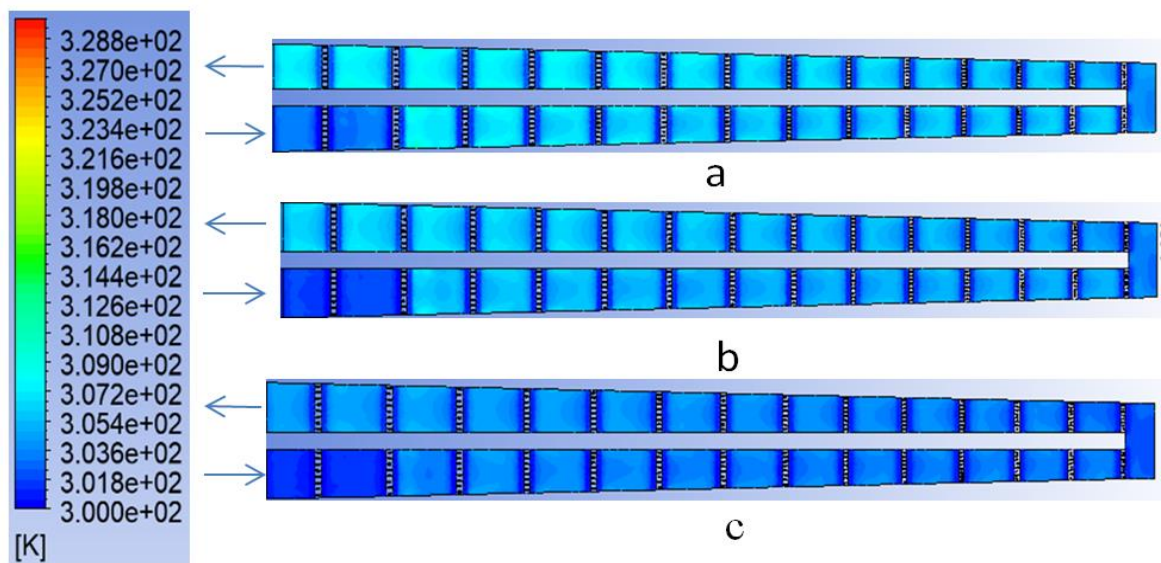
Fig (4.21). Heat transfer coefficient of air superficial velocity with respect of water superficial velocity

4.3.3.4 Effect of Increasing Water Superficial Velocity on Circle Slit Trapezoidal Rib

A. Temperature Distribution

Fig (4-22) , (4-23),(4-24) show the local temperature distribution of circle slit rib in two pass tapered channel with various water superficial velocity due to water superficial velocity. When water superficial velocity increase, the temperature decrease and heat transfer coefficient increase due to the decrease in the time residence of mixture (water and air) and the amount of air increases inside the channel, and adding of ribs increase surface area of heat transfer and interrupt the development of boundary layer of flow and creating turbulence flow inside the channel.

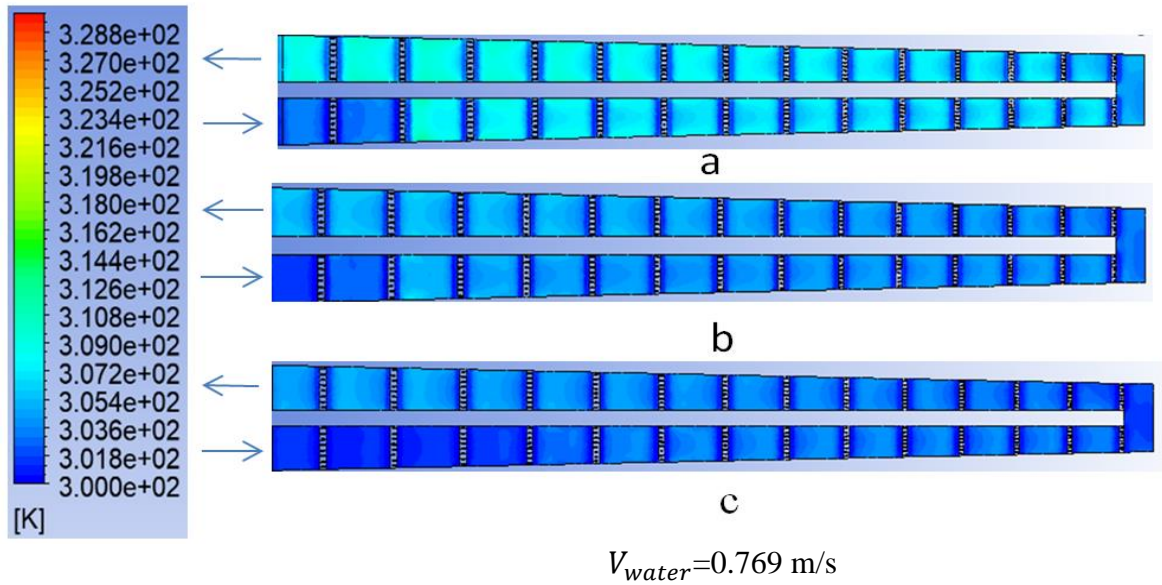
Temperature contour



$$V_{water}=0.3846\text{m/s}$$

Fig (4-22) . Temperature contour of circle slit ribs of increasing water velocity respect to water velocity V_{air} (a, b, c)=4.24 , 9.634 ,13.89 m/s respectively.

Temperature contour



Temperature contour

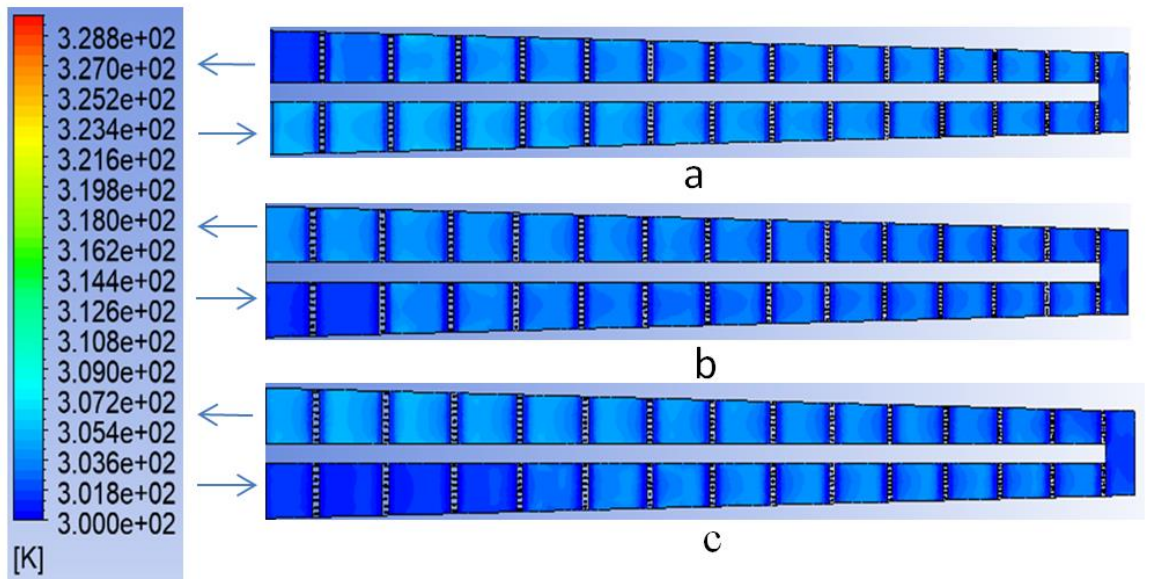


Fig (4-23) . Temperature contour of circle slit ribs of increasing water velocity respect to water velocity V_{air} (a, b ,c)=4.24 , 9.634 ,13.89 m/s respectively

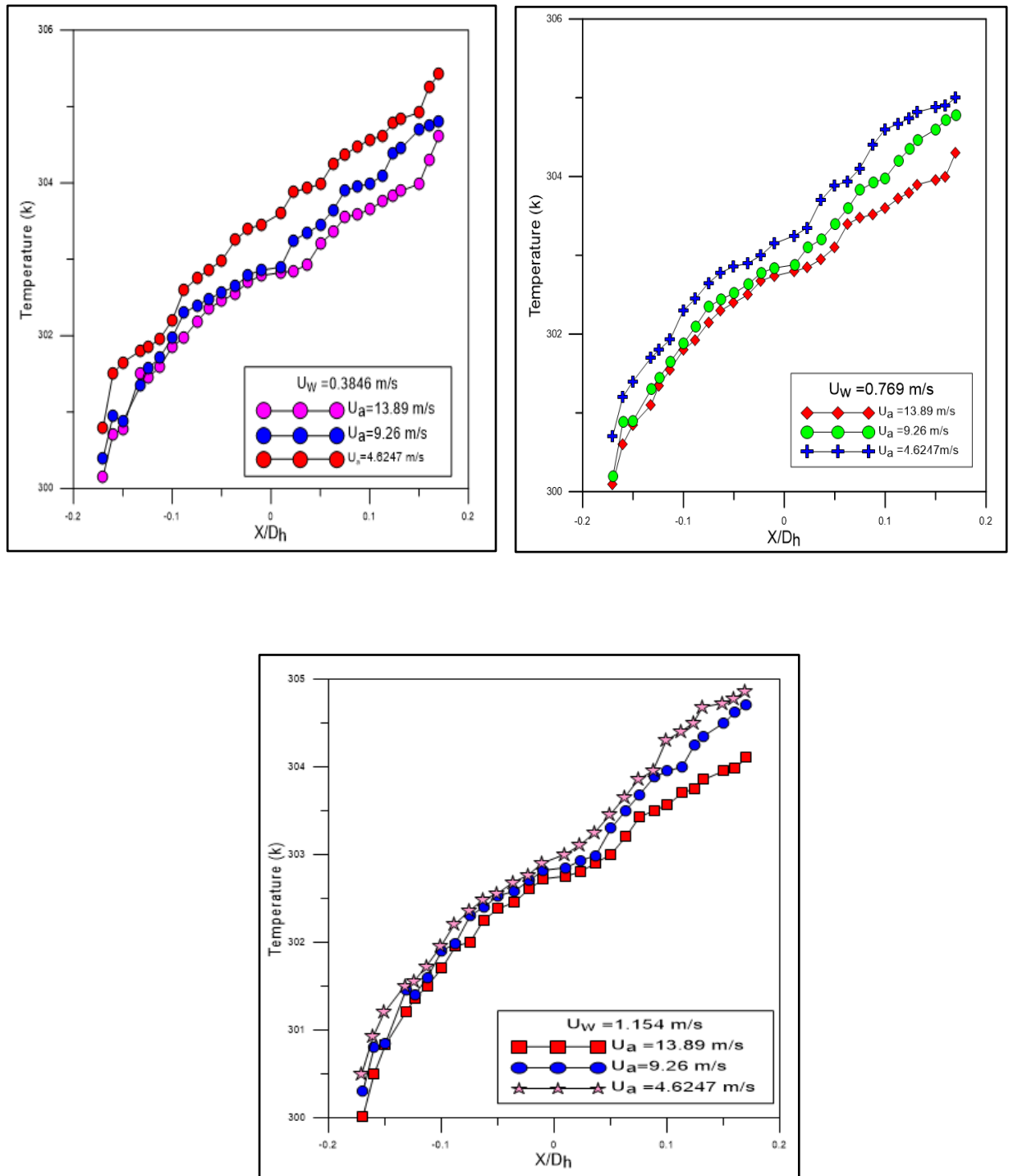


Fig .(4-24) . show the local temperature distribution along the tapered two pass channel with trapezoidal rib of circle slit at different water superficial velocity with respect to air superficial velocity .

B. Velocity Vector

The figures (4-25), (4-26) show the contour of velocity vector at different water superficial velocity with respect to air superficial velocity .

The figures show that when water superficial velocity increases , The boundary layer separation behind the slit rib can be seen. The flow separateD after going over the upstream slit rib. There is a primary recirculation bubble, with a small secondary recirculation region directly after the upstream slit rib. Further downstream, the flow reattaches and forms a short recovery region. This flow then impinges on the next slit rib, forming a recirculating region behind of it.

C. Pressure distribution

Figure (4-27) shows the contour of pressure distribution of circle slit trapezoidal ribs in tapered two pass channel at two phase flow of water and air superficial velocity , and the effect of increasing of water velocity with respect to air velocity clearly show in the contour of fig(4-26). In the first pass of the channel , the pressure linearly decreases toward the bend as shown in the contour . The bend effect on the pressure drop in the upstream duct is therefore small .The presence of the bend causes a large pressure drop in the bend .The pressure gradient after passing through the bend approaches that in the upstream duct , which means that the flow disturbed in the bend is redeveloping in the downstream. It can be noted that when the air velocity increases the pressure drop increase this is result in the increase of heat transfer .

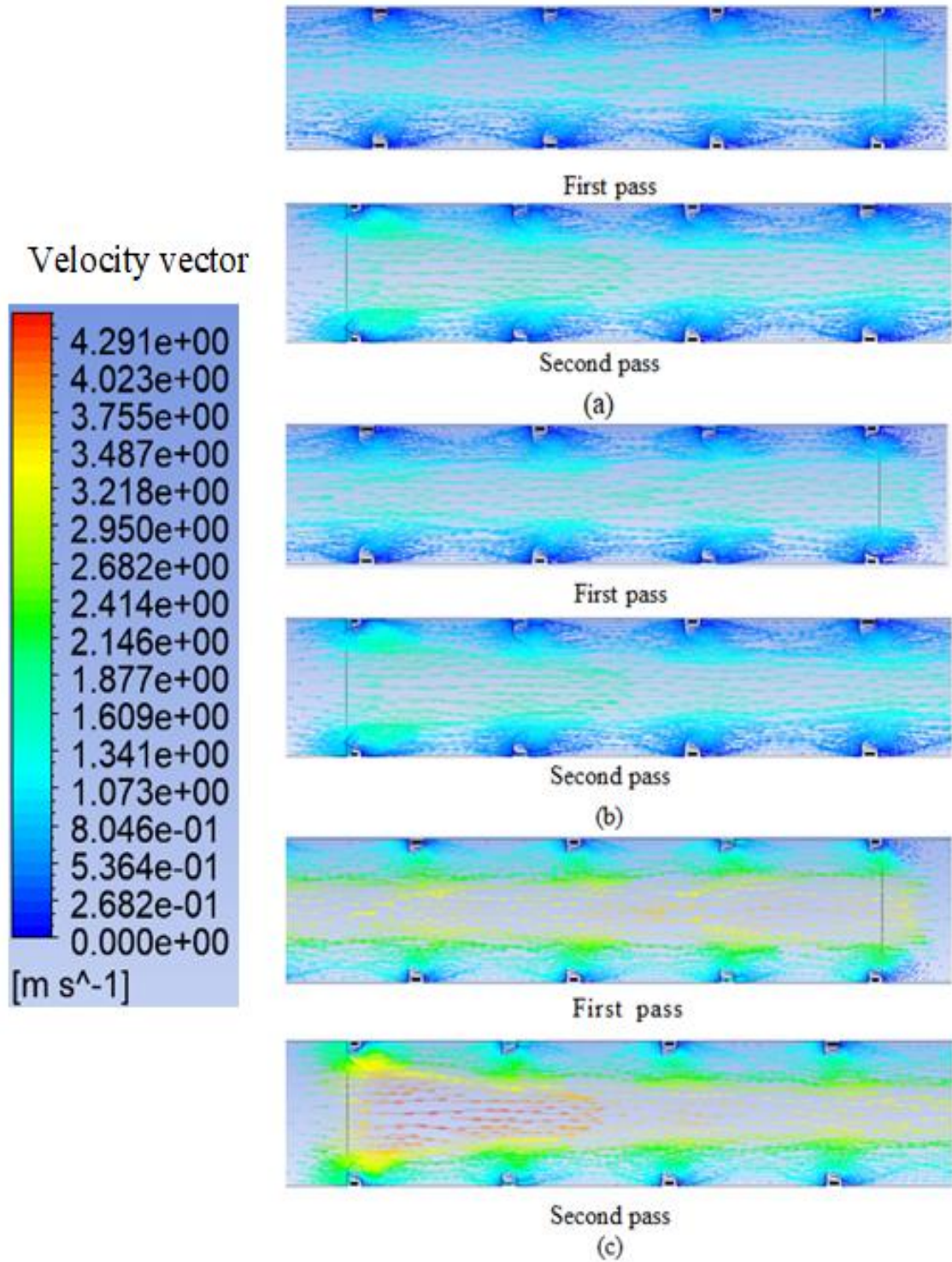


Fig (4-25) Velocity contour of circle slit ribs of air velocity $V_a = 0.3846\text{m/s}$ respect to water velocity V_a (a ,b ,c)= 4.624 , 9.624 , 13.89 m/s respectively

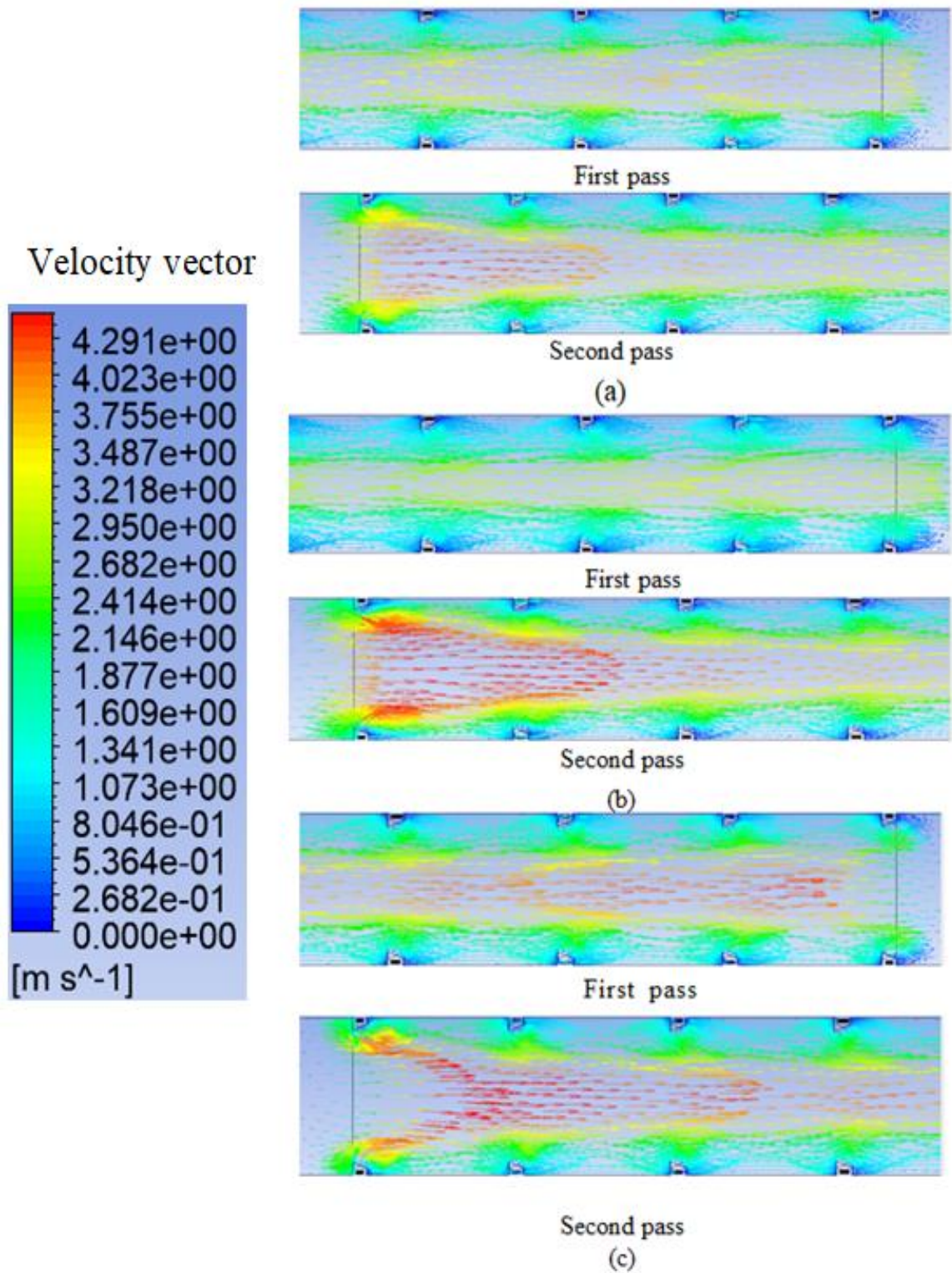


Fig (4-26) . Velocity contour of circle slit ribs of air velocity $V_a = 0.769\text{m/s}$ respect to water velocity V_a (a,b ,c)= 4.624 , 9.624 , 13.89 m/s respectively

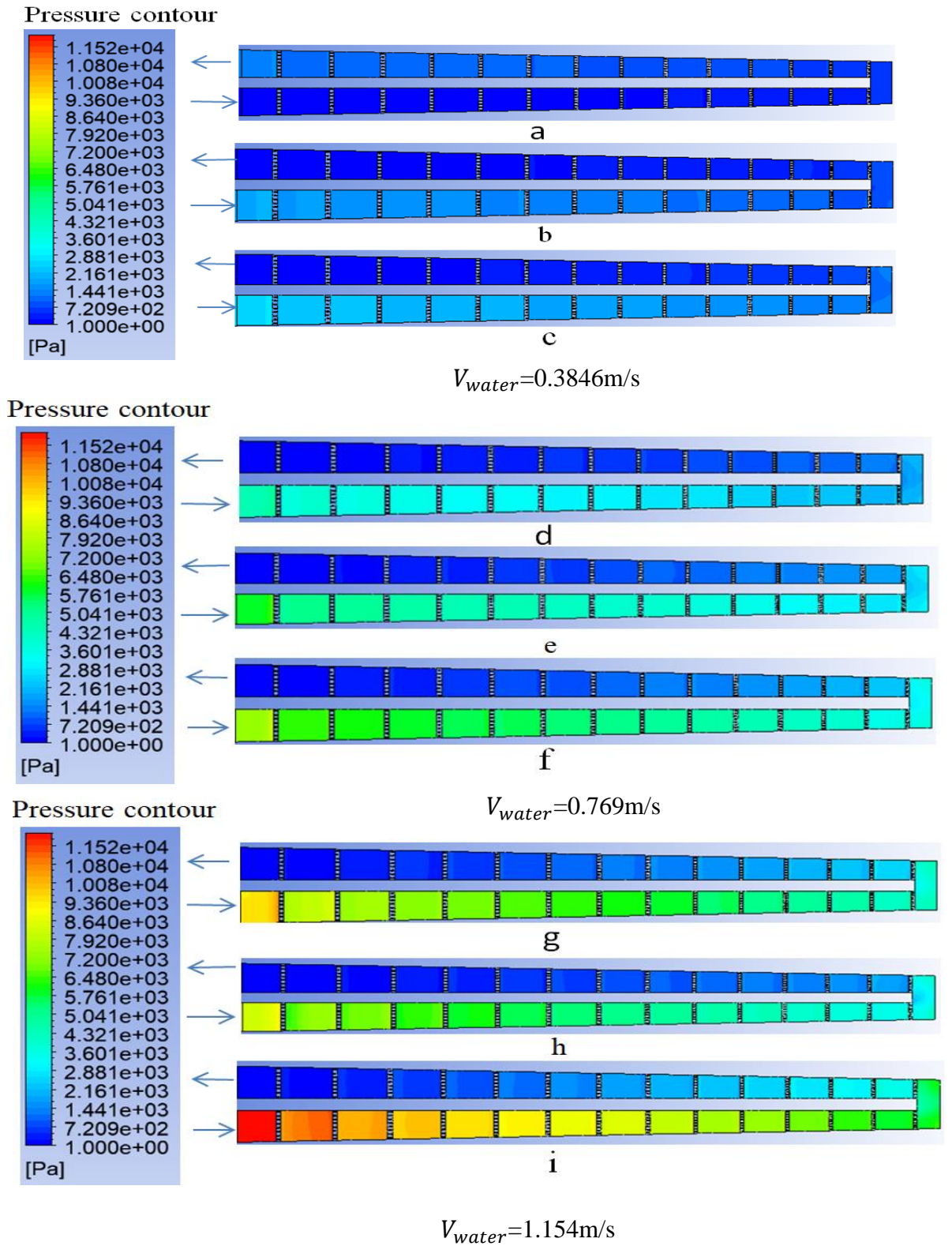


Fig (4-27) .pressure contour of circle slit ribs of increasing air velocity respect to water velocity V_{air} (a ,d, and g ; b, e and h ; c, f and i)=4.624,9.624,13.89 m/s respectively.

D. Heat Transfer Coefficient

Figure (4-28) show the local heat transfer coefficient increases as the water superficial velocity increases, due to a decrease in the time residence of the mixture (water and air) and an increase in the amount of water inside the channel, which has a constant volume that is already filled with water and air. The presence of ribs inside the channel increased the surface area of heat transfer and interrupted the development of the boundary layer of flow, causing turbulence due to the secondary flow generated. The local heat transfer coefficient increased when the air superficial velocity is 1.154 m/s as 6% ,4% in comparison with air velocity 0.3846 ,0.769 m/s respectively .

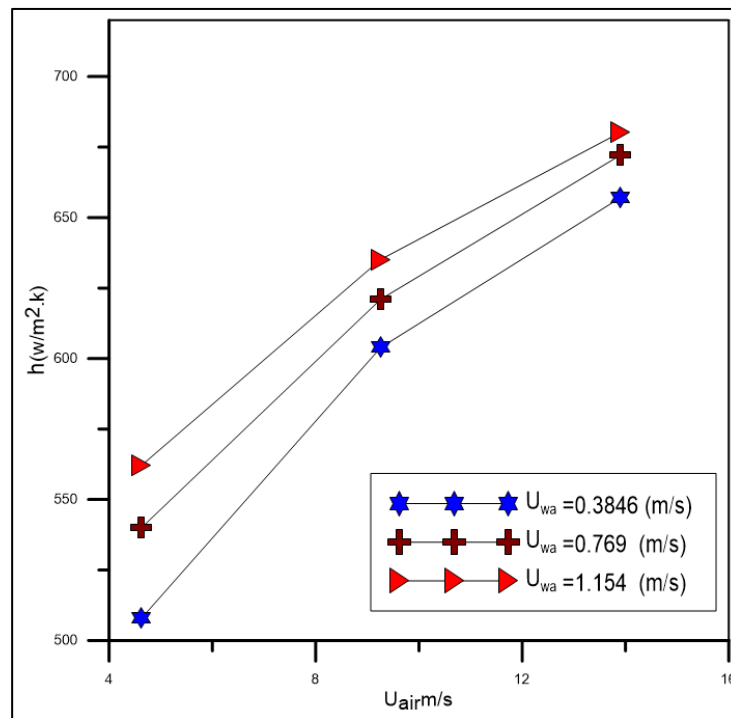


Fig (4.228). Heat transfer coefficient of water superficial velocity with respect of air superficial velocity

Chapter five

Conclusions and suggestions

Conclusions and Suggestions

5.1 Conclusions

In this section , the last conclusions have been drawn from the numerical studies of the heat transfer and temperature distribution in a horizontal tapered rectangular turbulated channel are summarized .Future study is also proposed, with the objective of improving and expanding multiphase flow learning in the horizontal tapered channel.

1. Investigation the three types of channels straight and tapered 1,2 channels, it was found that in case of increased tapering, the pressure drop increases, and this is at the expense of increasing the heat transfer coefficient.
2. When comparing heat transfer coefficient of ribbed channel(square , house and trapezoidal ribs) with the smooth channel, the heat transfer increases with the ribbed channel than the smooth channel about 10 % , 16% , 21 % respectively .
3. When comparing three types of ribs in the tapered channel (square ,house and trapezoidal rib) , it was found that the trapezoidal rib has a higher heat transfer coefficient and a better temperature distribution than the square and house ribs . the result indicate that the trapezoidal rib has more heat transfer enhancement than the square and house rib about 12% , 6% respectively .
4. By placing a hole in the inside of the ribs and comparing the ribs with holes and solid ribs, it was found that the ribs with holes prevent the formation of hot spots and increase heat transfer.
5. Through the use of three types of slit (square, ellipse and square) inside the ribs and comparing them, the ribs containing the

circular slit were found to have a heat transfer coefficient to and a better temperature distribution due to the structure of the circular slit and the better space it provides for the penetration of the flow to the ribs. The slit rib enhancement heat transfer in compare with the solid rib about 20% .

6. Increasing the water superficial velocity from (0.3846 to 1.154 m/s) and air superficial velocity from (4.624to 13.89 m/s), lead to increase the numerical results of heat transfer coefficient through ribbed two-pass channel with the increase velocity of air and water . The local heat transfer coefficient increased when the air superficial velocity 13.89 m/s as 18% ,10% in compare with air velocity 4.6247 ,9.26 m/s respectively . . The local heat transfer coefficient increased when the air superficial velocity 1.154 m/s as 6% ,4% in compare with air velocity 0.3846 ,0.769 m/s respectively .

5.2 Suggestions for Future Work

The following proposals for further development are summarized:

- Investigating the process of heat transmission, temperature distribution, and pressure decrease inside a conduit with other shape of ribs and slits.
- Investigating the use of various types of phases, such as nanofluid particles, to demonstrate the impact of this phase on heat transmission and temperature distribution via the testing section.
- Investigation the work experimentaly

References

1. Guangwen Jianga., Jianmin Gaoa., Xiaojun ShiWang Zhaoa , and, Yunlong Lia, “**Flow and Heat Transfer of mist/steam Two-phase Flow in Two-pass Rectangular Channels with Paralleled and V-shaped Rib Turbulators**” International Mechanical Engineering Congress and Exposition IMECE, Vol:8B,2018.
2. Laith Jaafer Habeeband Riyadh S. Al-Turaihi, “**Experimental Study and CFD Simulation of Two-Phase Flow around Multi-Shape Obstacles in Enlarging Channel**”, American Journal of Mechanical Engineering, , Vol. 1 , No. 8, 2013,pp: 470-486 .
3. M.R. Ansari and B. Arzandi “**Two-phase gas–liquid flow regimes for smooth and ribbed rectangular ducts**” International Journal of Multiphase Flow, Vol.38,No.1,pp: 118–125.
4. Humam Kareem Jalghaf, Riyadh S. Al-Turaihi and Laith Jaafer Habeeb , “**Air-Water Flow Investigation around Hot Circular Cylinder inside Channel**” ,Advances in Natural and Applied Sciences.Vol. 10,No.12 August 201 6 .
5. Zhi Tao , Meisong Yang , Hongwu Deng, Haiwang Li , Shuqing Tian “**Heat transfer study in a rotating ribbed two-pass channelwith engine-similar cross section at high rotation number**” ,Applied Thermal Engineering,Vol. 106 ,2016,pp: 681–696
6. Srinath V. Ekkad , Gautam Pamula, Manoj Shantiniketanam “**Detailed heat transfer measurements inside straight and tapered two-pass channels with rib turbulators**” ,Experimental Thermal and Fluid Science,Vol. 22, (2000), pp:155-/,163
7. Je-Chin Han ,Committee Members, Sai Lau ,Hamn-Ching Chen ,Jorge Alvarado and , Dennis O’Neal “**Heat Transfer in Smooth and Ribbed Rectangular Two-Pass Channels with a Developing Flow Entrance at High Rotation Numbers**”, P.h.d . , Texas A&M University,2009

8. Lei Wang and Bengt Sundén ,“**Experimental investigation of local heat transfer in a square duct with various-shaped ribs**” ,Heat Mass Transfer ,Vol.43,No.8,2006,pp:759-766
9. Adnan Qayoum and Pradipta Panigrahi ,“**Experimental Investigation of Heat Transfer Enhancement in a Two-pass Square Duct by Permeable Ribs**”, Heat Transfer Engineering, 1–12.2018
10. Jian Liu , Safeer Hussain , Wei Wang , Lei Wang , Gongnan Xie , Bengt Sundén “**Heat Transfer Enhancement and Turbulent Flow in a Rectangular Channel Using Perforated Ribs with Inclined Holes**” , Journal of Heat Transfer, Vol:14 (2019)
11. Arjumand Rasool and Adnan Qayoum ”**Numerical Investigation of Fluid Flow and Heat Transfer in a Two-Pass Channel with Perforated Ribs**” Pertanika J. ,science and technology, Vol: 26, No:4 (2018).
12. Naveen Sharma, Andallib Tariq and Manish Mishra , “**Detailed heat transfer and fluid flow investigation in a rectangular duct with truncated prismatic ribs**”, Experimental Thermal and Fluid Science , Vol. 96, No. 2018, pp : 383-396
13. Satyanand Abraham and Rajendra P. Vedula ,“ **Heat transfer and pressure drop measurements in a square cross-section converging channel with V and W rib turbulators**”, Experimental Thermal and Fluid Science, Vol. 70, No.2016, pp: 208–219.
14. Fifi NM Elwekeel, Qun Zheng and Antar MM Abdala ,“**Air/mist cooling in a rectangular duct with varying shapes of ribs**” , Proceedings of the Institution of Mechanical Engineers, Part C: Journal of Mechanical Engineering Science, Vol.228, No.11, 2013 pp:1925–1935
15. Arjumand Rasool , Adnan Qayoum ,“**Numerical analysis of heat transfer and friction factor in two-pass channels with variable rib shapes**” , International Journal of Heat and Technology , Vol.36, No.1, 2018, pp. 40-48

16. Prashant Singh, Srinath Ekkad , “**Experimental study of heat transfer augmentation in a two-pass channel featuring V-shaped ribs and cylindrical dimples**” , Applied Thermal Engineering ,Vol:116 ,(2017),pp: 205–216 .
17. Sourabh Kumar and R. S. Amano ” **Numerical Simulation of Two Pass Gas Turbine Blade Internal Cooling Channels with 90 Degree Varying Height Ribs**”,Proceedings of the ASME International Mechanical Engineering Congress & Exposition, Vol:6, No: IMECE2012-89064, pp: 245-253
18. Mi-Ae Moon, Min-Jung Park, Kwang-Yong Kim ”**Evaluation of Heat Transfer Performances of Various Rib Shapes**” International Journal of Heat and Mass Transfer ,Vol:71 ,(2014) ,pp:275–284
19. Shyy Woei Chang , Wei-Ling Cai and Ruei-Jhe Wu ,” **Heat Transfer Enhancement by Detached S-Ribs for Twin-Pass Parallelogram Channel**” ,Inventions 2018, 3, 50
20. Jian Liu, Safer Hussain , Wei Wang, Lei Wang ,Gongnan Xie and Bengt Sundén, ” **Experimental and numerical study of heat transfer due to developing flow in a two-pass rib roughened square duct**” International Journal of Heat and Mass Transfer vol:102(2016) ,p: 1245—1256
21. Azher M. Abed , Doaa Fadhil Kareem , Hasan Sh Majdi, and Ammar Abdulkadhim,“**Experimental and CFD Analysis of Two-Phase Forced Convection Flow in Channels of Various Rib Shapes**”, Journal of Advanced Research in Fluid Mechanics and Thermal Sciences, Vol:77, No 1 ,(2021) ,pp:36-50
22. Naveen Sharma, Andallib Tariq and Manish Mishra, “**Experimental Investigation of Heat Transfer Enhancement in Rectangular Duct with Pentagonal Ribs**” Heat Transfer Engineering, 2018
23. Andallib Tariq , Naveen Sharma and Naveen Sharma , “**Aerothermal Characteristics of Solid and Slitted Pentagonal Rib Turbulators**” ,Journal of Heat Transfer , Vol. 140 ,No :6, 2018,pp: 061901-1

24. Md Shaukat Ali, Andallib Tariq, and B K Gandhi, “**lct and piv investigations behind trapezoidal-rib with a slit mounted on bottom wall of a rectangular duct**” ,Proceedings of the ASME Gas Turbine India Conference GTINDIA2012.
25. Daren Zhenga, , Xinjun Wang, and , Qi Yuana “**Numerical investigation on the flow and heat transfer characteristics in arectangular channel with V-shaped slit ribs**” Infrared Physics and Technology ,Vol:101, (2019),pp: 56–67.
26. Guoqiang Xu and Yang Li, Hongwu Deng “**Effect of rib spacing on heat transfer and friction in a rotating two-pass square channel with asymmetrical 90-deg rib turbulators**” , Applied Thermal Engineering,Vol:80,2015,pp:386-395.
27. Sarah Oleiwi and Riyadh Al-Turaihi ,“**The effect of ribs height in two phase flow (air-water) on heat transfer coefficient in vertical ribbed duct**” ,Ain Shams Engineering Journal, 2019 .
28. Tieyu Gao, Jiangnan Zhu, Jun Li and Qingfeng Xia ,“**Numerical study of the influence of rib orientation on heat transfer enhancement in two-pass ribbed rectangular channel**” engineering applications of computational fluid mechanics, vol. 12, no. 1,2017, pp:1-20.
29. Tieyu Gao , Junxiong Zeng, Jiangnan Zhu, Jun Li and Jianying Gong “**Effects of rib angle and rib orientation on flow and heat transfer in two-pass ribbed channels**” Journal of Mechanical Science and Technology ,Vol:32,No :1, (2018),pp: 513-526.
30. Jiang Lei Je-Chin Han and Michael Huh , “**Effect of Rib Spacing on Heat Transfer in a Two Pass Rectangular Channel (AR = 2:1) at High Rotation Numbers**” Journal of Heat Transfer, , Vol. 134, 2018 , 091901-1 .
31. Natthaporn Kaewchoothong, Kittinan Maliwan , Chayut Nuntadusit, Takeishi Kenichiro “**Effect of Inclined Ribs on Heat Transfer**

- Coefficient in Stationary Square Channel**”, Theoretical & Applied Mechanics Letters ,Vol:7,No:6(2017),pp: 1-8
32. Riyadh S. Al-Turaihi, Sarah Hasan Oleiwi, “**Heat Transfer of Two Phases (water – air) in Horizontal Smooth and Ribbed Ducts**”, International Journal of Energy Applications and Technologies Vol. 3, No. 2, 2016, pp. 21 – 29,
33. Xiangyun Liu , Zhi Tao, Shuiting Ding and Guoqiang Xu , “**Experimental investigation of heat transfer characteristics in a variable cross-sectioned two-pass channel with combined film cooling holes and inclined ribs**”, Applied Thermal Engineering, Vol. 50, (2013) 1186e1193 .
34. Tieyu Gaoa , Jiangnan Zhuh, Jun Lia, Jianying Gong, Qingfeng Xia, “**Improving Heat transfer Performance in Two-pass Ribbed Channel by the Optimized Secondary Flow via Bend Shape Modification**” , International Communications in Heat and Mass Transfer
35. Ramesh Erelli, Arun K. Saha, P.K. Panigrahi , “**Influence of turn geometry on turbulent fluid flow and heat transfer in a stationary two-pass square duct** ” , International Journal of Heat and Mass Transfer, Vol. 89,(2015) ,pp:667-684
36. Krishnendu Saha and Sumanta Acharya “**Effect of Bend Geometry on Heat Transfer and Pressure Drop in a Two-Pass Coolant Square Channel for a Turbine**”, Journal of Turbomachinery ,MARCH, Vol. 135,2013, 021035-1.
37. Runzhou Liu , Haiwang Li , Ruquan You and Zhi Tao , “**Experimental investigation of turbulent flow in a two-pass channel with different U shaped bends**” ,AIP Advances 10, 065311 (2020)
38. Longfei Wang, Songtao Wang, Xun Zhou, Fengbo Wen and Zhongqi Wang , “**Numerical Prediction of 45° Angled Ribs Effects on U-shaped Channels Heat Transfer and Flow under Multi Conditions**”, Int J Turbo Jet Eng 2017; aop .

39. Kosuke Hayashi, Junichiro Kazi , Naoyuki Yoshidaa, Akio Tomiyama ,**“Pressure drops of air-water two-phase flows in horizontal U-bends”**, International Journal of Multiphase Flow, Vol. 131 ,(2020) ,103403 .
40. T.S. Dhanasekaran, Ting Wang ”**Computational analysis of mist/air cooling in a two-pass rectangular rotating channel with 45-deg angled rib turbulators”** , International Journal of Heat and Mass Transfer, Vol: 61 ,(2013) ,554-564 .
41. Riyadh S. Al-Turaihi and Doaa Fadhil kareem ,**“The Effect of the Two Phase Flow (Water –Air) Over Triangle Ribs on Heat Transfer Coefficient in Vertical Rectangular Duct”**, European Journal of Scientific Research ,Vol. 140 No 3 July, 2016, pp.248-262
42. Riyadh S. Al-Turaihi ,**“Experimental Investigation of Two-Phase Flow (Gas –Liquid) Around A Straight Hydrofoil In Rectangular channel”** Journal of Babylon University/Engineering Sciences/ Vol.21, No. 5, 2013.
43. Laith Jaafer Habeeb and Riyadh S. Al-Turaihi ,**“Steady and Unsteady Bubbly Two-phase Flow (Gas-Liquid Flow) Around A Hydrofoil in Enlarging Rectangular Channel”**, International Journal of Computational Engineering Research, Vol:3,2013
44. Hyder M. Abdul Hussein ,Sabah Tariq Ahmed and Laith Jaafar Habeeb **“Two-phase Flow for Gas-liquid, Gas-solid, Liquid-solid, and Liquid-liquid in a Horizontal Smooth and Turbulator Conduit – A Review”**, Journal of Mechanical Engineering Research and Developments, Vol. 43, No. 7 2020, pp.(26-50)
45. Yao-Hsien Liu, Lesley M. Wright, Wen-Lung Fu, and Je-Chin Han **“Rib Spacing Effect on Heat Transfer and Pressure Loss in a Rotating Two-Pass Rectangular Channel (AR=1:2) with 45-Degree Angled Ribs”** ,heat transfer parts ,A and B ,Vol.3,2006 .
46. ANSYS, **“ANSYS Fluent Meshing User's Guide”**, ANSYS, Inc., Release 2020R1, January 2020.

47. Ansys 15.0 Help, Fluent Theory Guide, Mixture Multiphase Model.
48. ANSYS, “ANSYS Fluent in ANSYS Workbench User's Guide”, ANSYS, Inc., Release 2020R1, January 2020.
49. Vallee,C., Hohne, T., Prasser, H-M., Suhnel, T., "**Experimental investigation and CFD simulation of horizontal stratified two-phase flow phenomena**", Nuclear Engineering and Design, Vol. 238, No.3 2008, pp.(637-646)
50. YUNUS A. ÇENGEL and AFSHIN J. GHAJAR “**Heat and mass transfer: fundamentals and applications**”, fifth edition , McGraw-Hill Education.2015 .

الخلاصة

عادة ما تكون شفرات التوربينات الغازية مستدقة من محور إلى طرف لتقليل التحميل الحراري. توجد هذه القنوات داخل شفرات التوربينات عالية الأداء لتوفير تبريد فعال للسطح الخارجي للشفرة ، والذي يتعرض لتدفق غاز عالي الحرارة.

في هذا العمل تمت دراسة جريان ثنائي الطور (ماء - هواء) بوجود انتقال الحرارة في قنوات مستقيمة ومدببة افقية مزلعة مستطيلة. تم اجراء الدراسة نظريا لاختبار تأثير شكل القنوات ، تأثير سرعة الدخول والشكل الهندسي للأضلاع عند تدفق حراري ثابت على توزيع درجة الحرارة داخل قناة الاختبار وكذلك معامل انتقال الحرارة. سرعة الماء والهواء المستخدمة ما بين (1.154 -0.3845 m/s) و (13.89 – 4.624 m/s) بالتتابع اما التدفق الحراري ثابت (10000W/m^2).

تم استخدام برنامج solid work 2018 لتصميم الشكل الهندسي ثلاثي الابعاد. وتمت المحاكاة باستخدام برنامج Ansys fluent 20.R1 . ابعاد القناة المستقيمة ، يبلغ طولها cm 60، ومساحة المقطع العرضي $2.2 \times 5 \text{ cm}^2$ تكون متساوية عند الدخول ومنطقة الانحناء ، اما القناة المدببة تكون ابعاد منطقة الانحناء نصف منطقة الدخول لتكون عند الدخول $2.2 \times 5 \text{ cm}^2$ وعند الانحناء $2.5 \times 2.2 \text{ cm}^2$ حتى تكون بشكل مدبب . تم اختبار ثلاث اشكال هندسية للأضلاع مربعة وشكل البيت وشبه المنحرف تم وضعها في اعلى القناة وعند القاعدة لتكون بشكل متقابل . تم عمل ثلاث اشكال هندسية للثقوب بداخل الضلع شبه المنحرف واختبار تأثيرها على معامل انتقال الحرارة .

بينت النتائج النظرية ان معامل انتقال الحرارة الموقعي تحسنت بنسبة (16%, 10% 21%) داخل قناة الاختبار المزودة بعائق عند مقارنتها في القناة الملساء ، تحسنت بنسبة (12% 6%) داخل قناة الاختبار المزودة بضلع ذو شكل شبه المنحرف عند مقارنتها بالأضلاع الاخرى، و تحسنت بنسبة (20%) داخل قناة الاختبار المزودة بضلع ذو شق عند المقارنة مع الضلع الصلب، عندما تزداد سرعة الماء من (1.154- 0.3845 m/s) ، وعندما تزداد سرعة الهواء من (13.89 – 4.624 m/s) ، بالتتابع، عند تدفق حراري ثابت (10000 W) .



جمهورية العراق

وزارة التعليم العالي والبحث

العلمي

جامعة بابل - كلية الهندسة

تقصي مميزات الجريان ثنائي الطور داخل قنوات ثنائية المسار مستقيمة ومستدقة مع وجود العوائق

رسالة مقدمة الى كلية الهندسة – جامعة بابل كجزء من متطلبات نيل درجة
ماجستير علوم في الهندسة الميكانيكية

من قبل

بركات حسن عبدالامير

بإشراف

أ.د. رياض صباح الطريحي